

Supporting Information
for the Article

**Illuminating the Multiple Lewis Acidity of Triaryl-Boranes via Atropisomeric
Dative Adducts**

Benjámín Kovács, Tamás Földes, Márk Szabó, Éva Dorkó, Bianka Kótai, Gergely Laczkó, Tamás Holczbauer, Attila Domján, Imre Pápai, and Tibor Soós

Table of Contents

Experimental Procedures.....	3
1.1. NMR spectroscopy.....	3
1.2. Structure Calculation	4
Results and Discussion.....	6
2. Computed Borane and Hydride Complex Structures.....	6
3. Lewis Base Screening via Single-Pulse NMR	10
4. Computed Piperidine-Borane Adduct Structures	23
5. ¹⁹ F Chemical Shift Calculations	28
6. ¹⁹ F Signal Assignment and Structure Validation	30
7. Kinetic and Thermodynamic Studies Using ¹⁹ F-EXSY	31
8. PES Scans	40
9. Aqueous Complexes and X-ray Crystallography	43
10. Additional Borohydride and FIA Calculations	50
11. Additional Activation-Strain Analysis.....	51
12. ¹⁹ F NMR spectra of the Quinuclidine+Borane Systems.....	52
References	53
List of Atomic Coordinates.....	54

Experimental Procedures

1.1. NMR spectroscopy

The synthesis and characterization of boranes **I**, **II** and **III** were performed as described previously.^[11] For the NMR measurements the solid products were dissolved in toluene-*d*8 (99.6%, Sigma Aldrich Chemical Co.) at ~0.1 M initial concentration. The solvent was dried on 3–4 Å molecular sieves (Merck KgaA) for 12 hours which had been activated at 120°C under vacuum and stored under inert atmosphere in a glove box. The samples were transferred into screw cap NMR tubes.

The ¹H, ¹¹B and ¹⁹F dimensions were referenced to the residual solvent signal, BF₃ and TFA, respectively. The 1D ¹¹B, ¹⁹F, ¹H, ¹⁹F DOSY (Diffusion Ordered Spectroscopy) measurements were recorded with a narrow bore Varian NMR SYSTEM spectrometer operating at 400 MHz ¹H frequency, equipped with an inverse broadband HX probe (Z gradient=20 G/cm) or a Varian NMR SYSTEM spectrometer operating at 600 MHz ¹H frequency, equipped with an inverse triple resonance HFC probe or a dual resonance ¹H-¹⁹F/X probe (Z gradient=60 G/cm in both cases). The ¹H-decoupled 1D ¹⁹F (¹⁹F-¹H}), ¹⁹F-¹H HOESY (Heteronuclear Overhauser Effect Spectroscopy) and ¹⁹F-¹⁹F-EXSY (Exchange Spectroscopy) experiments were performed using the 600 MHz instrument exclusively. For these measurements the ¹⁹F pulse was always calibrated with the typical 90° ¹⁹F pulse length being ~13 μs (HFC) or ~16 μs (¹H-¹⁹F/X). The temperature of the samples was controlled by airflow with an accuracy of 0.1 K. All the samples were equilibrated for at least 30 min before the measurements.

Standard pulse sequences from the Varian's VnmrJ 4.2 software library were used throughout: 'NOESY' for ¹⁹F-EXSY, 'Dbppste_cc' for ¹⁹F DOSY, 'FH_HOESY' for ¹⁹F-¹H HOESY, 'Fhdec' for ¹H-decoupled 1D ¹⁹F, 's2pul' for 1D ¹¹B. The 1D ¹H and ¹⁹F measurements applied 32 scans (*NS*) with the interscan delay (*D1*) of 16.0 s. The ¹¹B spectra were recorded with *NS*=512 and *D1*=2.0 s. For the 1D ¹⁹F measurements the pulse angle was reduced from 90° to 30°. The ¹⁹F-¹H} spectra were recorded with decoupling during acquisition only using the waltz16 decoupling scheme with a decoupler frequency at 4 ppm. Typical acquisition times (*t*_{AQ}) for the ¹H, ¹⁹F and ¹¹B spectra were chosen around 4.0 s, 1.0 s and 0.5 s, respectively.

The ¹H-decoupled ¹⁹F spectra (¹⁹F-¹H}) of the piperidine (**p**) + **I** and **p+II** systems (**p+I**: Figure S18, **p+II**: Figure 5) were used to distinguish between ¹⁹F-¹⁹F and ¹⁹F-¹H *J*-couplings. While both types of *J*-couplings impact the signal patterns in the standard ¹⁹F spectrum the effects of ¹⁹F-¹H couplings are removed in the ¹⁹F-¹H} spectrum. Thus, in the latter the ¹⁹F-¹⁹F *J*-coupling values can be directly extracted from the fine structure of the ¹⁹F signals. Considering that in our systems the fluorine atoms are located on different aromatic rings, and therefore, are separated by six chemical bonds, the emerging ¹⁹F-¹⁹F *J*-couplings must exist through space (TS) rather than through bond.^[19] Indeed, TS *J*_{FF}-coupling occurs when two atoms, at least one of which has lone-pair electrons, are constrained at a distance smaller than the sum of their van der Waals radii and show quasi-exponential decay as a function of the distance between the coupled nuclei. In this way, the detection of ¹⁹F-¹⁹F TS couplings confirms the spatial vicinity of fluorine atom pairs in **p-I** and **p-II** atropisomers. (Section 6, Table S9)

The ¹⁹F-¹H HOESY is a well-established NMR technique for the structural characterization of fluorinated organic compounds.^[17] By correlating the frequencies of spatially close (<~5 Å) ¹H and ¹⁹F nuclei, in the slow exchange regime the 2D ¹⁹F-¹H HOESY spectrum is able to provide direct experimental insights into the relative orientation of **p** and the borane aryl rings and reveal the particular F-arrangements of the **p**-adduct conformers. (Section 6) However, the lowest applicable temperature for the required HFC probe is ~273 K which in case of the **p+III** mixture is close to the coalescence point of the ¹⁹F signals. (Figure S15) Due to this technical limitation, for the **p+III** system ¹⁹F-¹H HOESY studies were not performed. For the **p+I** and **p+II** systems the 2D ¹⁹F-¹H HOESY experiment was recorded with *D1*=10 s, *NS*=64, *t*₁=128 indirect time domain points, *t*₂=4906 direct time domain points, *t*_{AQ}~0.2 s and the respective mixing times (*τ*_{mix}) of 400 ms and 60 ms. For 2D processing the HOESY spectra were zero-filled to a 512x16384 real data matrix and multiplied with a Gaussian function along both dimensions before Fourier-transformation.

To characterize the dynamic behavior of the **p**-borane systems 2D ¹⁹F-¹⁹F EXSY measurements were performed in the slow exchange regimes. These were recorded uniformly with *D1*=10 s, *NS*=64, *t*₁=128, *t*₂=4096, *t*_{AQ}~0.2 s and *τ*_{mix} values adjusted to the dynamic properties of the system. (Table S1) For 2D processing the ¹⁹F-EXSY spectra were zero-filled to a 512x8192 real data matrix and multiplied with a Gaussian function along both dimensions before Fourier-transformation. Exchange rates between chemically nonequivalent fluorines (*k*_F) were determined by the full relaxation matrix analysis of the corresponding ¹⁹F-EXSY cross- and diagonal peak amplitudes using the EXSYCalc freeware (Mestrelab: <https://mestrelab.com/software/freeware/>). The cross-peak amplitudes are related to the *k*_F values and the applied *τ*_{mix} through the following expression:

$$\mathbf{R} = -\frac{\ln \mathbf{A}}{\tau_{\text{mix}}} = -\frac{\mathbf{X}(\ln \mathbf{A})\mathbf{X}^{-1}}{\tau_{\text{mix}}} \quad (1)$$

In Equation 1 matrix **R** contains the *k*_F values as off-diagonal elements whereas matrix **A** contains the peak amplitudes at *τ*_{mix} divided by the corresponding diagonal peak intensity in the reference spectrum recorded with *τ*_{mix}=0. Matrix **R** matrix is obtained according to the eigen-values eigen-vector method where **Λ** is the matrix of the eigenvalues of **A** and **X** is the square matrix of the eigenvectors of **A**.^[24] As for the **p+I** and **p+II** systems multiple fluorine exchanges can be assigned to the same chemical exchange process the exchange rate of a chosen process (*k*_{ex}) was determined by averaging the corresponding *k*_F fluorine exchange rates. (See the *k*_F values for the **p-II** conformational exchanges at 293.0 K in Table S12 vs the averaged *k*_{ex} values in Table S13 as example.) For the **p+III** (Table S11) and **p+I** systems (Table S16) the *k*_{ex} values were determined at a single respective temperature point only, that is, at 253.0 and 323.0 K. For the **p-II** system multiple ¹⁹F-EXSY-s were measured

in the range from 293.0 K to 333.0 K (Table S13) to determine thermodynamic parameters (Tables S14–S15) from the extracted k_{ex} values. Here, the energy barrier of activation (ΔG^\ddagger) was calculated using the Eyring-theory:

$$\Delta G^\ddagger = RT \left[\ln \left(\frac{k_b T}{h} \right) - \ln (k_{ex}) \right] \quad (2)$$

In Equation 2 T is the applied temperature, R is the universal gas constant, h is the Planck constant and k_b is the Boltzmann constant. The processes' entropy of activation (ΔS^\ddagger) and enthalpy of activation (ΔH^\ddagger) were determined by fitting a linear to the points of the Eyring-plot with the ordinary least-squares method. That is, the ΔS^\ddagger and the ΔH^\ddagger were calculated from the intercept of the fitted linear and the y axis, and the slope of the fitted linear, respectively. The detected exchange processes are detailed in Section 7 for each **p**-adduct.

Table S1. The corresponding temperature (T) and mixing time values (τ_{mix}) applied for the ^{19}F -EXSY experiments to characterize the conformational interconversions of the **p**-borane adducts.

p -borane	T / K	τ_{mix} / ms
p-III	253.0	400
p-II	293.0	1000
	300.0	500
	303.0	400
	310.0	200
	317.0	100
	323.0	50
	333.0	33
p-I	323.0	600

The corresponding sp^2 borane, dative **p**-complex and aqueous **p**-complex forms (Section 9) were clearly distinguishable based on their differences in diffusional properties using diffusion NMR spectroscopy (DOSY). (Section 9) These double stimulated echo measurements applied bipolar gradients and convection compensation with $NS=32$ and $D1=4.0$ s. The diffusion encoding/decoding gradients varied linearly between 5% and 95% of their maximum output over 50 increments. For the **p-I** and **p-II** systems at 298.2 K the duration of these gradients and the diffusion delay time were set to 4 ms and 100 ms, respectively. These values were adjusted to respectively 2 ms and 200 ms when the **p-III** system was measured at low temperature. The obtained intensity decays were translated to the corresponding DOSY spectra using the VnmrJ 4.2 'DOSY' processing function.

1.2. Structure Calculation

To explore the conformational space of each molecule including **p**, boranes **I**, **II**, **III** (Table S2) and the **p**-adducts **p-I** (Table S6), **p-II** (Table S5), and **p-III** (Table S4), we performed Monte Carlo conformational searches with MacroModel in the Schrodinger program suite.^[25] The subsequent quantum mechanical density functional theory (DFT) computations were carried out using the B3LYP-D3^[26] dispersion-corrected exchange correlation functional with the Gaussian09 package.^[27] The generated structures were subjected to geometry optimizations using the 6-311G(d,p) basis set.^[28] The vibrational analysis confirmed that all obtained geometries correspond to local minima. Thermal and entropic corrections were evaluated using the ideal gas-rigid rotor-harmonic oscillator (RRHO) approximations at 243.15 K or 298.15 K and $c = 1 \text{ mol/dm}^3$ conditions. The solvation effect of the toluene medium was estimated by single-point energy calculations applying the SMD solvation model.^[29] To obtain more accurate complexation free energy results, we performed single-point energy calculations for the optimized geometries utilizing a low-order scaling, local natural orbital CCSD(T) (denoted as LNO-CCSD(T)) method as implemented in the MRCC program.^[30] The CCSD(T) correlation energy was extrapolated as

$$E_{N-T} = E_T + \frac{E_T - E_N}{2} \quad (3)$$

where N and T refer to "normal" and "tight" composite cutoff thresholds offered by the MRCC program. The LNO-CCSD(T) calculations were carried out using the correlation consistent basis set developed by Dunning.^[31] The complete basis set limit of the LNO-CCSD(T) energies were estimated relying on extrapolation techniques employing the aug-cc-pVTZ and aug-cc-pVQZ basis sets. From the results with the aug-cc-pVTZ (TZ) and the aug-cc-pVQZ (QZ) basis sets, we extrapolated towards the complete basis set (CBS) limit of the Hartree-Fock and the correlation energy according to [32]:

$$E_{\text{CBS}}^{\text{HF}} = E_{\text{QZ}}^{\text{HF}} + \frac{5(E_{\text{QZ}}^{\text{HF}} - E_{\text{TZ}}^{\text{HF}})}{4 \exp[6.57(\sqrt{4} - \sqrt{3})]} \quad (4)$$

$$E_{\text{CBS}}^{\text{C}} = \frac{3^3 E_{\text{TZ}}^{\text{C}} - 4^3 E_{\text{QZ}}^{\text{C}}}{3^3 - 4^3} \quad (5)$$

We estimated the CCSD(T)/CBS limit by extrapolating towards the CCSD(T) limit on the TZ basis and extrapolating towards the CBS limit with the normal threshold. The final LNO-CCSD(T)/CBS energies were calculated according to the following formula:

$$E_{\text{CCSD(T)}}^{\text{CBS}} = E_{\text{N}}^{\text{CBS}} + E_{\text{N-T}}^{\text{TZ}} - E_{\text{N}}^{\text{TZ}} \quad (6)$$

where $E_{\text{N}}^{\text{CBS}}$ is the sum of $E_{\text{CBS}}^{\text{HF}}$ and $E_{\text{CBS}}^{\text{C}}$, whereas $E_{\text{N-T}}^{\text{TZ}}$ and E_{N}^{TZ} refer to CCSD(T) correlation energies. The correlation of the core electrons was neglected. The Gibbs free energies (ΔG) were finally calculated by applying the obtained solvation and thermal corrections to the LNO-CCSD(T)/CBS(aug-cc-pVTZ,aug-cc-pVQZ) energies. These values were used to quantify the Lewis acidity strengths of the boranes with respect to **p**. In Equation 7 G_a , $G_{\text{borane}(\alpha)}$ and $G_{\text{base}(\alpha)}$ refer to the obtained Gibbs free energies of the chosen adduct conformer and the lowest lying conformer of the borane and **p**, respectively.

$$\Delta G^a = G_a - G_{\text{borane}(\alpha)} - G_{\text{base}(\alpha)} \quad (7)$$

In our calculations for the free **p**, the N lone electron pair favored the axial rather than the equatorial orientation by 0.7 kcal·mol⁻¹. The ΔG^a values were displayed with respect to the more stable conformer. In contrast, the **p**-adducts the favored orientation of the B–N bond is equatorial. Hydride affinity values (ΔG^h) were also defined according to Equation 7, but in these cases G_{base} was the Gibbs free energy of the free H⁻ anion ($G_{\text{hydride}} = -0.5276$ hartrees) whereas all the rotameric states of each borane were considered as Lewis acid partners. (Table S3) The ΔG^h values were defined in toluene. Notably, these values are still expected to bear significant errors due to the poor description of solvated H⁻ anion. Nevertheless, the relative values ($\Delta_\alpha \Delta G^h$), that reflect Lewis acidity relations between the diverse rotameric states of a borane, are expected to be more accurate. For the **p**-adducts a computed conformational distribution (P^c) was calculated from the corresponding stabilities based on the Boltzmann-equation:

$$\frac{N_{\chi_2}}{N_{\chi_1}} = \exp \left(\frac{G_{\chi_1}(T) - G_{\chi_2}(T)}{k_{\text{B}} \cdot T} \right) \quad (8)$$

In Equation 8 N_{χ_2}/N_{χ_1} stands for the population ratio of the conformers χ_1 and χ_2 at temperature T , the G values are the corresponding Gibbs free energies. For best comparability with the experimental data, the ΔG^a values were recomputed at 243.15 K applying the same protocol.

Results and Discussion

2. Computed Borane and Hydride Complex Structures

The computed sp^2 states and hydride adducts of boranes I, II and III are shown in Tables S2–23. In both types of structures two rings always adopt the tilt angle of $\sim 40^\circ$ – 45° while the orientation of the third ring varies from structure to structure. (Figure S1)

Table S2. The computed borane structures in tube representation along with their G_{borane} and ΔG_{borane} values latter being the difference with respect to the lowest lying energy conformational state (α) at 298.15 K. Cl: green, F: blue, B: pink, C: gray, H: white. The structures are shown in the same respective orientations as the 'Top view'-s in Figure 3A in the main text. To guide the eye, the spatial position of the halogen atoms on the fluorinated rings is indicated by upwards or downwards arrow in the corresponding color depending on whether the halogen atom is found above or below the plane defined by the boron atom and the aryl rings.

Borane	III	I	I
Conformer	α	α	β
Structure			
G_{borane} / hartree	-3113.6762	-2393.6886	-2393.6883
ΔG_{borane} / kcal·mol ⁻¹	0.0	0.0	0.2
Borane	II	II	II
Conformer	α	β	γ
Structure			
G_{borane} / hartree	-2753.6830	-2753.6830	-2753.6817
ΔG_{borane} / kcal·mol ⁻¹	0.0	0.3	0.8

Table S3. The computed borane–hydride complex structures along with the way of their formation and the corresponding ΔG_h values at 298.15 K. Cl: green, F: blue, B: pink, C: gray, H: white. The structures are shown with the B–H bond pointing towards the viewer. To guide the eye, the spatial position of the halogen atoms on the fluorinated rings is indicated by upwards or downwards arrow in the corresponding color depending on whether the halogen atom is found above or below the plane defined by the boron atom and the aryl rings. In most cases distinct ΔG_h and [borane–H][−] complex conformations could be determined depending on which side (top or bottom, see Figure 4 in the main text) was available for interaction with the H[−]. Uniformly, it shows more than 1 kcal·mol^{−1} favorable for the H[−] to attack the side of the borane rotamer which has the most Cl atoms.

borane–hydride complex (conformer)	[III–H] [−] (α)	[III–H] [−] (β)	[II–H] [−] (α)
Reaction route	III(α) [Bottom side] + H [−]	III(α) [Top side] + H [−]	II(α) [Bottom side] + H [−]
Structure			
G_h / hartree	−3114.3940	−3114.3919	−2754.4024
ΔG_h / kcal·mol ^{−1}	−52.9	−51.6	−54.0
borane–hydride complex (conformer)	[II–H] [−] (β)	[II–H] [−] (γ)	[II–H] [−] (δ)
Reaction route	II(β) [either side] + H [−]	II(γ) [either side] + H [−]	II(α) [Top side] + H [−]
Structure			
G_h / hartree	−2754.4000	−2754.3998	−2754.3975
ΔG_h / kcal·mol ^{−1}	−52.5	−52.4	−50.9

Table S3 (continued). The computed borane–hydride complex structures along with the way of their formation and the corresponding ΔG_h values at 298.15 K. Cl: green, F: blue, B: pink, C: gray, H: white. The structures are shown with the B–H bond pointing towards the viewer. To guide the eye, the spatial position of the halogen atoms on the fluorinated rings is indicated by upwards or downwards arrow in the corresponding color depending on whether the halogen atom is found above or below the plane defined by the boron atom and the aryl rings. In most cases distinct ΔG_h and [borane–H][−] complex conformations could be determined depending on which side (top or bottom, see Figure 4 in the main text) was available for interaction with the H[−]. Uniformly, it shows more than 1 kcal·mol^{−1} favorable for the H[−] to attack the side of the borane rotamer which has the most Cl atoms.

borane–hydride complex (conformer)	[I–H] [−] (α)	[I–H] [−] (β)	[I–H] [−] (γ)
Reaction route	I(β) [Bottom side] + H [−]	I(α) [Bottom side] + H [−]	I(α) [Top side] + H [−]
Structure			
G_h / hartree	−2394.4089	−2394.4076	−2394.4052
ΔG_h / kcal·mol ^{−1}	−54.6	−53.8	−52.3
borane–hydride complex (conformer)	[I–H] [−] (δ)		
Reaction route	I(β) [Top side] + H [−]		
Structure			
G_h / hartree	−2394.4033		
ΔG_h / kcal·mol ^{−1}	−51.1		

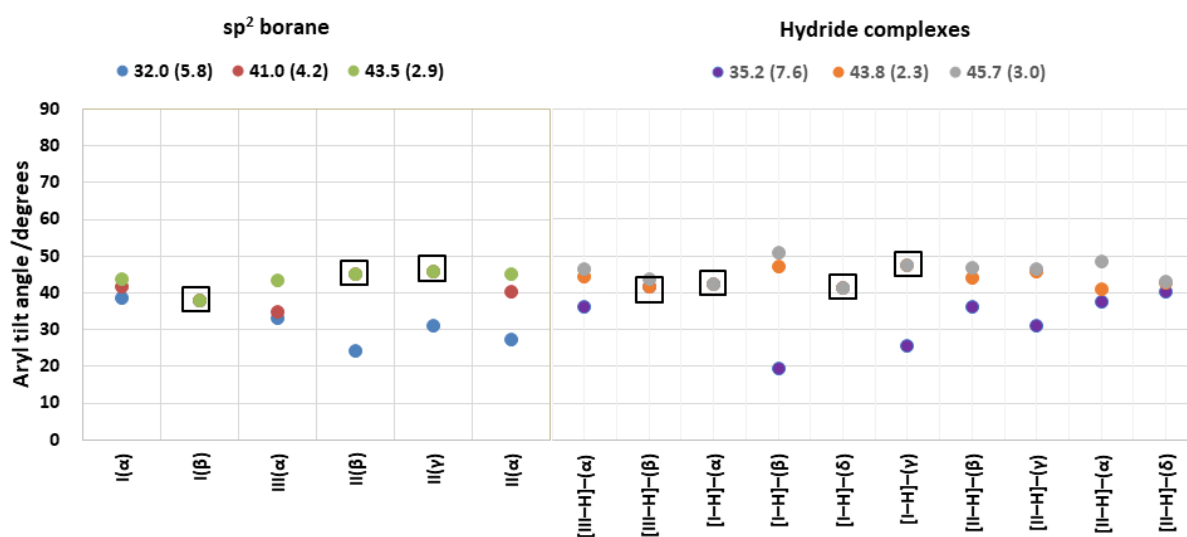


Figure S1. The tilt angles of the three aryl rings in the sp² borane and the borane–hydride complex structures. The tilt angles were defined by the C_x-B-C_y-C_z atoms. Degenerated angle values are indicated by squares. The average tilt angles per each ring are shown above with their standard deviation values in parenthesis.

3. Lewis Base Screening via Single-Pulse NMR

The asymmetrically halogenated boranes I-III were (separately) reacted with a chosen library of N-bases which was monitored through 1D ^1H , ^{19}F and ^{11}B NMR spectra. (Figure S2) The liquid N-bases were distilled over KOH to minimize their water content and added to the boranes with a Hamilton syringe through the septum of the cap. To illuminate the multiple Lewis acidity of the Lewis acidic boranes I-III, our goal was to find a Lewis base (LB) which is able to form a dative adduct with each of the investigated boranes; besides, the adduction process needed to allow for the emergence of multiple conformational states of each LB-borane adduct which are sufficiently long-lived to be detected by NMR. The formation of the dative LB-borane adduct could be directly confirmed by a ^{11}B signal at around 0 ppm. (Figures S3-S8) The linewidth (sharp vs broad) of the LB-borane ^{11}B NMR signal also reflects the dynamic properties of the adduct. Multiple distinct ^{19}F signals of a dative LB-borane adduct reflect the number of the emerging long-lived conformational (atropisomeric) states. In contrast, a single weighted-average borane-LB ^{19}F signal is the result of the fast exchange between its plausible conformational states which precludes their distinction and characterization (Figure 2B). As Figure S2 shows, although at room temperature the dative adduct formation of I and II could be confirmed with several Lewis bases, only a few of those yielded multiple ^{19}F signals for both the LB-I and LB-II adducts. The highest number of distinct LB-I and LB-II conformational states could be obtained when piperidine (**p**) was used as LB. Furthermore, the multiple conformational states of the piperidine-III adduct could be detected at lower temperatures. Thus, we chose **p** as the model base to illuminate the multiple Lewis acidity of boranes I-III. The single-pulse ^{11}B , ^{19}F and ^1H NMR spectra of the three **p**+borane systems are shown in Figures S3-S8, Figures S9-S18, and Figures S19-S24, respectively. The ^{19}F NMR spectra of the **quinuclidine** (C)+II or I systems is discussed in SI Section 12.

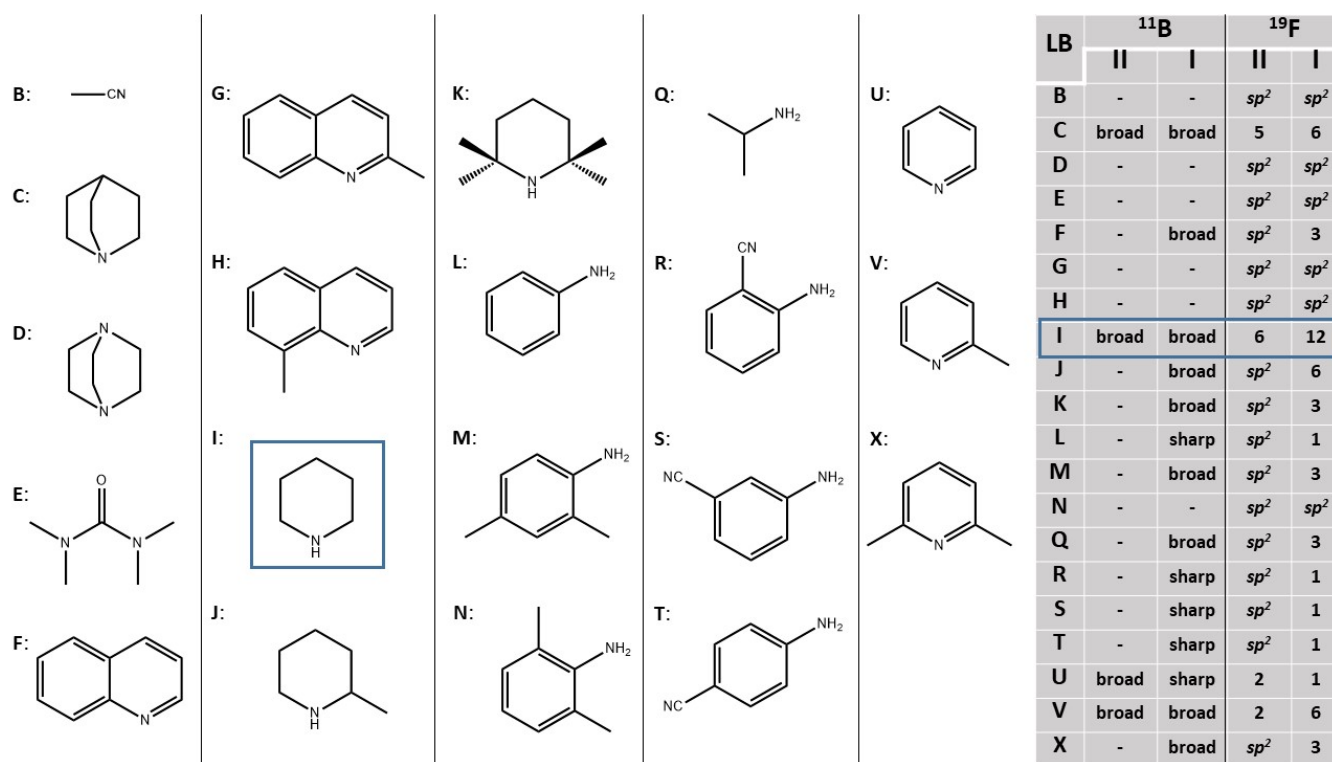


Figure S2. The N-bases (B-X) with which boranes I-II were reacted. The table presents the respective ^{11}B linewidths ('sharp' (40–60 Hz) or 'broad' (>100 Hz)) as well as number of ^{19}F NMR signals observed for these LB-borane mixtures at 298.2 K. Here, ' sp^2 ' indicates that despite adding the LB to the borane only the respective sp^2 borane signal could be detected. A single shifted average signal indicates free ring rotations in the sp^3 state. The most complex ^{19}F NMR spectra could be obtained when piperidine was added to the boranes. The ^{19}F NMR spectra of the **quinuclidine** (C)+II or I systems is discussed in SI Section 12.

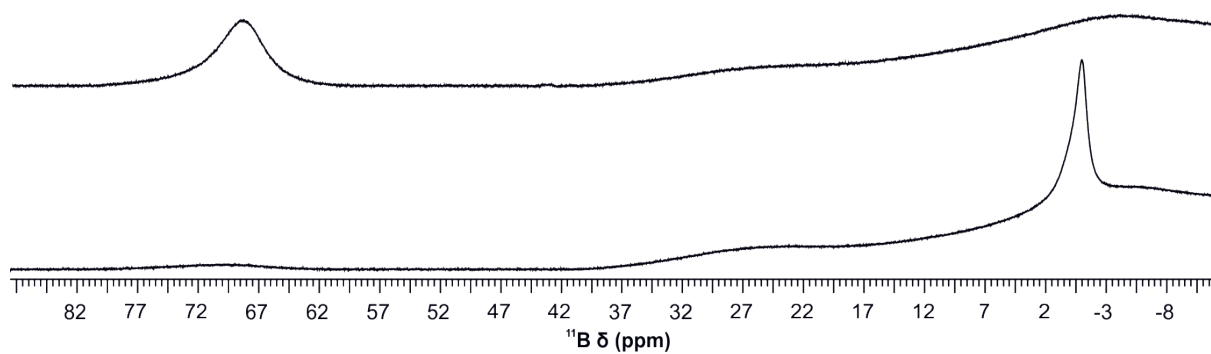


Figure S3. ^{11}B spectrum (128 MHz) of **III** (top) and the mixture of **p** and **III** using a **p** to **III** ratio of 3:1 (bottom) recorded at 243.2 K. In the ^{11}B spectrum of **p+III** the forming **p**-adduct atropisomers are represented by single weighted-average signal at ~ 0 ppm.

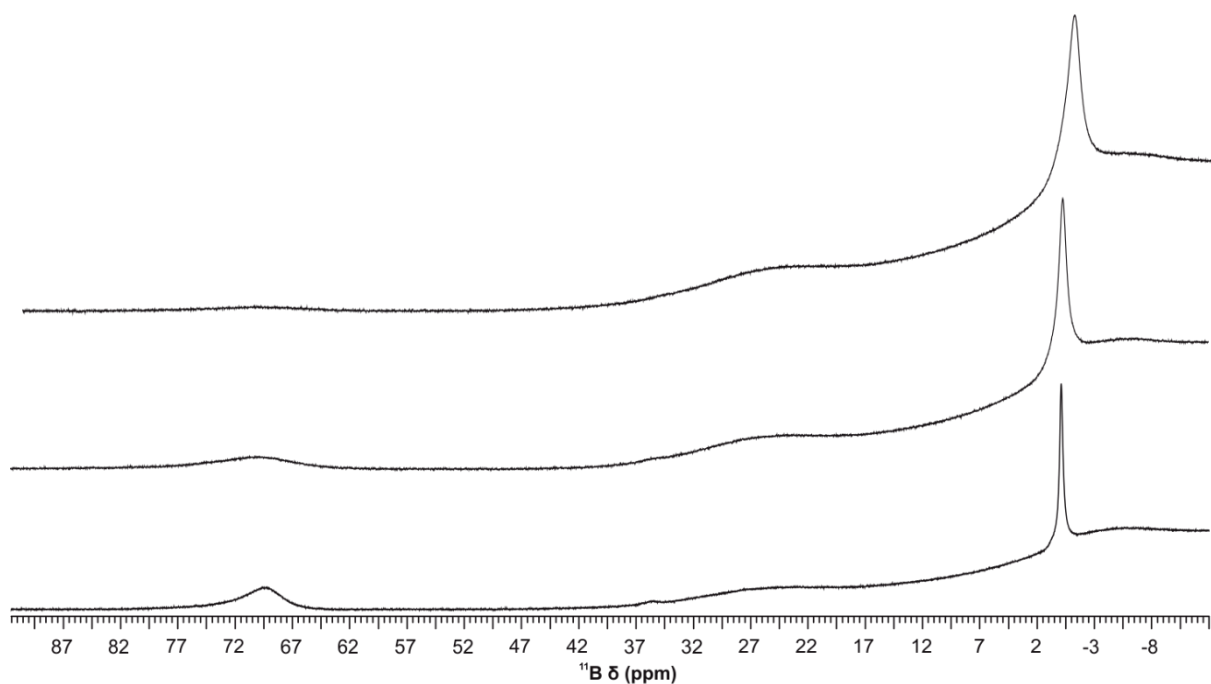


Figure S4. ^{11}B spectrum (128.3 MHz) of the mixture of **p** and **III** using a **p** to **III** ratio of 3:1 recorded at 243.2 K (top), 273.0 K (middle) and 323.0 K (bottom). The forming **p**-adduct atropisomers are represented by single weighted-average signal at ~ 0 ppm throughout.

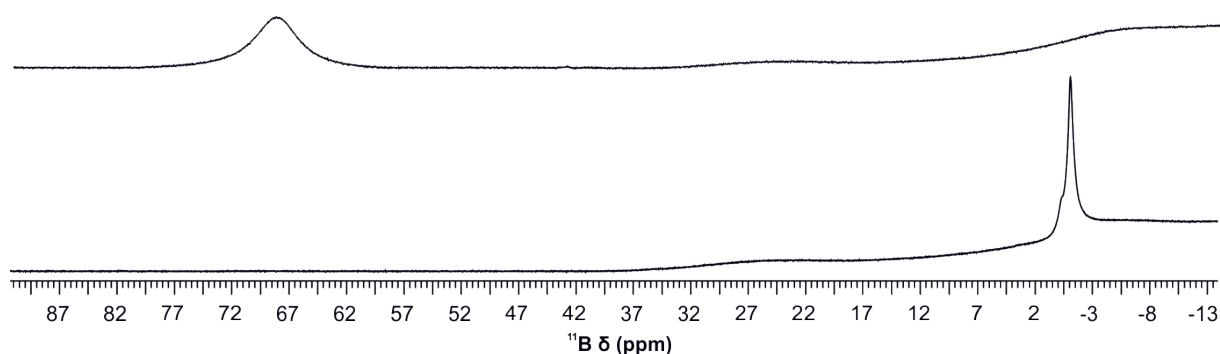


Figure S5. ^{11}B spectrum (128.3 MHz) of **II** (top) and the mixture of **p** and **II** using a **p** to **II** ratio of 3:1 (bottom) recorded at 298.2 K. In the ^{11}B spectrum of **p+II** the forming **p**-adduct atropisomers are represented by single weighted-average signal at ~ 0 ppm.

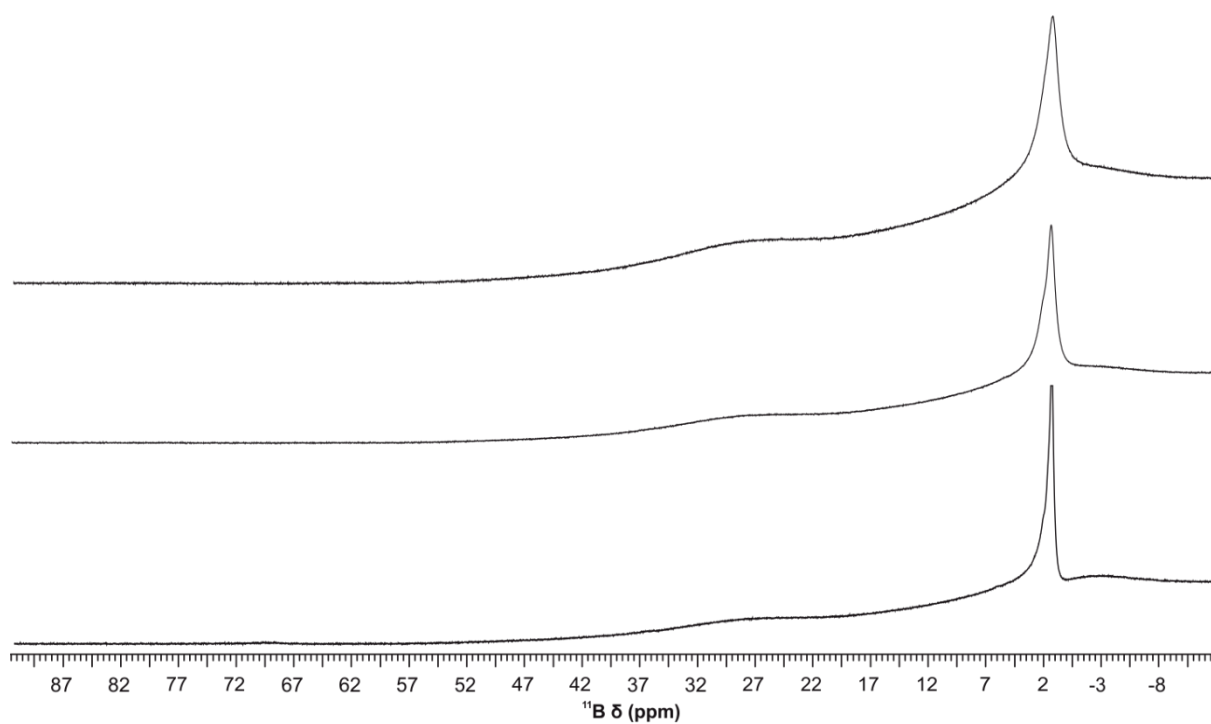


Figure S6. ^{11}B spectrum (128.3 MHz) of the mixture of **p** and **II** using a **p** to **II** ratio of 3:1 recorded at 243.2 K (top), 273.0 K (middle) and 323.0 K (bottom). The forming **p**-adduct atropisomers are represented by single weighted-average signal at ~ 0 ppm throughout.

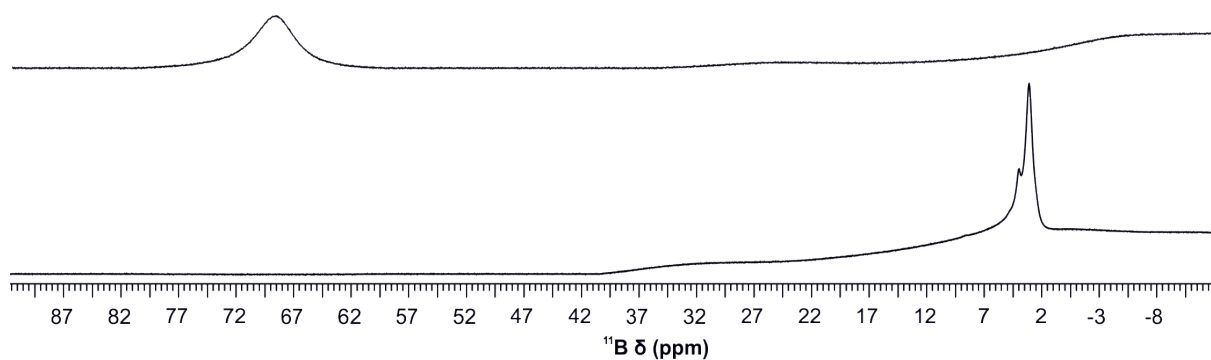


Figure S7. ^{11}B spectrum (128.3 MHz) of **I** (top) and the mixture of **p** and **I** using a **p** to **I** ratio of 3:1 (bottom) recorded at 298.2 K. In the ^{11}B spectrum of **p+I** the forming **p**-adduct atropisomers are represented by single weighted-average signal at ~ 0 ppm.

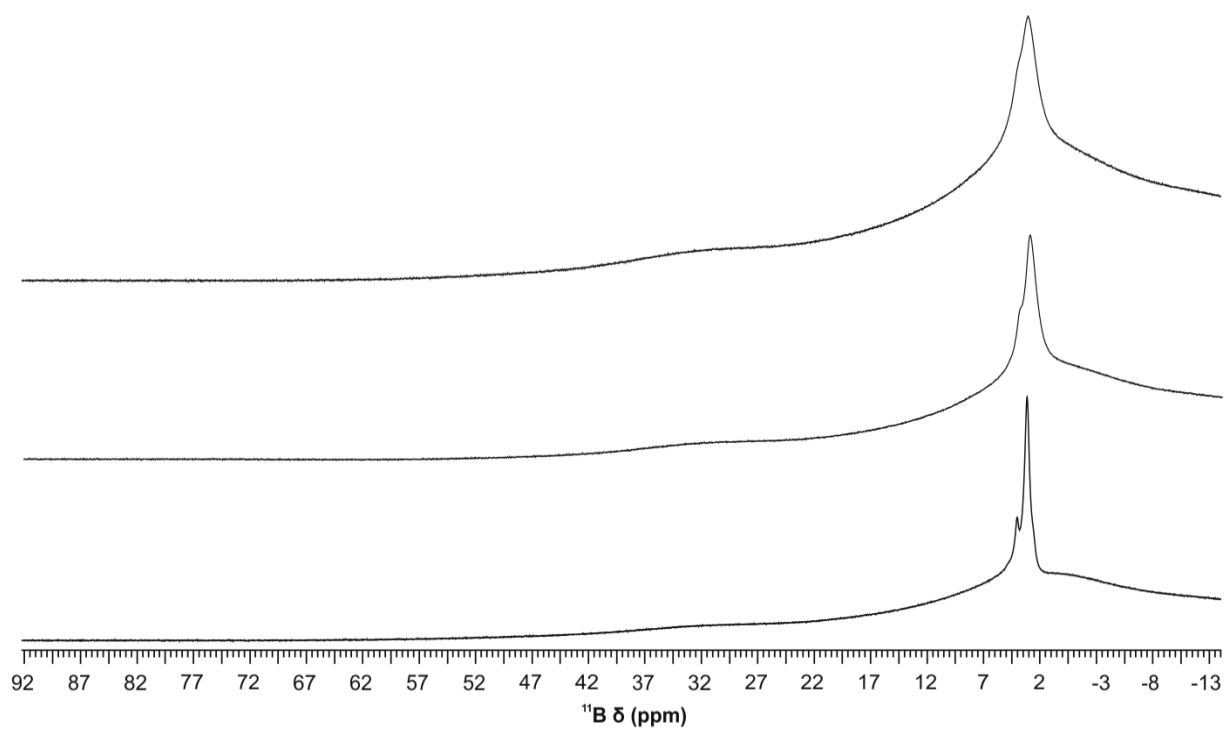


Figure S8. ^{11}B spectrum (128.3 MHz) of the mixture of **p** and **I** using a **p** to **I** ratio of 3:1 recorded at 243.2 K (top), 273.0 K (middle) and 323.0 K (bottom). The forming **p**-adduct atropisomers are represented by single weighted-average signal at ~ 0 ppm throughout.

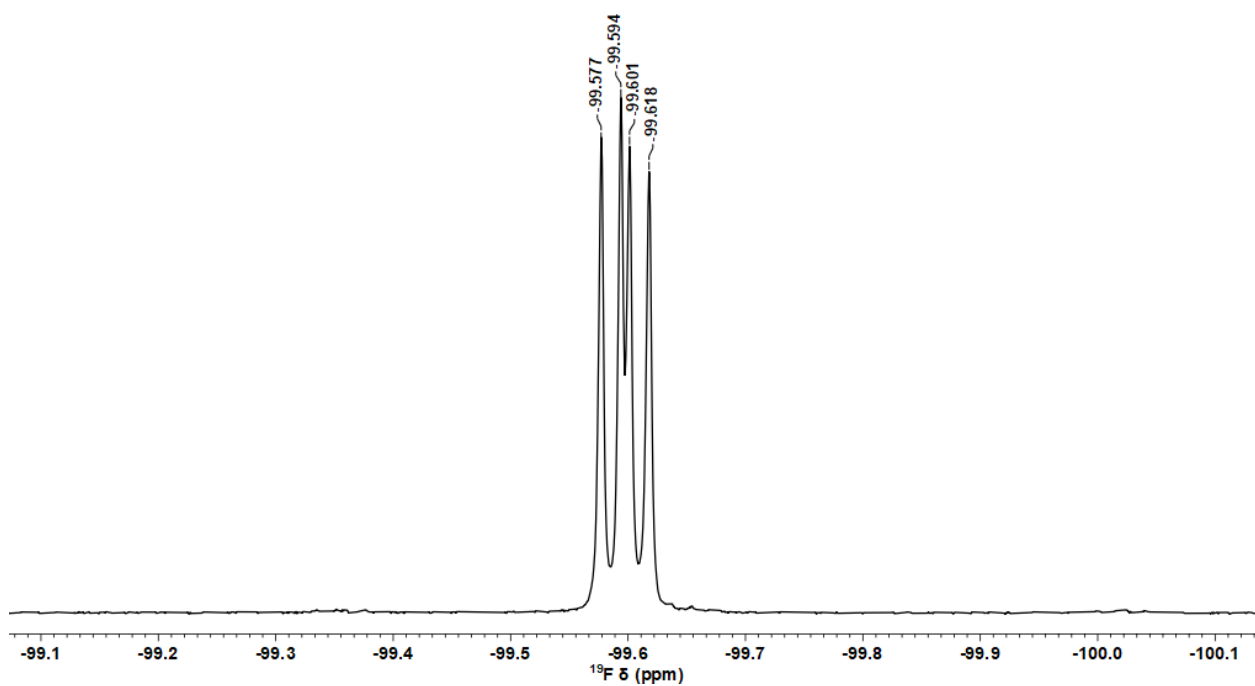


Figure S9. ^{19}F signal (376 MHz) of **III** recorded at 243.2 K.

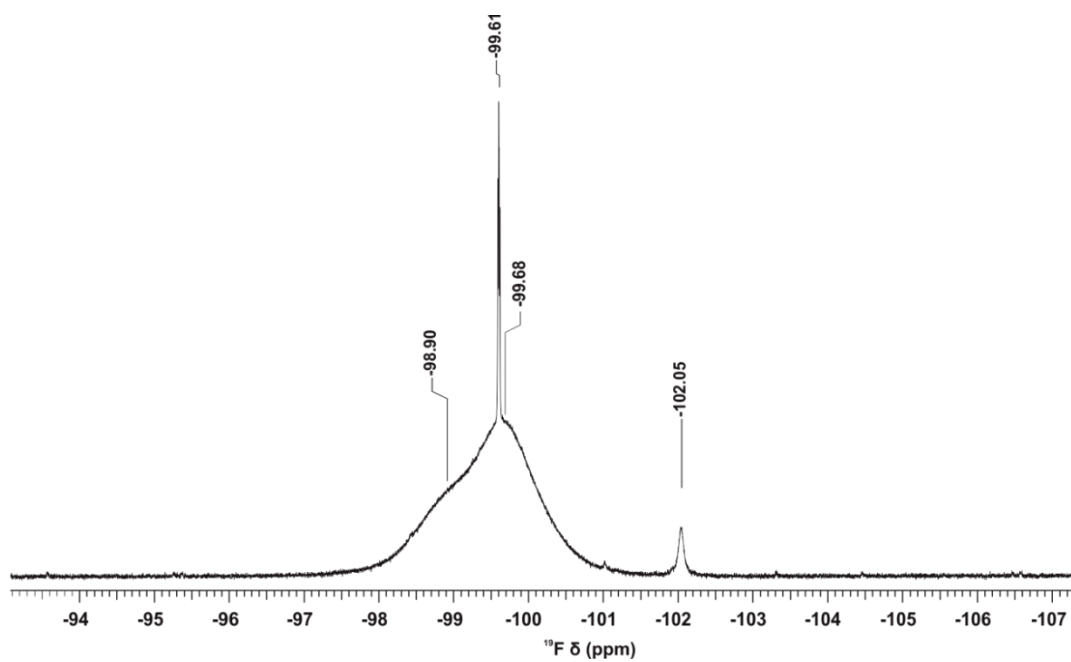


Figure S10. ^{19}F signal (564 MHz) of **II** at 243.2 K. Unfortunately, as a leftover product of the synthesis procedure some **III** cross-contaminated the sample which's sharp doublet of doublets is superimposed onto the signal of **II** at ~ -99.6 ppm.

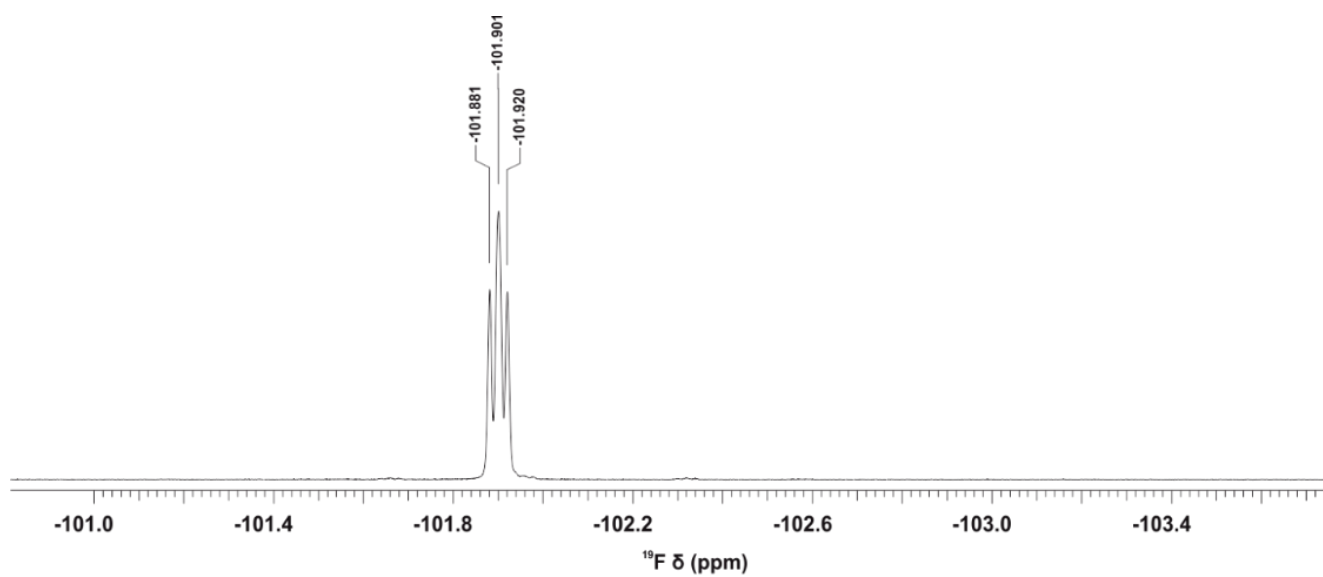


Figure S11. ^{19}F signal (564 MHz) of **I** recorded at 298.2 K.

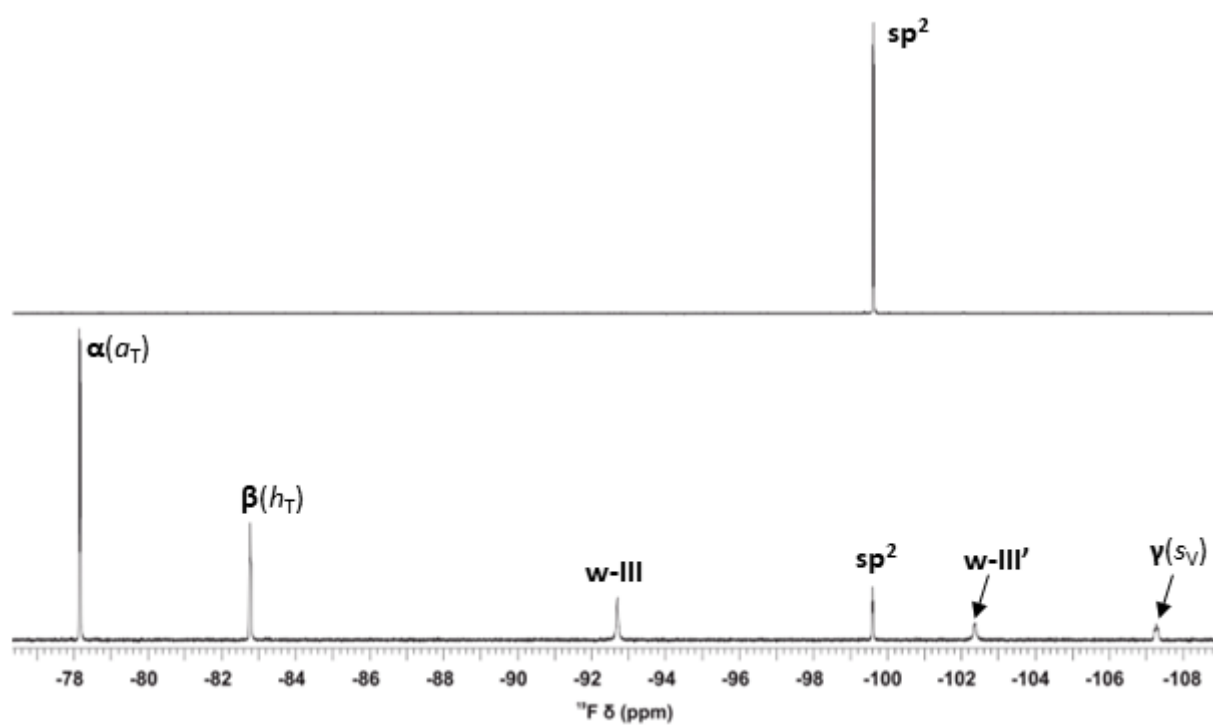


Figure S12. ^{19}F spectra (376 MHz) of **III** (top) and the mixture of **p** and **III** using a **p** to **III** ratio of 3:1 recorded at 243.2 K. In the latter in addition to the signals of **p-III** adduct atropisomers (**α** , **β** , **γ**) the signals of aqueous forms (**w-III**, **w-III'**) and that of the residual sp^2 **III** also emerge. For the signals of **p-III** atropisomers the spatial position of the represented fluorine atom is indicated in parenthesis.

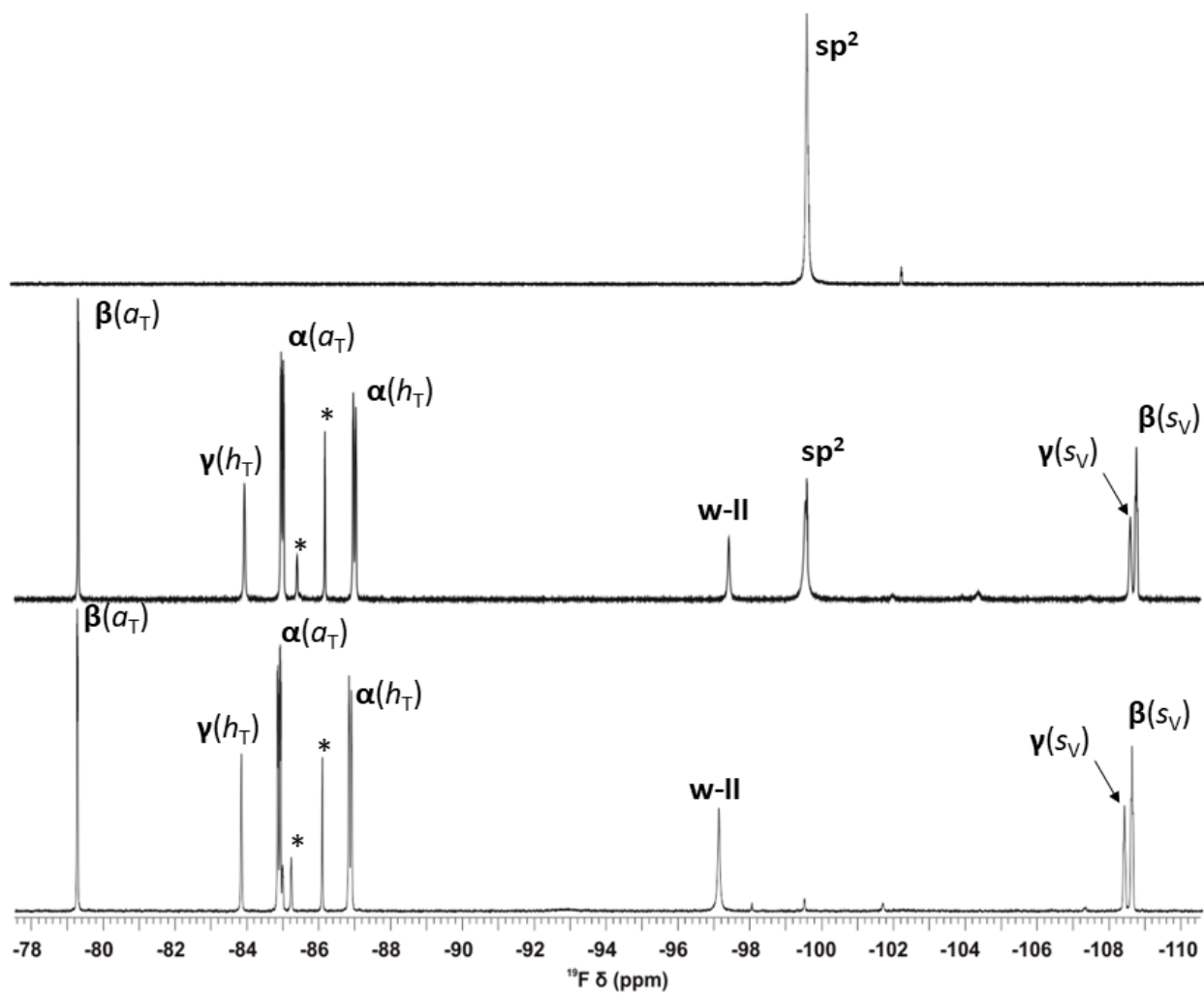


Figure S13. ^{19}F spectra (564 MHz) of **II** (top) and the mixture of **p** and **II** using a **p** to **II** ratio of 1:2 (middle) and 3:1 (bottom) recorded at 298.2 K. In addition to the signals of **p-II** adduct atropisomers (α , β , γ) the signals of the aqueous form (**w-II**) and that of the residual sp^2 **II** also emerge. For the signals of **p-II** atropisomers the spatial position of the represented fluorine atom is indicated in parenthesis.
**Signals of non-characterized contaminating compounds.*

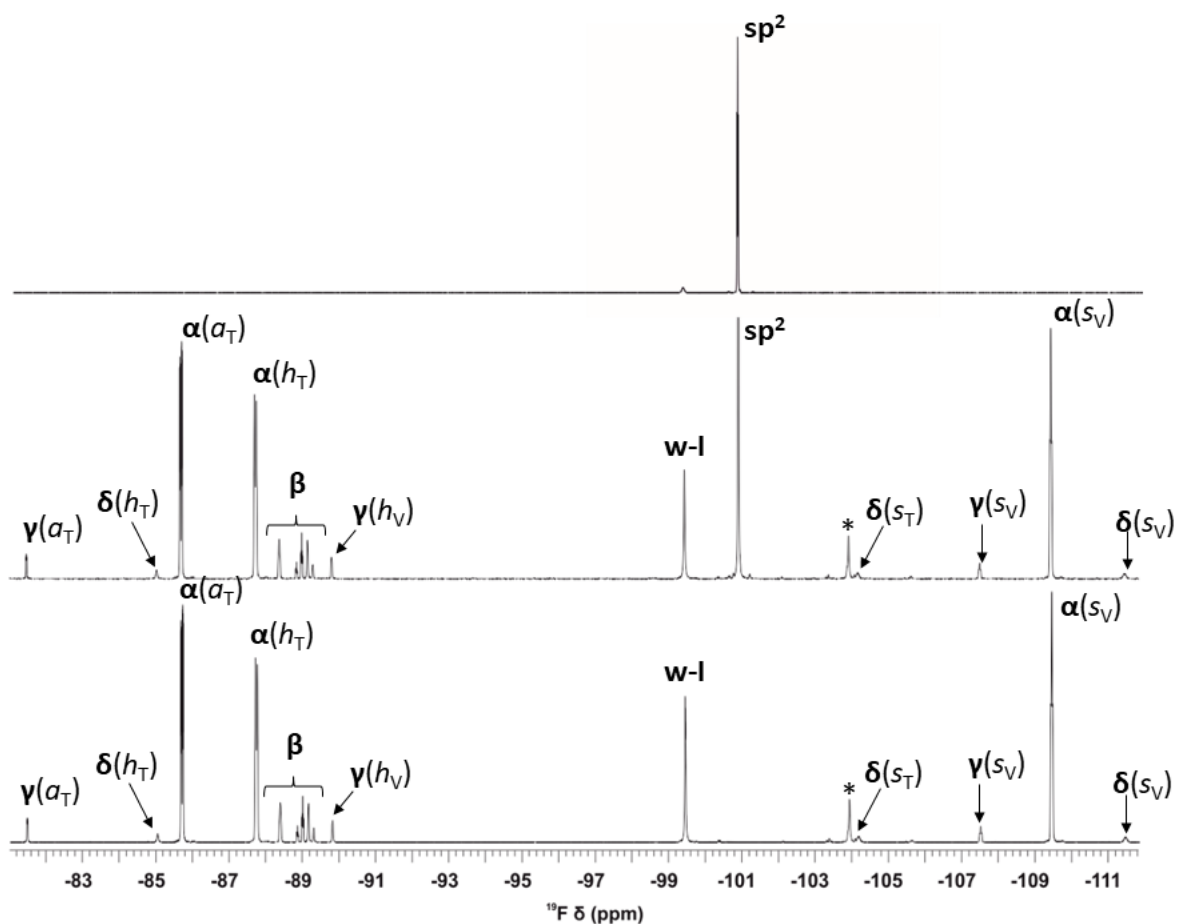


Figure S14. ^{19}F spectra (564 MHz) of **I** (top) and the mixture of **p** and **I** using a **p** to **I** ratio of 1:2 (middle) and 3:1 (bottom) recorded at 298.2 K. In addition to the signals of **p-I** adduct atropisomers (α , β , γ , δ) the signals of the aqueous form (**w-I**) and that of the residual sp^2 **I** also emerge. For the signals of **p-I** atropisomers the spatial position of the represented fluorine atom is indicated in parenthesis.
*Signals of non-characterized contaminating compounds.

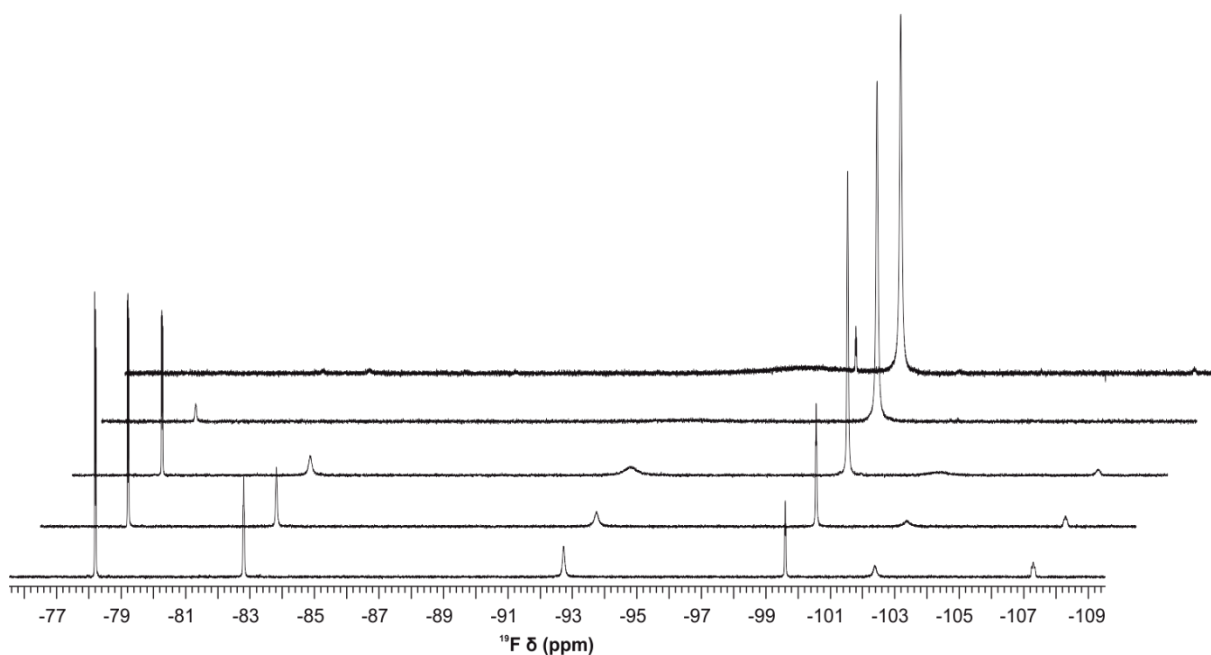


Figure S15. ^{19}F spectrum (376 MHz) of the mixture of **p** and **III** using a **p** to **III** ratio of 3:1 recorded at (from bottom to top) 243.2 K, 253.0 K, 273.0 K, 298.2 K and 323.0 K.

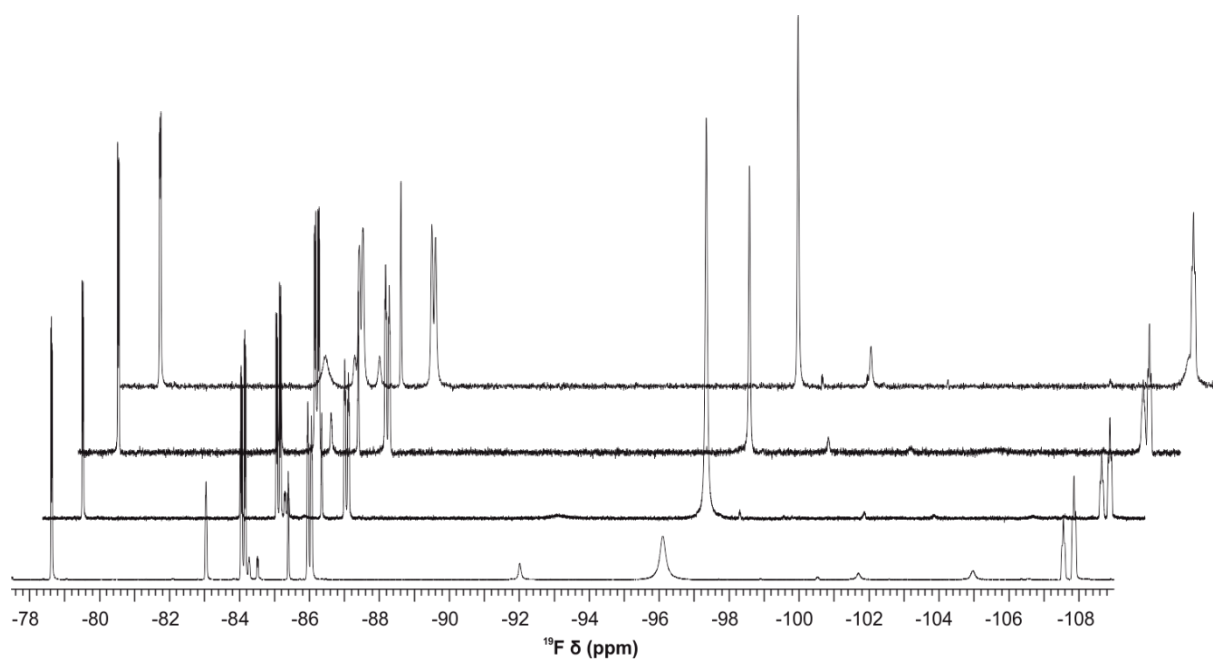


Figure S16. ^{19}F spectrum (564 MHz) of the mixture of **p** and **II** using a **p** to **II** ratio of 3:1 recorded at (from bottom to top) 243.2 K, 273.0 K, 298.2 K and 323.0 K.

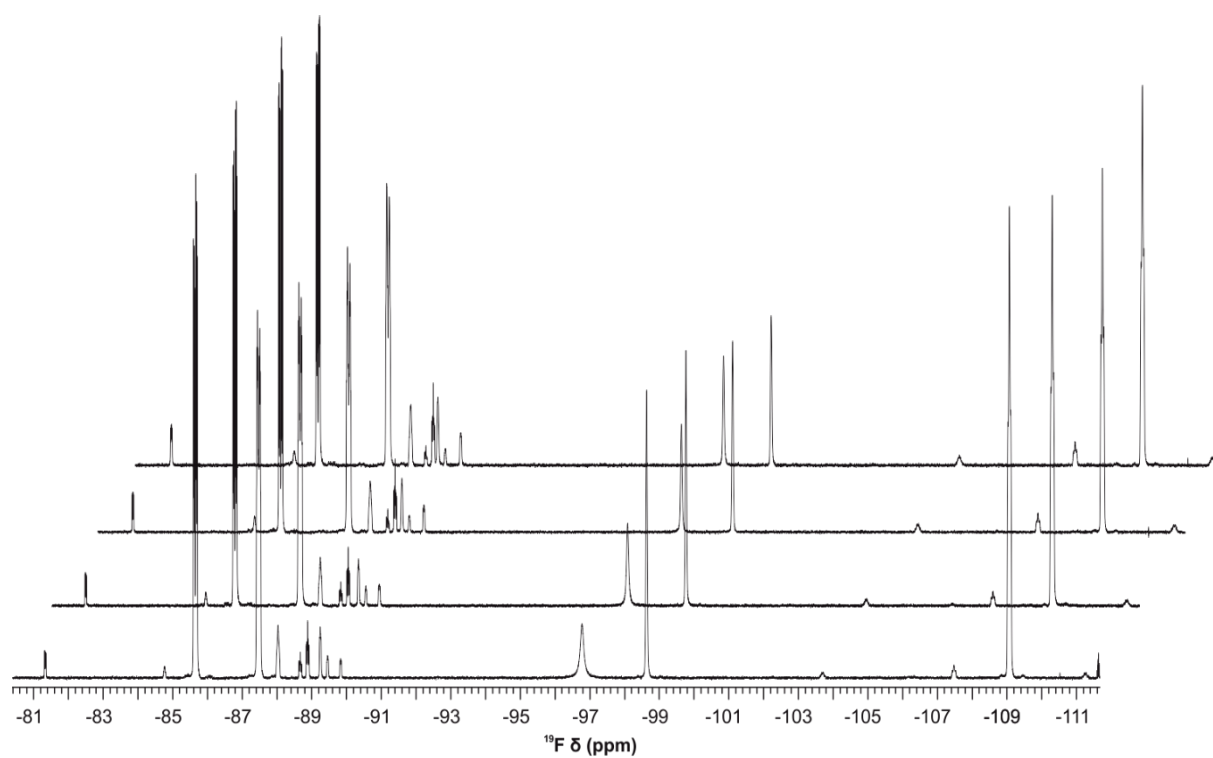


Figure S17. ^{19}F spectrum (564 MHz) of the mixture of **p** and **I** using a **p** to **I** ratio of 1:2 recorded at (from bottom to top) 243.2 K, 273.0 K, 298.2 K and 323.0 K.

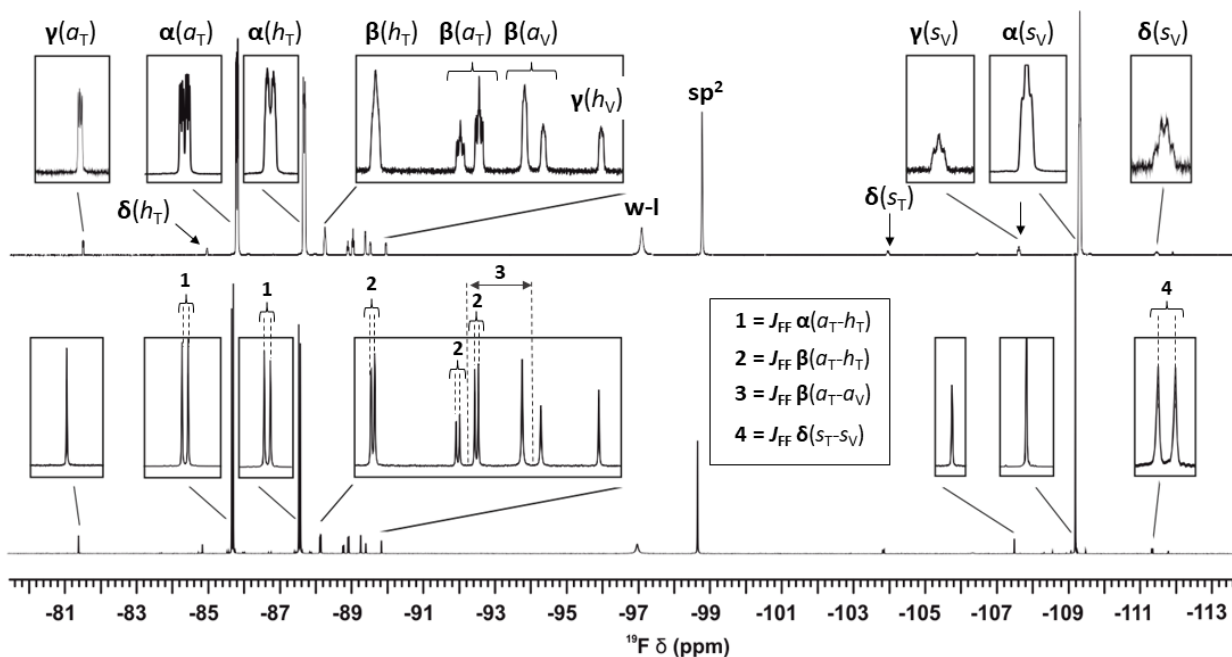


Figure S18. Single-pulse ^{19}F (top) and ^1H -decoupled ^{19}F (bottom) spectrum (564 MHz) of the mixture of **p** and **l** using a **p** to **l** ratio of 3:1 recorded at 298.2 K. In the ^1H -decoupled ^{19}F spectrum the fine structure of most signals simplifies into a singlet whereas those affected by through space ^{19}F - ^{19}F couplings (J_{FF}) display higher order fine structure. The obtained J_{FF} values are listed in Table S9 (Section 6).

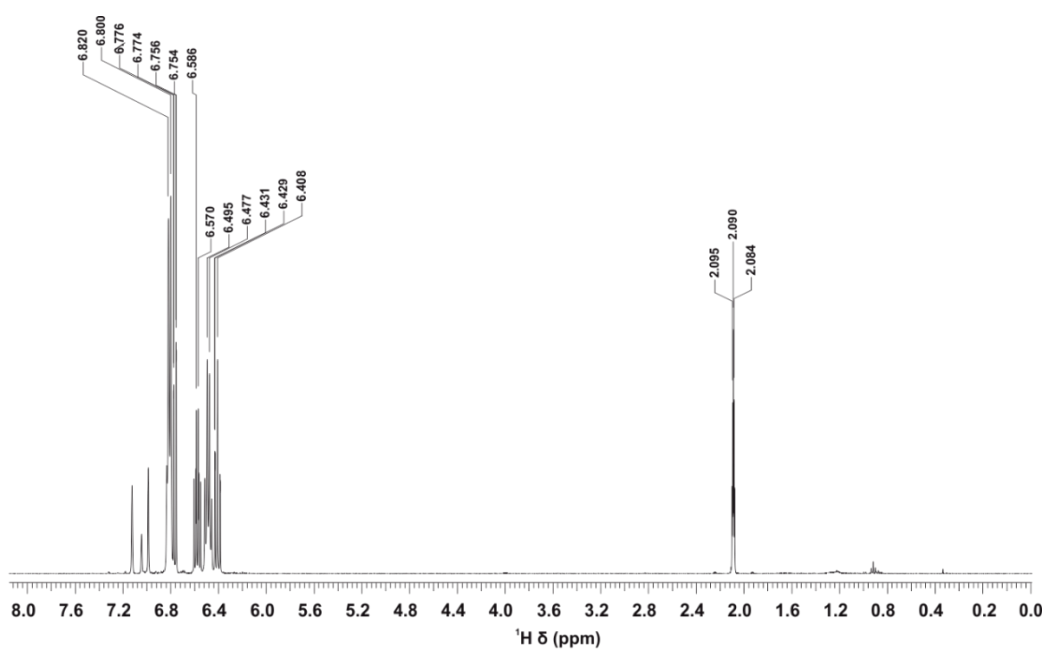


Figure S19. ^1H spectrum (400 MHz) of **III** at 243.2 K.

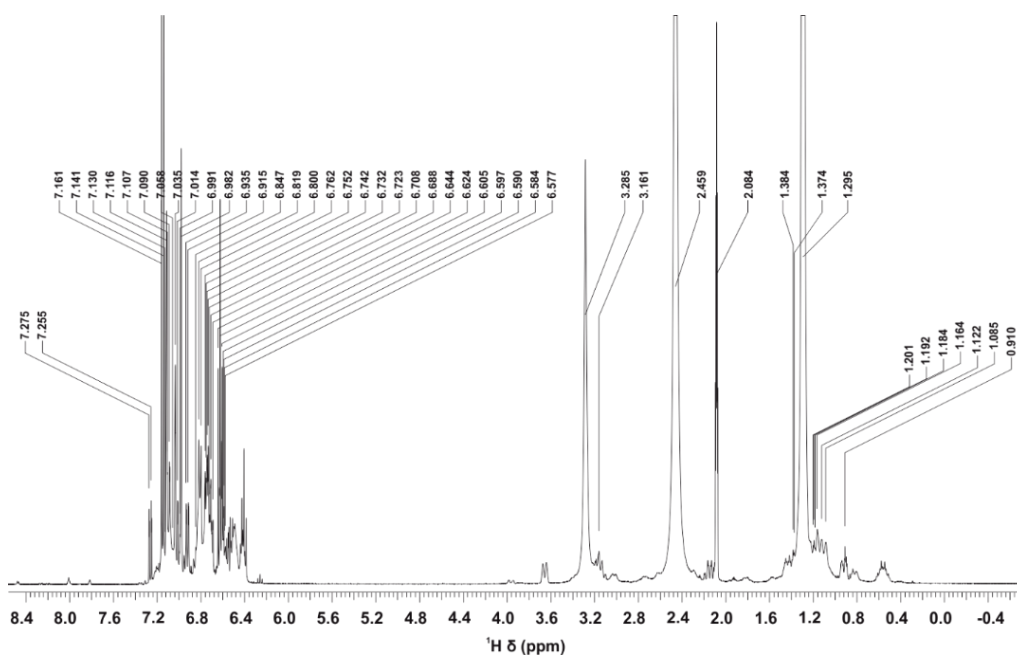


Figure S20. ^1H spectrum (400 MHz) of the mixture of **p** and **III** using a **p** to **III** ratio of 3:1 recorded at 243.2 K.

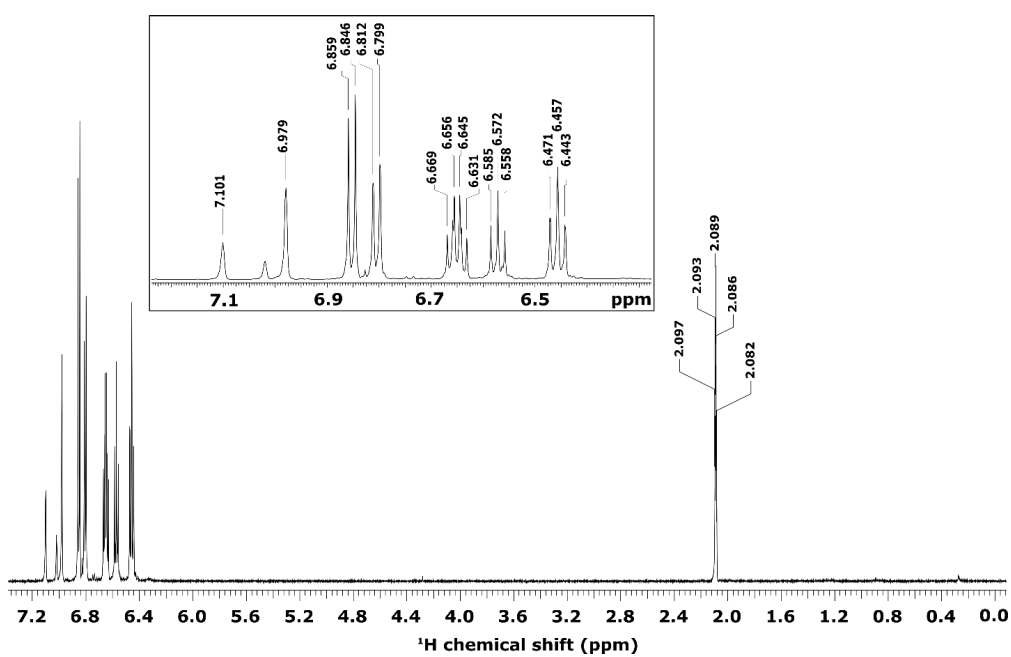


Figure S21. ^1H spectrum (600 MHz) of **II** recorded at 298.2 K.

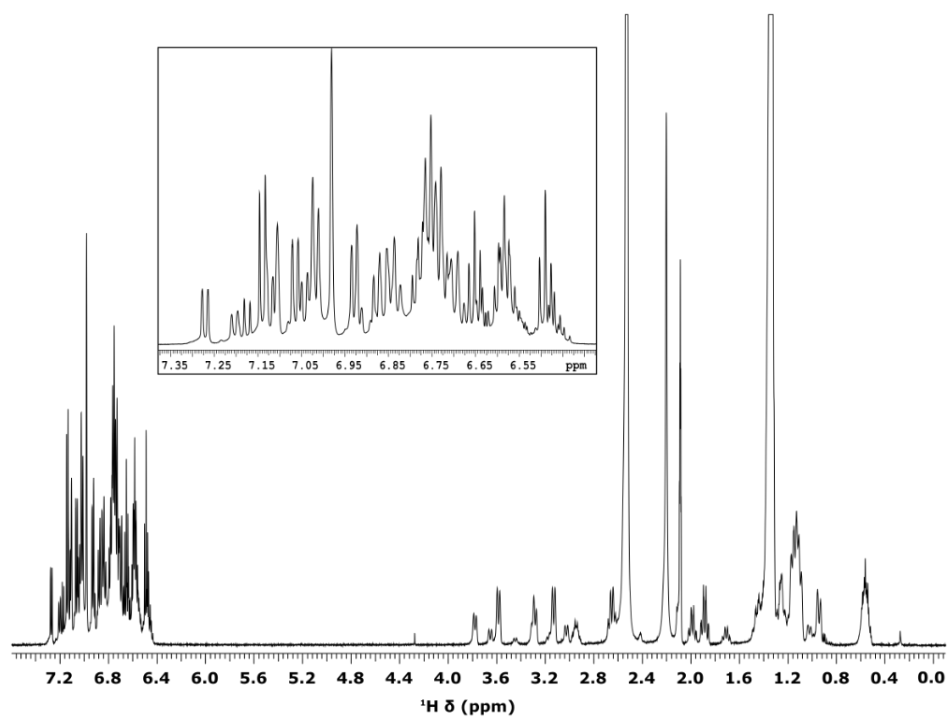


Figure S22. ^1H spectrum (600 MHz) of the mixture of **p** and **II** using a **p** to **II** ratio of 3:1 recorded at 298.2 K.

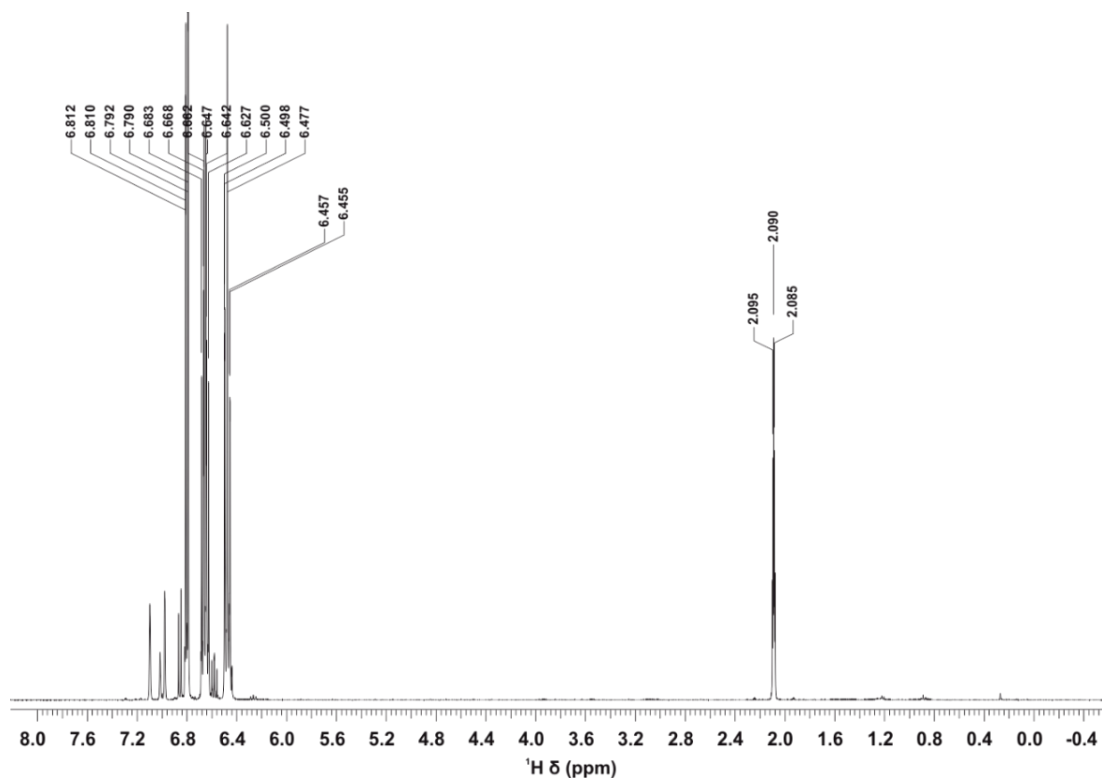


Figure S23. ^1H spectrum (600 MHz) of **I** recorded at 298.2 K.

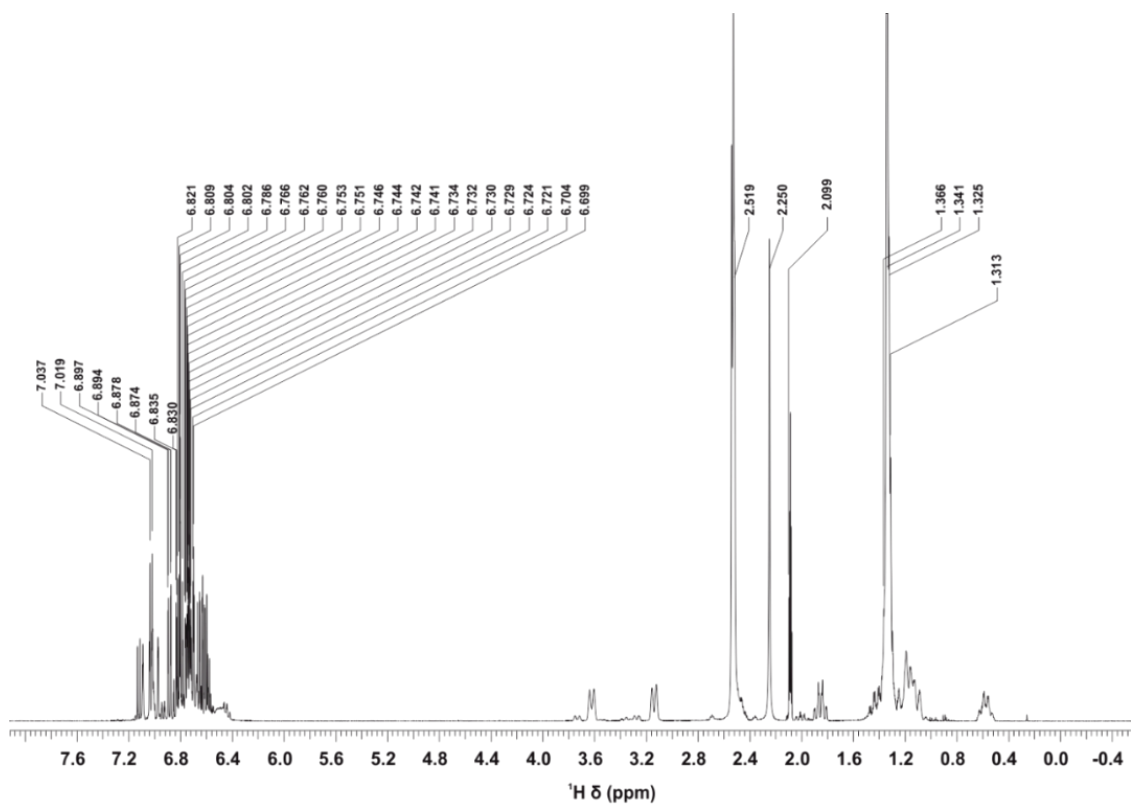


Figure S24. ^1H spectrum (600 MHz) of the mixture of **p** and **l** using a **p** to **l** ratio of 3:1 recorded at 298.2 K.

4. Computed Piperidine-Borane Adduct Structures

The electronic and steric interactions that emerge between **p** and respectively **I**, **II** and **III** define a uniform molecular shape for all the computed **p**-adduct structures. (Tables S4–S6) With respect to the equatorial B–N bond the three aryl rings adopt ‘horizontal’ (*h*), ‘tilted’ (*t*) and ‘vertical’ (*v*) orientations (Figure S25) based on the corresponding X–B–C_v–C_v’ torsion angles. In this particular molecular topology the N–H group of **p** forms hydrogen bonds with 1–1 halogen atom of both the tilted and vertical rings. We assigned these hydrogen bonding halogen atoms of the vertical and tilted rings as being in *syn* position with respect to the N–H bond (*syn*-vertical: *s_v*, *syn*-tilted: *s_T*) while their ortho-counterparts that point in the opposite direction were assigned as anti-positioned halogens (*a_v* and *a_T*). The distinction of the *syn* and *anti* positions on the vertical and tilted aryl rings was motivated by the remarkably distinct ¹⁹F NMR properties the fluorine atom displays upon hydrogen bonding compared to the situation when the ortho-Cl atom interacts with the N–H group instead. The horizontal ring is oriented almost perpendicularly with respect to the B–N bond. This creates steric clash (back-strain) between the *horizontal* and *anti* halogen atoms. Due to the differences in the emerging steric hindrance, we further distinguished the two *horizontal* halogen ligands of the computed **p**-adduct structures based on whether they point towards the vertical (*h_v*) or the tilted (*h_T*) aryl ring.

The atropisomers of **p-I**, **p-II** and **p-III** are thus defined based on their unique F/Cl atom distributions between the six possible halogen atom positions in space being *s_v*, *s_T*, *a_v*, *a_T*, *h_v* and *h_T*. By permutation, only considering the ring rotations, this yields 8, 12, and 6 plausible atropisomers in total for **p-I**, **p-II** and **p-III**, respectively. Our conformational search found most of these as 6, 7 and 4 atropisomers of **p-I**, **p-II** and **p-III**, respectively, were computed. We found that the missing structures impose unfavored interactions that the system can overcome with relative ease by minor rearrangements. For example, while the orientations *h*, *t* and *v* are defined at the point of complex formation, small conrotation (<30°) of rings *t* and *v* is still allowed and can switch them. This means the interaction with the nearby N–H group can induce rearrangement in the initial conformation search process and neglects the energetically less stable state. In the computed structures the fluorine in *syn* position is typically allocated to the vertical ring (*s_v*). This arrangement provides short N–H⋯F distance (~1.9 Å) and acceptable arrangement between the fluorine and the amine group to form a hydrogen bond which stabilizes the local geometry and rigidifies the vertical ring. When this fluorine is rotated away to the *s_T* position, it is less capable of interaction due to its larger N–H⋯F distance (>2.0 Å) and an acute angle, sub-optimal for a hydrogen bond. Moreover, the chlorine atom, which is concurrently pushed to the *s_v* position, can only form a much weaker hydrogen bond. Concomitantly, the ring with the tilted orientation shows preference for the fluorine atom to be in the anti-position (*a_T*). This also alleviates the back-strain emerging primarily between the highly congested *h_T*, *a_T* and *a_v* positions. As the *a_T* halogen is exposed to the steric repulsion from both the *h_T* and *a_v* ligands the smaller van der Waals radius of the fluorine atom than that of the chlorine atom mitigates the steric congestion. Based on these, a fluorinated ring with its F atom in the unfavored *s_T* or *a_v* position is expected to converge into the respective more stable *s_v* or *a_T* position. This explains the absence of computed structures that would display a fluorine in the *s_T* and/or *a_v* positions unless, as shown by particular **p-I**, and **p-II** structures, both *syn* (**p-I(δ)**, **p-I(6)**, **p-II(5)**) or indeed, *anti* positions (**p-I(β)**, **p-I(5)**, **p-II(4)**) are occupied by F atoms.

Notably, amongst the computed **p**-adduct structures several atropisomer pair(s) are defined that mutually differ in the phase of the horizontal fluorinated ring, that is, whether the fluorine ligand is in the *h_T* or the *h_v* position. This being the case for the **α/γ**, **β/5**, and **δ/6** atropisomer pairs of **p-I**; the **α/6** and **γ/5** atropisomer pairs of **p-II**; and the **β** vs **γ** atropisomers of **p-III**. Uniformly, of these atropisomer pairs the one with the fluorine placed in the *h_T* rather than the *h_v* position shows more stable by at least 1.7 kcal mol⁻¹ according to the computations. This, again, is due to the high steric congestion between the *h_T*, *a_T* and *a_v* positions which is mitigated when the asymmetrically halogenated horizontal ring places its fluorine ligand in the *h_T* position, while the chlorine atom in the *h_v* position is allowed to take up more space next to the vertical ring.

We also note that our conformational search provided plausible, albeit relatively less-stable conformers for the **p-I** system in which the B–N bond is axial.

Table S4. The computed atropisomers of **p-III** along with their G_a and ΔG^a values at 243.15 K. The diverse atropisomeric states are designated with Greek letters which refer to the order of their detected stability with the α -state being the most abundant atropisomeric state. The non-detected atropisomer is designated as **p-III(4)**. Cl: green, F: blue, B: pink, N: purple, C: gray, H: white. To guide the eye, the F-atom is highlighted by an arrow for each structure. The respective F atom positions are specified according to the scheme in Figure 6 in the main text.

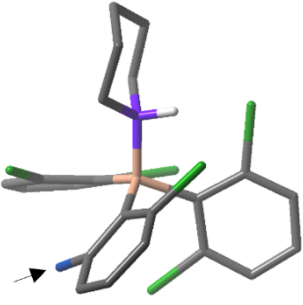
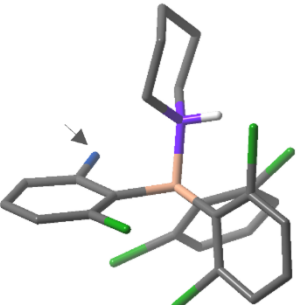
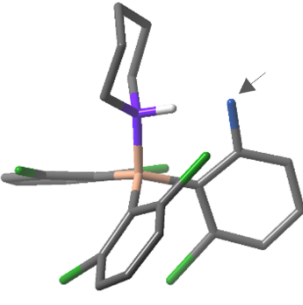
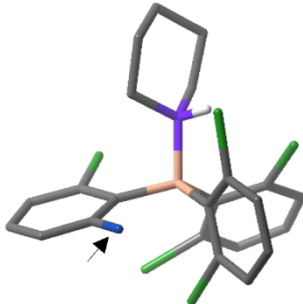
		p-III		
Atropisomer		α	β	γ
Structure				
F-positions		a_T	h_T	s_V
G_a / hartree		-3365.1224	-3365.1229	-3365.1211
ΔG^a / kcal·mol ⁻¹		-0.1	-0.3	0.8
Atropisomer		4		
Structure				
F-positions		h_V		
G_a / hartree		-3365.1178		
ΔG^a / kcal·mol ⁻¹		2.8		

Table S5. The computed atropisomers of **p-II** along with their G_a and ΔG^a values at 243.15 K. The diverse atropisomeric states are designated with Greek letters which refer to the order of their detected stability with the α -state being the most abundant atropisomeric state. The non-detected atropisomers are designated with numbers. Cl: green, F: blue, B: pink, N: purple, C: gray, H: white. To guide the eye, the F-atoms are highlighted by arrows. The respective F atom positions are specified according to the scheme in Figure 6 in the main text.

p-II			
Atropisomer	α	β	γ
Structure			
F-positions	$h_T + a_T$	$s_V + a_T$	$h_T + s_V$
G_a / hartree	-3005.1388	-3005.1379	-3005.1384
ΔG^a / kcal·mol ⁻¹	-6.0	-5.5	-5.8
Atropisomer	4	5	6
Structure			
F-positions	$a_T + a_V$	$s_T + s_V$	$a_T + h_V$
G_a / hartree	-3005.1366	-3005.1348	-3005.1347
ΔG^a / kcal·mol ⁻¹	-4.7	-3.5	-3.4
Atropisomer	7		
Structure			
F-positions	$s_V + h_V$		
G_a / hartree	-3005.1344		
ΔG^a / kcal·mol ⁻¹	-3.3		

Table S6. The computed atropisomers of **p-I** along with their G_a and ΔG^a values at 243.15 K. The diverse atropisomeric states are designated with Greek letters which refer to the order of their detected stability with the α -state being the most abundant atropisomeric state. The non-detected atropisomers are designated with numbers. Cl: green, F: blue, B: pink, N: purple, C: gray, H: white. To guide the eye, the F-atoms are highlighted by arrows. The axial arrangement of the lone electron pair of N (7, 8, 9) is clearly less favored than the equatorial (α , β , γ , δ , 5, 6) in these structures. The respective F atom positions are specified according to the scheme in Figure 6 in the main text.

				p-I		
Atropisomer	α	β	γ	δ	5	6
Structure						
F-positions	$h_T + a_T + s_V$	$h_T + a_T + a_V$	$h_V + s_V + a_T$	$h_T + s_T + s_V$	$a_T + a_V + h_V$	$s_T + s_V + h_V$
G_a / hartree	-2645.1544	-2645.1516	-2645.1509	-2645.1513	-2645.1489	-2645.1470
ΔG^a / kcal·mol ⁻¹	-12.4	-10.6	-10.1	-10.4	-8.9	-7.7
Atropisomer						
Structure						
F-positions	$s_V + a_T + h_T$	$s_T + s_V + h_T$	$h_V + s_V + a_T$			
G_a / hartree	-2645.1426	-2645.1401	-2645.1380			
ΔG^a / kcal·mol ⁻¹	-5.0	-3.4	-2.0			

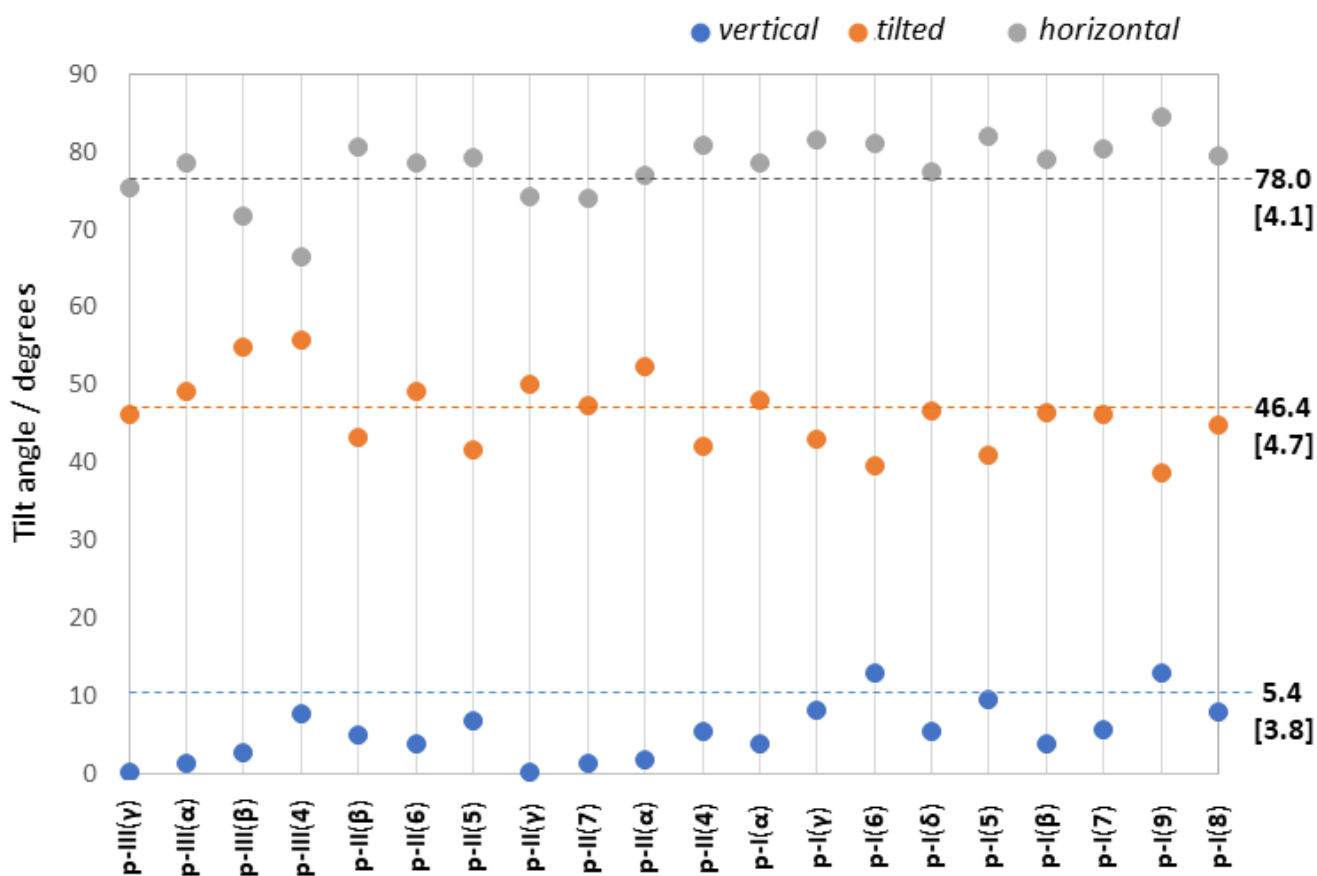


Figure S25. The tilt angles of the three borane aryl rings in the dative **p**-adduct structures. The tilt angles were defined by the X-B-C_γ-C_γ' atoms. For each structure, the three aryl rings feature remarkably distinct tilt angles averaging respectively ~5°, ~46° and ~78° such that they unambiguously define the *vertical*, *tilted* and *horizontal* ring orientations. The average tilt angle values are indicated with their standard deviations in parenthesis.

5. ^{19}F Chemical Shift Calculations

Chemical shielding factors were obtained with the default GIAO method^[33] for each computed sp^2 borane and p -adduct structure with equatorial B–N bond at the B3LYP-D3/6-311+G(2d,p) level of theory. The theoretical ^{19}F chemical shifts (σ^{C}) were calculated using the chemical shielding obtained for CFCl_3 . (Figure S26 and Tables S7–S8) In the obtained ~ 40 ppm ^{19}F chemical shift window the sp^2 state and the three distinct fluorine atom positions in the p -adduct structures being *horizontal*, *anti* or *syn* define their respective domains with the general order of *syn* < sp^2 < *horizontal* < *anti*. This assessment aided us in the interpretation of the p + borane mixtures' ^{19}F spectra and the assignment of the computed structures. (Section 6) When the corresponding computed and experimental (σ^{E}) ^{19}F chemical shifts of the detected structures are compared (Tables S7–S8) we notice that the computed values show consistently lower by 10–20 ppm than the corresponding experimental ^{19}F chemical shifts. This emerges because these chemical shift calculations were performed in vacuum. Regardless, as shown in Figure S30 the great correlation between their σ^{C} and σ^{E} values supports the assignment of the detected p -atropisomers to the computed structures.

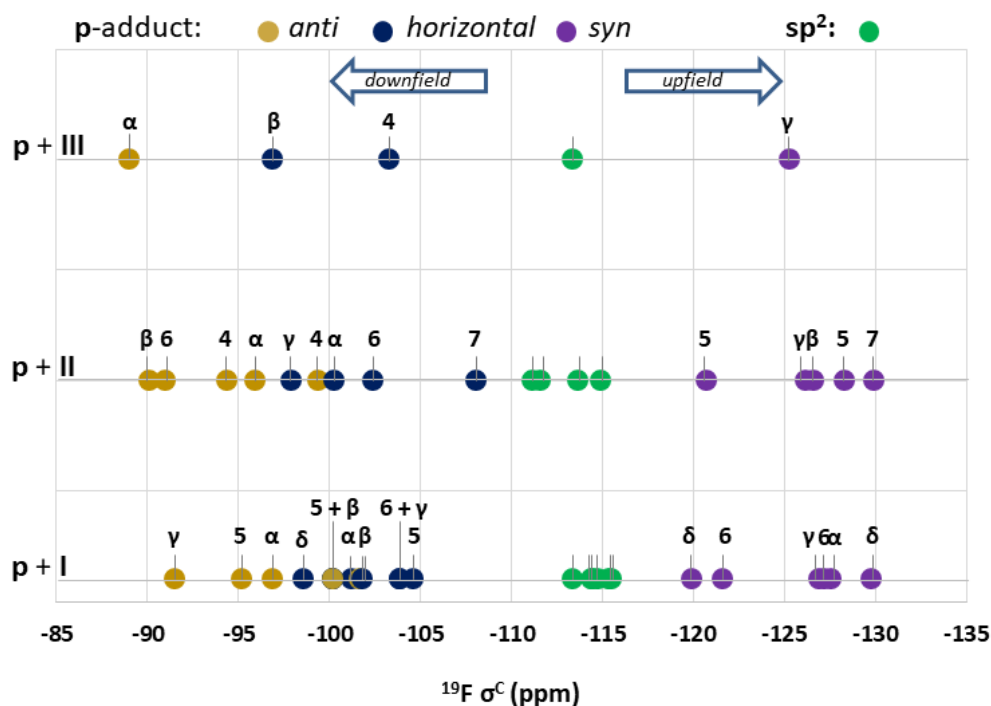


Figure S26. The computed ^{19}F chemical shifts (σ^{C}) of the sp^2 borane and p -adduct atropisomer structures. (Tables S8 and S9) The computed sp^2 signals are shown in green. The p -adduct signals are assigned with the corresponding atropisomeric state whereas the color coding specifies the spatial position of the fluorine atom.

Table S7. The computed (σ^{C}) and experimental (σ^{E}) ^{19}F chemical shifts per borane structure.

Structure	σ^{C} (F1) / ppm	σ^{C} (F2) / ppm	σ^{C} (F3) / ppm	σ^{E} / ppm
III(α) ^[a]	-113.4			-99.6 (sharp multiplet, Figure S9)
II(α)	-111.2	-114.9		-99.3 (broad, Figure S10)
II(β)	-111.6	-111.6		
II(γ)	-113.7	-113.7		
I(α)	-113.4	-114.4	-115.5	-100.8 (sharp multiplet, Figure S11)
I(β)	-114.5	-114.8	-115.4	

[a] Values obtained at 243.2 K rather than 298.2 K.

Table S8. The computed (σ^C) and experimental (σ^E) ^{19}F chemical shifts per **p**-adduct structure.

Structure	Detected atropisomer?	F1			F2			F3		
		Position	σ^C / ppm	σ^E / ppm	Position	σ^C / ppm	σ^E / ppm	Position	σ^C / ppm	σ^E / ppm
p-III(α) ^[a]	yes	a_T	-89.0	-78.3						
p-III(β) ^[a]	yes	h_T	-96.9	-82.9						
p-III(γ) ^[a]	yes	s_V	-125.3	-107.3						
p-III(4) ^[a]	no	h_V	-103.3							
p-II(α)	yes	a_T	-95.9	-85.0	h_T	-100.3	-86.9			
p-II(β)	yes	a_T	-90.1	-79.4	s_V	-126.6	-108.8			
p-II(γ)	yes	h_T	-97.9	-83.9	s_V	-126.2	-108.5			
p-II(4)	no	a_T	-94.4		a_V	-99.4				
p-II(5)	no	s_T	-120.7		s_V	-128.3				
p-II(6)	no	a_T	-91.0		h_V	-102.4				
p-II(7)	no	h_V	-108.1		s_V	-129.9				
p-I(α)	yes	a_T	-96.9	-85.8	h_T	-101.2	-87.6	s_V	-127.6	-109.1
p-I(β)	yes	a_T	-100.2	-88.9	a_V	-101.7	-89.5	h_T	-101.8	-88.1
p-I(γ)	yes	a_T	-91.5	-81.4	h_V	-103.9	-90.0	s_V	-126.9	-107.6
p-I(δ)	yes	h_T	-98.6	-84.9	s_T	-119.9	-103.7	s_V	-129.8	-111.3
p-I(5)	no	a_T	-95.2		a_V	-100.2		h_V	-104.6	
p-I(6)	no	h_V	-103.9		s_T	-121.6		s_V	-127.2	

[a] Values obtained at 243.2 K rather than 298.2 K.

6. ^{19}F Signal Assignment and Structure Validation

In the slow-exchange regimes the ^{19}F NMR spectra of the **p+I**, **p+II** and **p+III** mixtures showed uniform trends in ^{19}F signal characteristics. As detailed in the following, three distinct types of ^{19}F signals could be observed throughout which we correlated with the proposed *horizontal*, *syn* or *anti* spatial position of the fluorine atom. (Figure S27)

The ^{19}F signals of the **p**-adducts appear normally below -107 ppm (upfield-shifted region) or above -90 ppm (downfield-shifted region). The only exception from this was made by a signal in the ^{19}F spectrum of the **p+I** mixture (i.e. -103.7 ppm at 298.15 K) that could be assigned to the *h*-positioned fluorine of the **p-I**(δ) atropisomer. (Figure S14) Nevertheless, it was clear that in the **p**-adducts the fluorine(s) display their ^{19}F signals at remarkably distinct frequencies than in the sp^2 borane states (~ -100 ppm, see for **p+III**: Figure S12, **p+II**: Figure S13, **p+I**: Figure S14) which reflects their adduction with **p**. In all cases, the number of **p**-adduct ^{19}F signals (**p+III**: 3, **p+II**: 6, **p+I**: 12) showed a multiple of the respective number of fluorine atoms (**p+III**: 1, **p+II**: 2, **p+I**: 3) suggesting the formation of respectively 3, 3 and 4 atropisomers of **p-III**, **p-II** and **p-I**. Indeed, in the **p**-adduct state the fluorines of the multifluorinated compounds **I** and **II** are chemically nonequivalent as each is represented by a distinct ^{19}F signal whereas in the sp^2 state the boranes feature a single weighted-average ^{19}F signal. This points towards the rigidity of the aryl rings in the dative **p**-adducts in contrast to their free rotation at NMR timescale in the sp^2 state.

The computed ^{19}F chemical shifts (Section 5) revealed that for any **p**-adduct atropisomer the ^{19}F signal of a *syn* positioned F atom is expected to show up in the upfield-shifted region exclusively, while the downfield-shifted ^{19}F signal region shall be populated by those of *horizontal* and *anti*-positioned F atoms. This was supported through ^{19}F - ^1H HOESY measurements^[17] performed for the **p+II** (Figure S28) and **p+I** (Figure S29) systems. In the obtained ^{19}F - ^1H HOESY spectra the upfield-shifted ^{19}F signals are correlated with many **p** hydrogen resonances including those of the alkyl 2- CH_2 as well as 3- CH_2 groups (as defined in Figure 6 in the main text) in addition to the N-H proton (H^{N}). This means that a fluorine with upfield-shifted signal is found in the vicinity to most part of the **p** ring while it is also in contact with the N-H group itself. The interaction with the H^{N} spin explains the overall enhanced electronic shielding, and also, the exceptionally high ^{19}F - ^1H *J*-couplings of 20–25 Hz that inflict apparent signal broadenings on the upfield-shifted ^{19}F signals of all the **p**-adducts.^[18] All these confirm that the upfield-shifted ^{19}F signals indeed represent fluorine atoms in *syn* spatial position. The downfield-shifted ^{19}F signals of the **p-I** and **p-II** adducts are either correlated with **p** hydrogens limited to 2- CH_2 group(s) or do not show any correlation with **p** ^1H frequencies at all. These two distinct ^{19}F - ^1H HOESY patterns distinguish the proposed *horizontal* and *anti* fluorine positions. Indeed, as in the *horizontal* position the fluorine atom is on the opposite side of the **p** ring than the N-H bond, only particular 2- CH_2 protons remain sufficiently close to establish ^{19}F - ^1H HOESY contacts. In the *anti* positions, however, the fluorine is too far from the **p** ring to generate any ^{19}F - ^1H HOESY cross-peaks above the level of detection but with neighboring aromatic protons. The ^{19}F signal fine structure turned out to be characteristic in the *horizontal* and *anti* positions as well. That is, the *horizontal* ^{19}F signals are typically broader and lack any complex fine structure, while those of *anti* fluorines show sharp multiplets complexified by multiple ^{19}F - ^1H *J*-couplings (of 5–12 Hz) that arise between the fluorine and the aromatic proton spins of the same borane ring. Apart from recognizing the correlations in the frequency, linewidth, and fine structure of the ^{19}F signals with the atom allocated to the *syn*, *horizontal* or *anti* positions, their detailed explanation did not constitute the goal of this work.

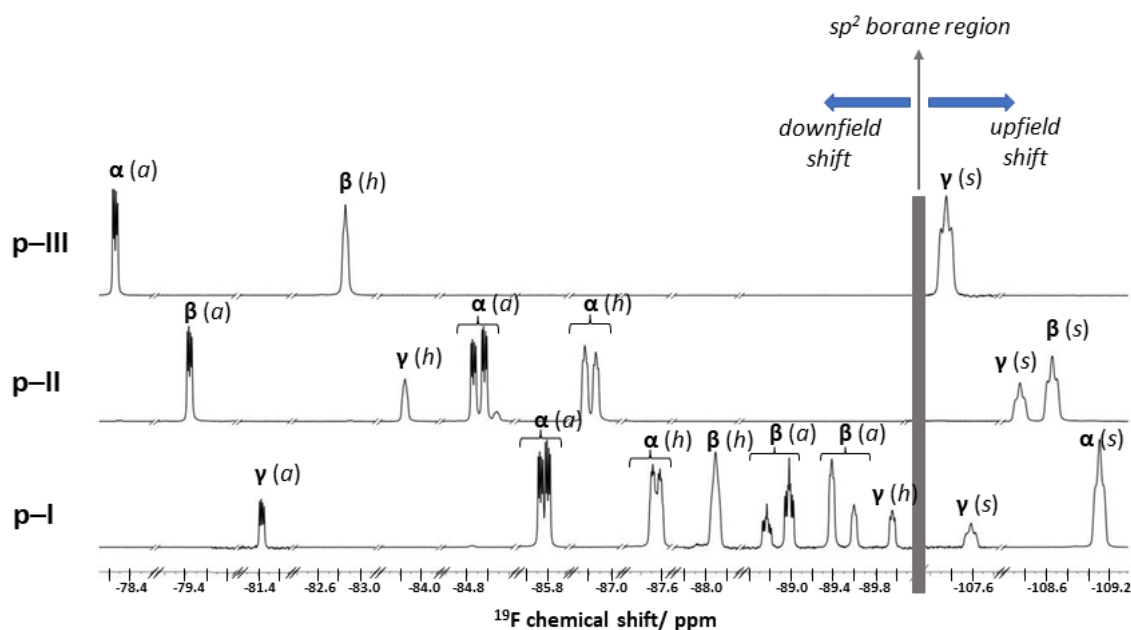


Figure S27. The ^{19}F signals (376 MHz) of the **p-I**, **p-II** and **p-III** adducts at 243.2 K. For the best visibility of the peak fine structures the signal intensities were rescaled arbitrarily. The spatial position of the represented fluorine atom is indicated for each **p**-adduct atropisomer signal in parenthesis. Here, the **p-I**(δ) signals are omitted for clarity, but they are shown in Figure S14.

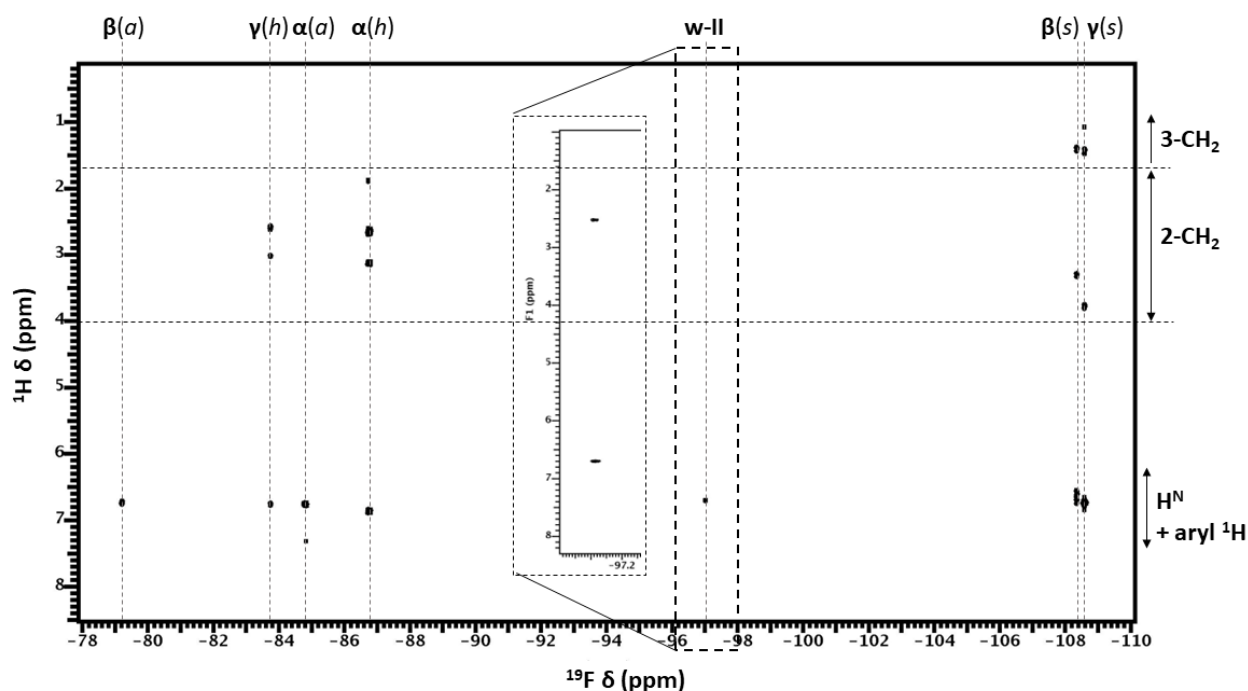


Figure S28. The ^{19}F - ^1H HOESY spectrum of the **p-II** system using a **p** to **II** ratio of 3:1. The spectrum was recorded at 283.0 K with the mixing time of 60 ms. The cross-peaks are assigned to the diverse atropisomeric states (Greek letters) of **p-II** along the ^{19}F dimension. The spatial position of the represented fluorine atom is indicated in parenthesis. Along the ^1H dimension the distinct chemical shift ranges of the 3- CH_2 , 2- CH_2 and H^{N} groups of **p** are shown explicitly. *Inset*: magnifying the signal intensities along the ^{19}F frequency of the aqueous **w-II** complex (Section 9) reveals a correlation with particular alkyl **p** protons frequencies.

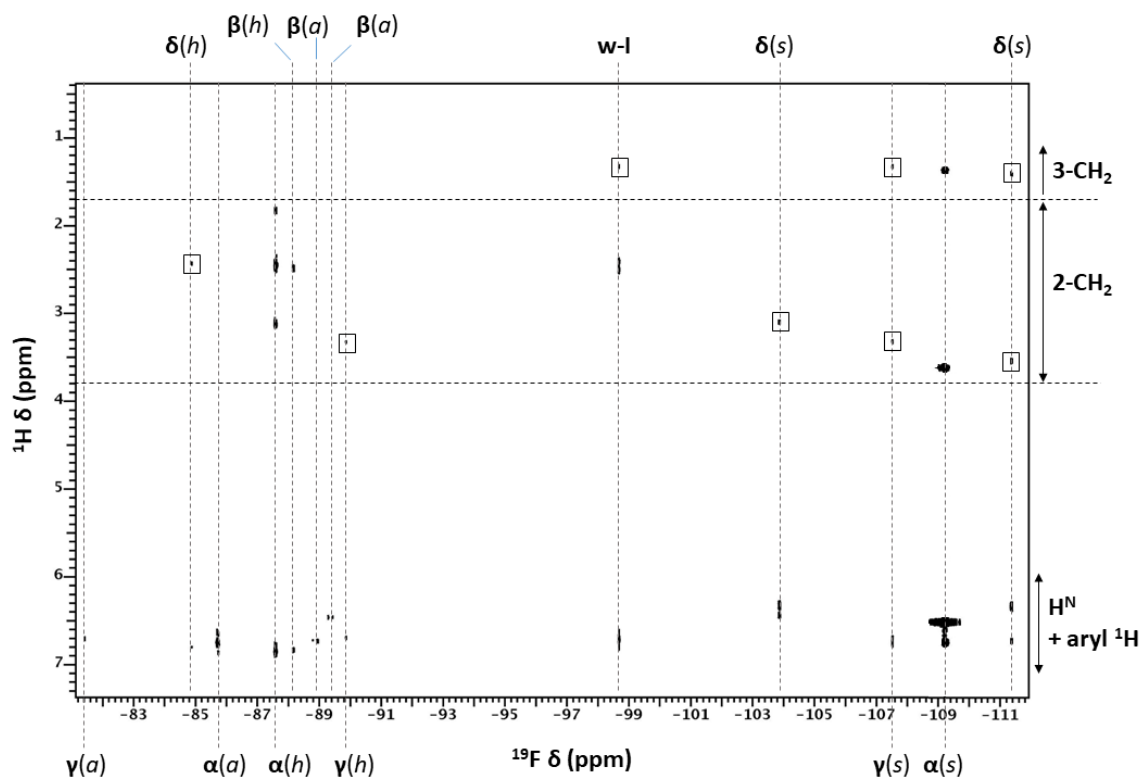


Figure S29. The ^{19}F - ^1H HOESY spectrum of the **p-I** system using a **p** to **I** ratio of 3:1. The spectrum was recorded at 273.0 K with the mixing time of 400 ms. The cross-peaks are assigned to the diverse atropisomeric states (Greek letters) of **p-I** along the ^{19}F dimension. The spatial position of the represented fluorine atom is indicated in parenthesis. Along the ^1H dimension the distinct chemical shift ranges of the 3- CH_2 , 2- CH_2 and H^{N} groups of **p** are shown explicitly. Certain cross-peaks of the low abundance γ and δ atropisomers are highlighted with squares for clarity. Notably, the ^{19}F signal of the aqueous **w-I** complex (Section 9) is correlated with particular alkyl **p** proton frequencies.

Identifying the ^{19}F NMR signals of the **p-I**, **p-II** and **p-III** adducts with the proposed *syn*, *horizontal* or *anti* spatial position of the represented fluorine atom allowed us to assign their respective sets of atropisomers to the computed structures. That is, the three slow exchanging ^{19}F signals of the **p-III** adduct (Figure S27) display an *anti*, a *horizontal*, and a *syn* positioned fluorine, respectively, thus, the three **p-III** atropisomers could be respectively assigned to the computed **p-III(α)**, **p-III(β)** and **p-III(γ)** structures. The second most abundant atropisomer of the **p-II** adduct features two ^{19}F signals that represent an *anti*, and a *syn* fluorine, respectively, thus, it could be assigned to the computed **p-II(β)** structure etc. Note that based on ^{19}F chemical shift, peak width and ^1H - ^{19}F coupling arguments it was not possible to specify whether the fluorinated horizontal ring points the F atom towards the vertical (h_{V}) or the tilted (h_{T}) aryl ring. As discussed in Section 4, however, for these **p**-borane adducts a more stable conformation is expected to form with the F atom being placed in the h_{T} rather than the h_{V} position. By exploiting the presence of through space (TS) ^{19}F - ^{19}F J -couplings (J_{FF}) this could be confirmed experimentally for multiple **p-II** (Figure 5) and **p-I** atropisomers (Figure S18). The emerging TS $J_{\text{FF-s}}$ reflect the spatial vicinity of the coupled ^{19}F nuclei.^[19] In our systems TS $J_{\text{FF-s}}$ could be observed between *horizontal-anti*, *anti-anti* or *syn-syn* fluorine pairs. (Table S9) That is, the two signals of the **p-II(α)** atropisomer are both split by the large TS J_{FF} of 39.5 Hz as a result of the spatial vicinity (2.5 Å in the computed structure) of the α_{T} - and h_{T} -positioned fluorines. Indeed, in the h_{V} position (see the non-detected **p-II(β)** structure in Table S5) the horizontal fluorine would be found too distant (~ 5 Å) from the α_{T} fluorine to generate measurable TS J_{FF} . Furthermore, the detected **p-I(α)** and **p-I(γ)** atropisomers both feature the combination of 1 α_{T} , 1 s_{V} and 1 *horizontal* fluorine but differ from each other in the h_{T} or h_{V} direction of the latter. Again, the spatial vicinity of the α_{T} - and h_{T} -positioned fluorines (2.6 Å) in the **p-I(α)** atropisomer is reflected by their large TS J_{FF} of 26.4 Hz. In contrast, the isolated fluorine atoms (α_{T} , s_{V} , h_{V}) of the **p-I(γ)** atropisomer do not show any measurable TS J_{FF} . Additional large TS $J_{\text{FF-s}}$ could be detected for the **p-I(β)** and **p-I(δ)** atropisomers (Table S9) which confirm the spatial vicinity of their respective *syn-syn* and *anti-anti* fluorine pairs. For these atropisomers, however, the particular TS J_{FF} with the horizontal fluorine does not specify its h_{T} or h_{V} direction due to the symmetry of the F/Cl distribution on the vertical and tilted rings.

All in all, using ^{19}F NMR spectroscopy and energetic arguments derived from the computations we could unambiguously assign the detected 4, 3 and 3 atropisomers of **p-I**, **p-II** and **p-III**, respectively, to the corresponding computed structures. Our assignment is further supported by the overall good agreement between the experimental and the computed conformational distributions (Table S10) as well as ^{19}F chemical shift data (Figure S30).

Table S9. The *through space* (TS) ^{19}F - ^{19}F scalar couplings (J_{FF}) detected for particular **p-I** and **p-II** atropisomers. The values were obtained from the corresponding ^1H -decoupled ^{19}F spectra (**p-I**: Figure S18, **p-II**: Figure 5).

p-adduct (atropisomer)	Coupled F-pair	Value of TS J_{FF} (Hz)
p-II (α)	$a_{\text{T}} - h_{\text{T}}$	39.5
p-I (α)	$a_{\text{T}} - h_{\text{T}}$	26.4
p-I (β)	$a_{\text{T}} - h_{\text{T}}$	15.3
p-I (β)	$a_{\text{T}} - a_{\text{V}}$	80.0
p-I (δ)	$s_{\text{T}} - s_{\text{V}}$	20.2

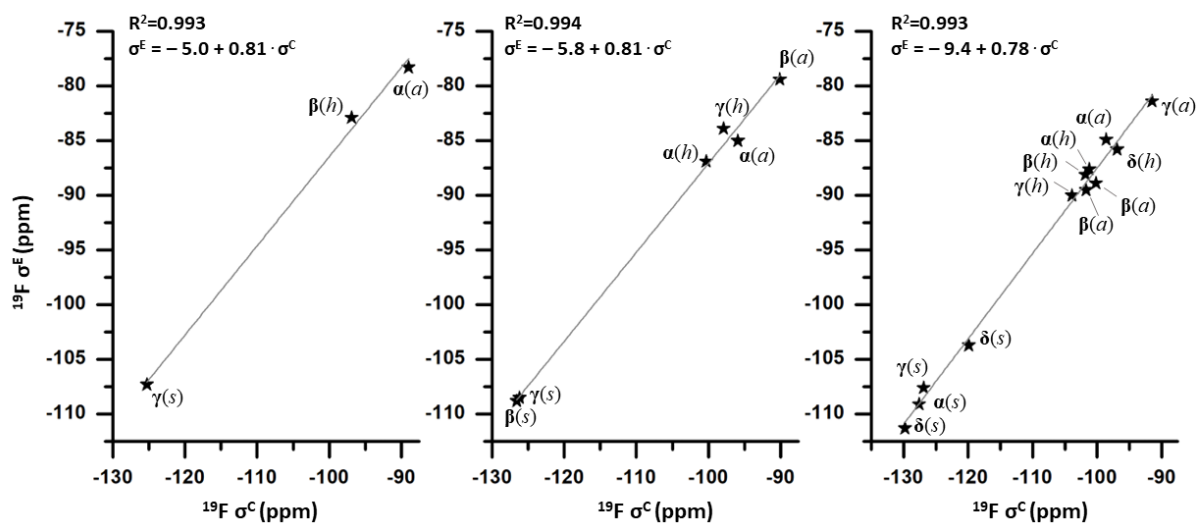


Figure S30. The correlation between the computed (δ^{C}) and the experimental (δ^{E}) ^{19}F chemical shifts of the detected **p**-adduct atropisomers. The values were obtained at 243.2 K for **p-III** and at 298.2 K for both **p-II** and **p-I**. The spatial position of the fluorine atom is marked in parenthesis.

Table S10. The experimental (P^E) and computed (P^C) conformational distributions of the three investigated **p**-borane adducts at 243.2 K. The P^E values were obtained from the corresponding ^{19}F signal integrals. The P^E values were calculated as described in Section 1.2.

p -borane adduct	Detected atropisomers (fluorine spatial positions)	P^E (%)	P^C (%)
p-III	p-III(α) (a_T)	61.2	32.3
	p-III(β) (h_T)	29.7	61.7
	p-III(γ) (s_V)	9.1	6.0
p-II	p-II(α) (a_T, h_T)	50.8	52.5
	p-II(β) (a_T, s_V)	29.7	16.3
	p-II(γ) (h_T, s_V)	19.5	31.2
p-I	p-I(α) (a_T, s_V, h_T)	85.2	94.8
	p-I(β) (a_T, a_V, h_T)	9.5	2.5
	p-I(γ) (a_T, s_V, h_V)	3.2	1.0
	p-I(δ) (s_V, s_T, h_T)	2.1	1.7

7. Kinetic and Thermodynamic Studies Using ^{19}F -EXSY

p+III system: In the mixture of **p** and **III** at 253.0 K the **p-III(α)** atropisomer does not show exchange with other species while the **p-III(β)** and **p-III(γ)** atropisomers show complete dissociation and interconversion into each other as well. The dissociation of both **p-III(β)** and **p-III(γ)** is much faster than their conversion into one another. The two aqueous forms of **p+III** (**w-III** and **w-III'**, see Section 9) show exchange with each other only. (Figure S31) The exchange rate (k_{ex}) values of these processes are collected in Table S11.

Table S11. Exchange rates (k_{ex}) of the species in the mixture of **p** and **III** at 253.0 K. The distinct atropisomers of **p-III** are indicated with Greek letters whereas the aqueous forms of **p** and **III** are indicated with **w** and **w'**.

p+III system	Dissociation and reassociation of p-III				Conformational interconversions of p-III		Exchanges of the aqueous forms of p+III	
	$\beta \rightarrow \text{sp}^2$	$\text{sp}^2 \rightarrow \beta$	$\gamma \rightarrow \text{sp}^2$	$\text{sp}^2 \rightarrow \gamma$	$\beta \rightarrow \gamma$	$\gamma \rightarrow \beta$	$w \rightarrow w'$	$w' \rightarrow w$
$k_{\text{ex}} (\text{s}^{-1})$	10.0	2.8	5.6	0.4	0.2	0.2	1.2	1.9

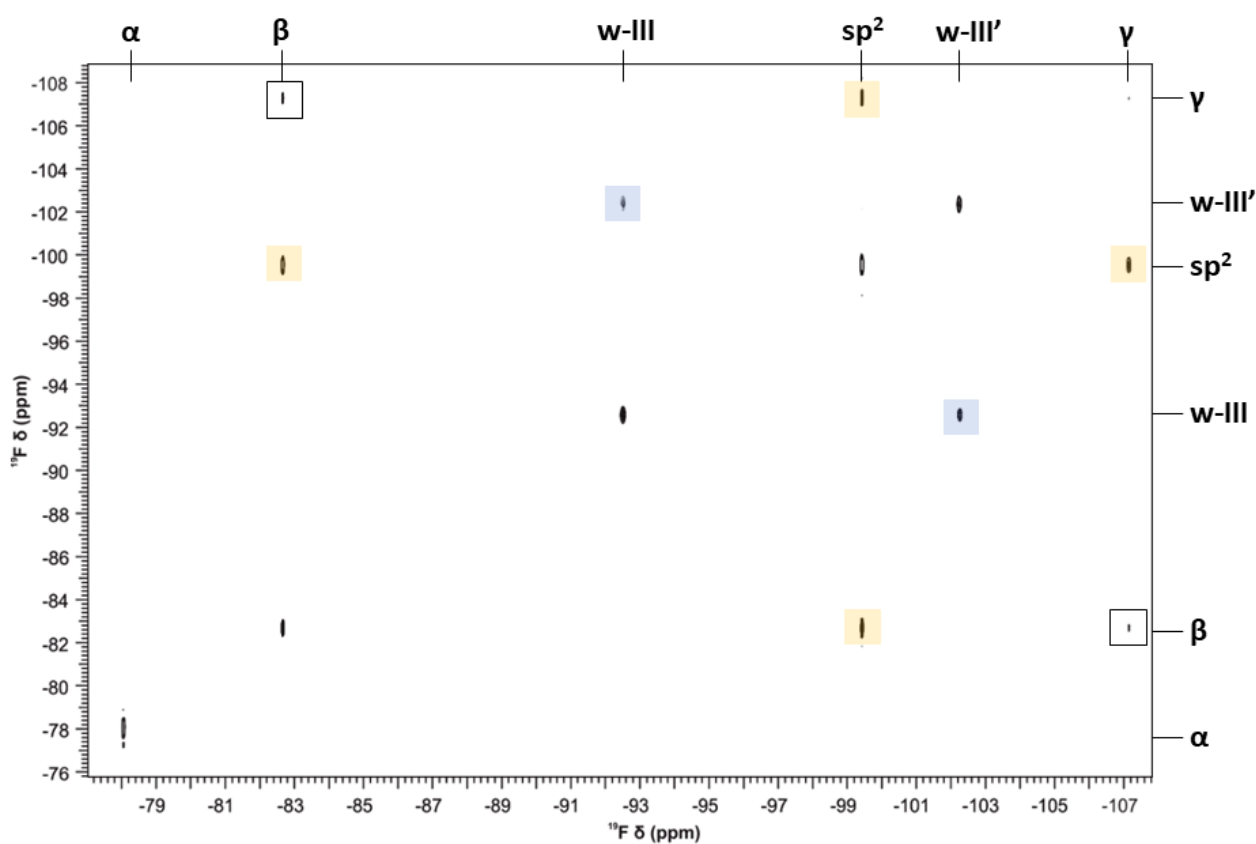


Figure S31. The ^{19}F -EXSY spectrum (564 MHz) of the **p+III** system using a **p** to **III** ratio of 3:1. The spectrum was recorded at 253.0 K with the mixing time of 400 ms. The ^{19}F frequencies are assigned along both dimensions with the distinct **p-III** atropisomer signals indicated with Greek letters. Cross-peaks indicating the exchanges that involve the sp^2 **III** form, the two aqueous forms of **p+III** (**w-III** and **w-III'**) or the atropisomers of **p-III** exclusively, are highlighted with orange, blue and white squares, respectively.

p+II system: In the mixture of **p** and **II** between 293.0 K and 333.0 K all the **p-II** atropisomers show complete dissociation and interconversion with each other at sufficiently long mixing times. Due to the presence of the cross-contaminating sp^2 **III** (see Figure S10) we could not quantify the kinetics of the dissociation and reassociation processes. This, nonetheless, based on the short mixing time ^{19}F -EXSY spectrum of the **p+II** mixture containing the excess of **II** (Figure S32) the dissociation of the **p-II** adduct atropisomers is a faster process than their interconversion. At 293.0 K the aqueous form of **p+II** (**w-II**) shows chemical exchange with the sp^2 **II** only but as the temperature increases it gradually participates in the exchanges with the **p-II** adduct as well. (Figure 7) The fluorine exchange rate (k_F) values (Section 1.1.) associated with the conformational interconversions of **p-II** at 293.0 K are collected in Table S12 for illustration (other k_F values: *not shown*). The k_{ex} values of the diverse exchange processes of the **p-II** species are collected in Table S13.

Table S12. Fluorine exchange rates (k_F) associated with the **p-II** conformational interconversions at 293.0 K. The distinct atropisomers of **p-II** are indicated with Greek letters whereas the spatial position of the chosen fluorine atom is shown in parenthesis. The initial and final position of the fluorine upon the conformational exchange is indicated in the left column and top row, respectively. The k_F -s of the same conformational interconversion process are always within an order of magnitude regardless of the initial and final position of the chosen fluorine.

p-II k_F (s^{-1})		Final position					
		α (h_T)	α (a_T)	β (a_T)	β (s_V)	γ (h_T)	γ (s_V)
Initial position	α (h) \rightarrow			0.01	0.02	0.28	0.27
	α (a) \rightarrow			0.02	0.01	0.35	0.29
	β (a') \rightarrow	0.01	0.01			0.04	0.03
	β (s) \rightarrow	0.02	0.01			0.06	0.02
	γ (h) \rightarrow	1.0	1.2	0.02	0.09		
	γ (s') \rightarrow	0.61	0.35	0.07	0.03		

Table S13. Exchange rates (k_{ex}) of the species in the mixture of **p** and **II** at different temperatures. The distinct atropisomers of **p-II** are indicated with Greek letters whereas the aqueous form of **p+II** is indicated with **w**. A hyphen means that no exchange between the indicated species was detectable or the signal-to-noise ratio of the corresponding EXSY cross-peaks did not reach the level of quantification, thus, the exchange rates were not quantified.

p+II system	k_{ex} (s^{-1})											
	Conformational exchanges of p-II						Exchanges with the aqueous form of p+II					
	$\alpha \rightarrow \beta$	$\beta \rightarrow \alpha$	$\alpha \rightarrow \gamma$	$\gamma \rightarrow \alpha$	$\beta \rightarrow \gamma$	$\gamma \rightarrow \beta$	$\alpha \rightarrow w$	$w \rightarrow \alpha$	$\beta \rightarrow w$	$w \rightarrow \beta$	$\gamma \rightarrow w$	$w \rightarrow \gamma$
293.0	0.01	0.01	0.30	0.79	0.04	0.05	–	–	–	–	–	–
300.0	0.02	0.03	0.66	2.08	0.12	0.22	–	–	–	–	–	–
303.0	0.08	0.10	1.39	4.52	0.21	0.34	0.03	0.04	–	–	0.13	0.11
310.0	0.21	0.40	2.56	10.21	0.37	0.87	0.18	0.30	0.02	–	0.60	0.32
317.0	0.51	0.83	4.69	19.75	0.56	1.69	0.75	1.04	0.11	0.11	2.31	0.77
323.0	0.92	1.31	6.34	41.31	0.59 ^[a]	3.03	1.82	2.08	0.26	0.24	7.95	1.39
333.0	3.69	4.42	4.96 ^[a]	82.62	0.68 ^[a]	7.68	11.80	11.40	1.72	1.46	32.84	2.48

[a] Outlier values that were omitted from the fitting of the Eyring equation.

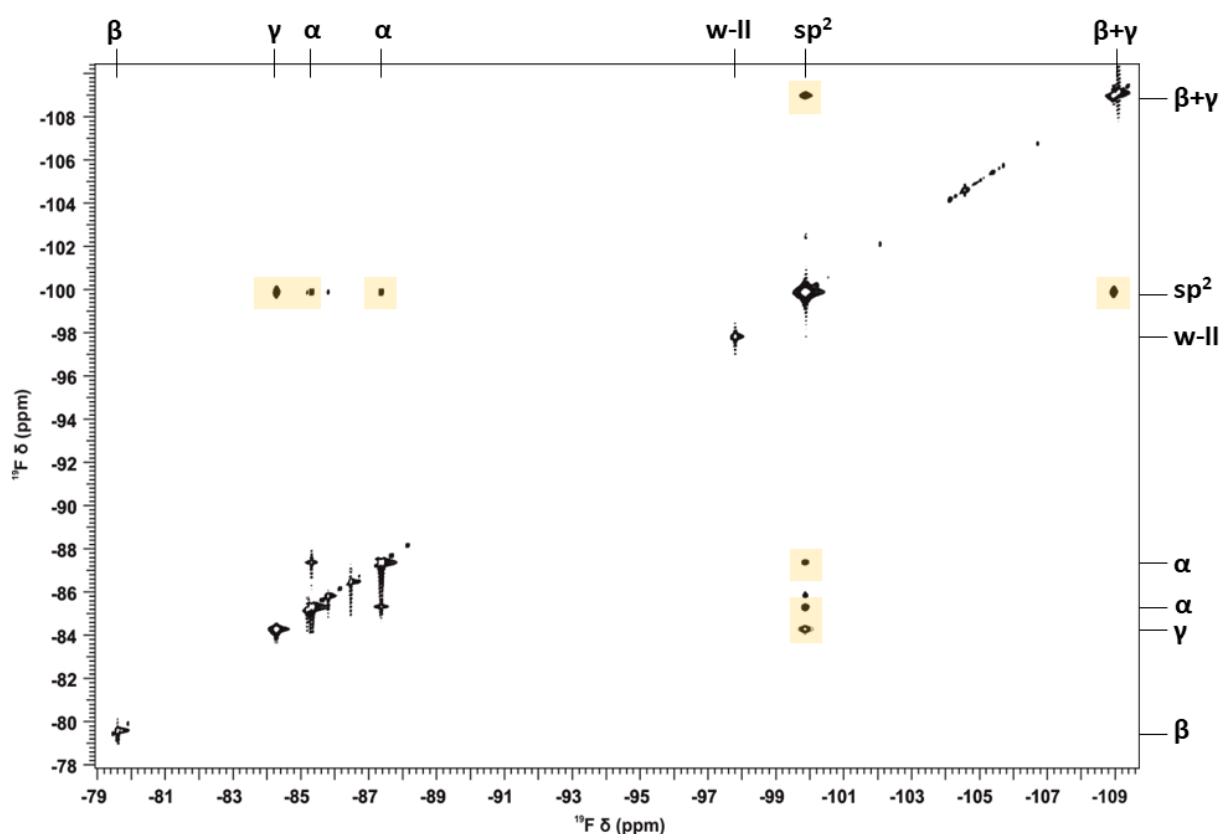


Figure S32. The ^{19}F -EXSY spectrum (564 MHz) of the **p+II** system using a **p** to **II** ratio of 1:2. The spectrum was recorded at 313.0 K with the mixing time of 2 ms. The ^{19}F frequencies are assigned along both dimensions with the distinct **p-II** atropisomer signals indicated with Greek letters. The EXSY cross-peaks of the identified **p-II** adduct conformers (highlighted in orange) indicate their exchanges with the sp^2 **II**. At this short mixing time cross-peaks that would correlate the ^{19}F frequencies of the distinct **p-II** atropisomers remain below the level of detection which means that the **p-II** conformational interconversions are slower processes than the dissociation and reassociation of the **p-II** adduct. A The ^{19}F -EXSY spectrum of the **p+II** system with higher mixing time can be found in the main text (Figure 7).

Table S14. The experimental ΔG^\ddagger values of the **p-II** conformational interconversions calculated from the corresponding k_{ex} -s (Table S13) at 300.0 K. The distinct atropisomers of **p-II** are indicated with Greek letters.

Conformational exchanges of p-II						
Process	$\alpha \rightarrow \beta$	$\beta \rightarrow \alpha$	$\alpha \rightarrow \gamma$	$\gamma \rightarrow \alpha$	$\beta \rightarrow \gamma$	$\gamma \rightarrow \beta$
$\Delta G_{300\text{K}}^\ddagger$ (kcal·mol $^{-1}$)	19.9	19.7	17.8	17.1	18.8	18.5

Table S15. The enthalpy (ΔH^\ddagger) and entropy (ΔS^\ddagger) of activation values of the exchanges detected for the **p+II** system. The distinct atropisomers of **p-II** are indicated with Greek letters whereas the aqueous form of **p** and **II** is indicated with **w**. The standard errors on the values that originate from the error in the regression are indicated in squared brackets.

Conformational exchanges of p-II						
Process	$\alpha \rightarrow \beta$	$\beta \rightarrow \alpha$	$\alpha \rightarrow \gamma$	$\gamma \rightarrow \alpha$	$\beta \rightarrow \gamma$	$\gamma \rightarrow \beta$
ΔH^\ddagger (kcal·mol $^{-1}$)	28.3 [3.7]	29.0 [4.8]	18.9 [3.3]	22.1 [2.5]	19.6 [5.0]	22.8 [2.9]
ΔS^\ddagger (cal·mol $^{-1}$ ·K $^{-1}$)	29.2 [12.0]	32.0 [15.5]	3.9 [10.8]	17.0 [8.2]	2.3 [16.7]	14.3 [9.3]
Exchanges with the aqueous form of p+II						
Process	$\alpha \rightarrow \text{w}$	$\text{w} \rightarrow \alpha$	$\beta \rightarrow \text{w}$	$\text{w} \rightarrow \beta$	$\gamma \rightarrow \text{w}$	$\text{w} \rightarrow \gamma$
ΔH^\ddagger (kcal·mol $^{-1}$)	38.4 [0.4]	35.5 [2.6]	38.5 [1.8]	40.6 [3.0]	36.9 [1.4]	26.3 [1.2]
ΔS^\ddagger (cal·mol $^{-1}$ ·K $^{-1}$)	64.1 [9.4]	53.0 [8.2]	57.8 [5.7]	64.1 [9.4]	59.2 [4.3]	23.7 [3.9]

p+I system: In the mixture of **p** and **I** at 323.0 K all the **p-I** atropisomers show complete dissociation and interconversion into each other. (Figure S33) The dissociation of any **p-I** atropisomer occurs 1–2 magnitudes of order faster than their conversion into another **p-I** atropisomer. The aqueous form of **p** and **I** (**w-I**) does not show any exchange. The corresponding k_{ex} values are collected in Table S16.

Table S16. Exchange rates (k_{ex}) of the species in the mixture of **p** and **l** at 323.0 K. The distinct atropisomers of **p-l** are indicated with Greek letters.

Process	Conformational interconversions of p-l						Dissociation and reassociation of p-l			
	$\alpha \rightarrow \beta$	$\beta \rightarrow \alpha$	$\alpha \rightarrow \gamma$	$\gamma \rightarrow \alpha$	$\alpha \rightarrow \delta$	$\delta \rightarrow \alpha$	$\alpha \rightarrow \text{sp}^2$	$\text{sp}^2 \rightarrow \alpha$	$\beta \rightarrow \text{sp}^2$	$\text{sp}^2 \rightarrow \beta$
$k_{\text{ex}} (\text{s}^{-1})$	0.003	0.01	0.01	0.58	0.03	0.41	0.40	0.22	0.14	0.02
Process	$\beta \rightarrow \gamma$	$\gamma \rightarrow \beta$	$\beta \rightarrow \delta$	$\delta \rightarrow \beta$	$\gamma \rightarrow \delta$	$\delta \rightarrow \gamma$	$\gamma \rightarrow \text{sp}^2$	$\text{sp}^2 \rightarrow \gamma$	$\delta \rightarrow \text{sp}^2$	$\text{sp}^2 \rightarrow \delta$
$k_{\text{ex}} (\text{s}^{-1})$	0.01	0.05	0.07	0.11	0.28	0.04	6.04	0.13	1.53	0.006

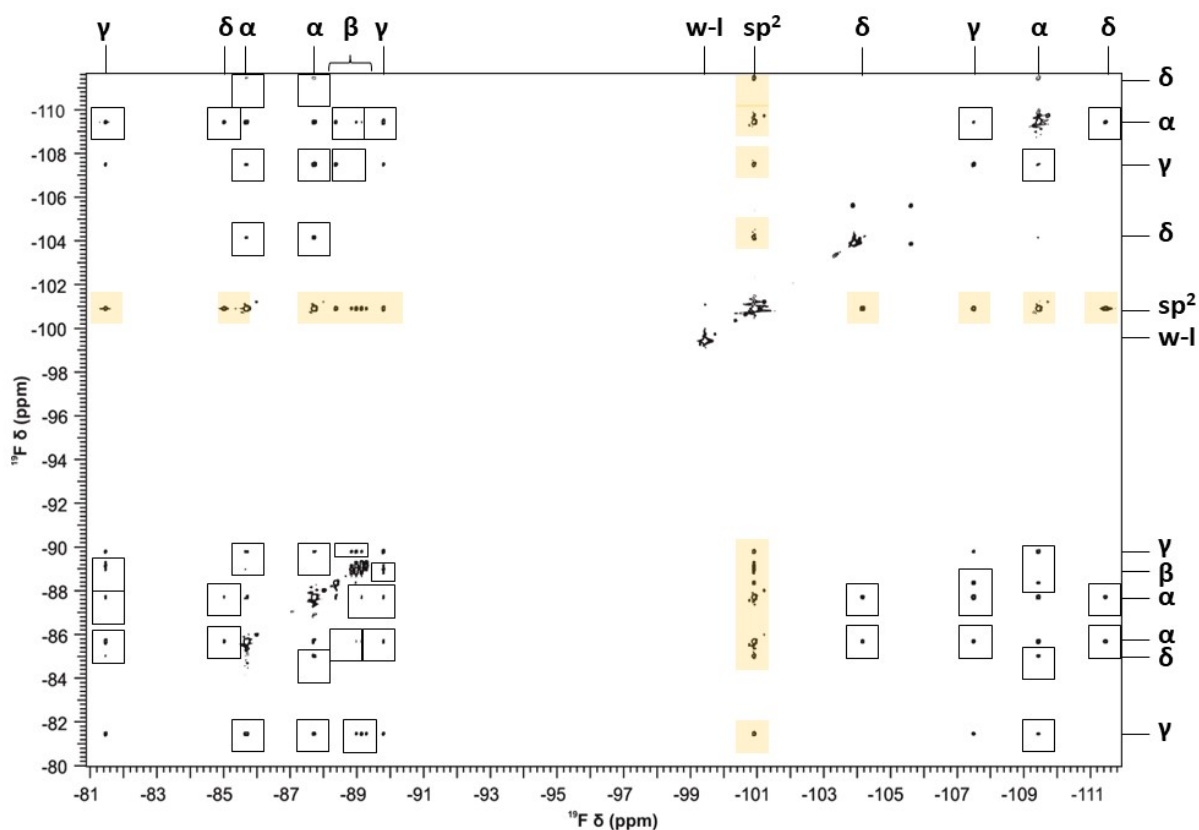


Figure S33. ^{19}F EXSY spectrum (564 MHz) of the mixture of **p** and **l** using a **p** to **l** ratio of 1:2. The spectrum was recorded at 323.0 K with the mixing time of 600 ms. The ^{19}F frequencies are assigned along both dimensions with the distinct **p-l** atropisomer signals indicated with Greek letters. Cross-peaks indicating fast dissociative equilibria between the sp^2 and sp^3 states of **l** are highlighted in orange. Cross-peaks indicating the slow atropisomeric exchanges of the dative **p**-adduct are highlighted with white squares. The kinetically stable aqueous complex **w-l** does not show exchanges with any other forms.

According to Reviewers' suggestions we added the ^{19}F EXSY spectrum of the **p+II** system using a **p:II** ratio of 3:1 (Figure S34). Under these circumstances the sp^2 form is not detectable, and thus, the dynamic exchanges between the dative **p-II** adduct atropisomers and the II sp^2 state is not detectable. This, nonetheless, the atropisomeric exchanges of the **p-II** adduct remain detectable.

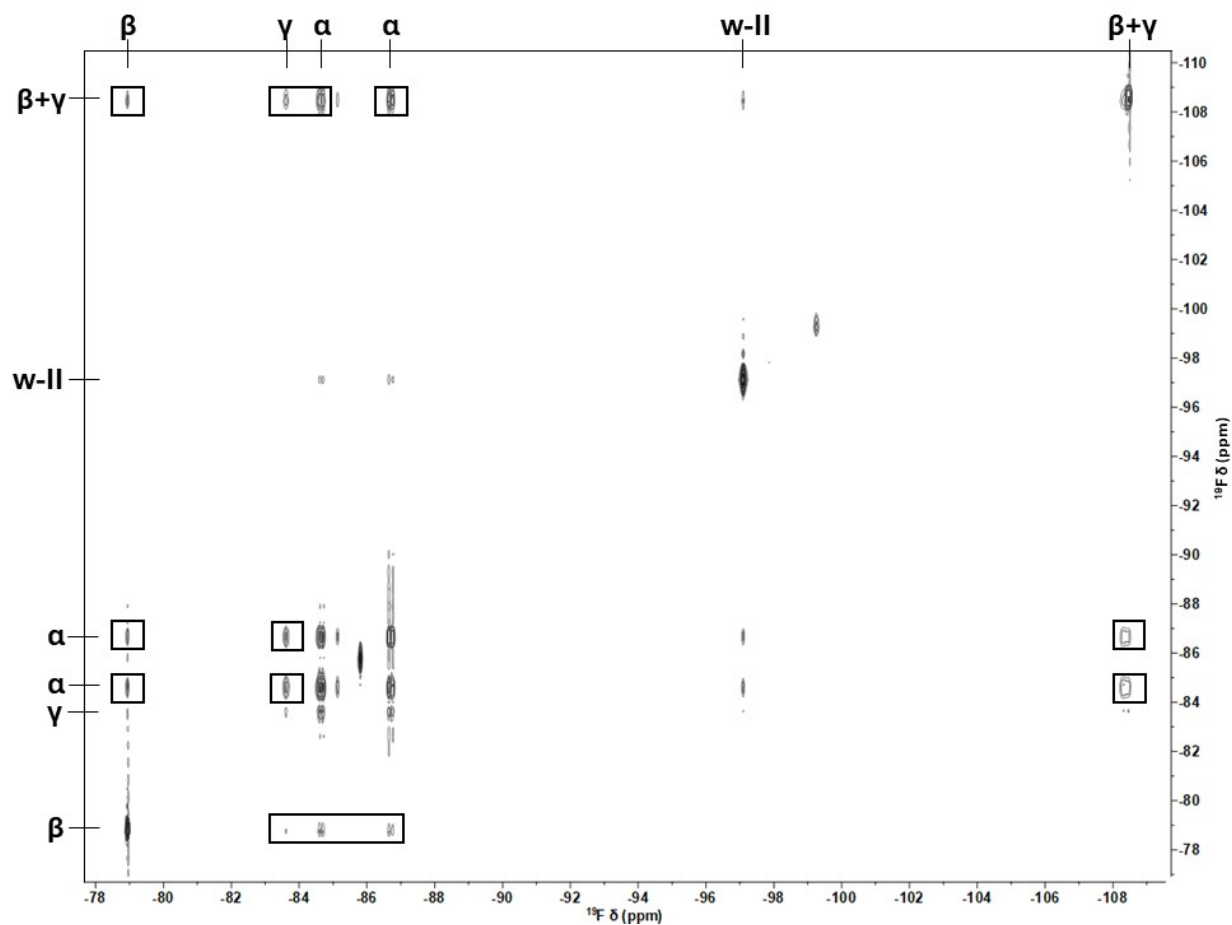


Figure S34. The ^{19}F -EXSY spectrum (564 MHz) of the **p+II** system using a **p** to **II** ratio of 3:1. The spectrum was recorded at 313.0 K with the mixing time of 150 ms. The ^{19}F frequencies are assigned along both dimensions with the distinct **p-II** atropisomer signals indicated with Greek letters. Cross-peaks indicating the exchanges of the **p-II** adduct atropisomers are highlighted with squares.

8. PES Scans

To confirm the mechanism of the interconversion between the atropisomers of **p**-borane adducts, the barrier heights that can be associated with these events were estimated via a series of potential energy surface (PES) scans carried out for the **p-II** adduct. The PES scans were performed at the same level of theory as the unconstrained geometry optimizations. Starting from the energetically lowest lying atropisomeric state **p-II**(α), the **p** moiety and the borane aryl rings were rotated separately around the respective bonds formed with the central boron atom so as to mimic the intramolecular rearrangements required for the conformational interconversions (Figure S35). In these calculations, only one ring was rotated at a time while all other intramolecular coordinates, including the B–N distance and those of the other rings, were unconstrained and allowed to relax freely. The relative electronic energies and B–N distances inferred by the ring rotations are plotted in Figure S36. Accordingly, in the **p-II** structure, the **p** (A) and the borane aryl ring (B, C and D) rotations are clearly hindered as the points with the highest energies lie between 25 and 53 kcal·mol⁻¹ above the starting point. These values are remarkably higher than the experimental activation barriers of the conformational interconversions ($\Delta G_{300\text{K}}^\ddagger$), which are in the 17.1–19.9 kcal·mol⁻¹ range as obtained from the exchange rates at 300 K (Table S14). We wish to highlight that the dissociation of the **p-II** adduct during these PES scans could be observed. These events were identified by the occasional increase of the B–N bond length from the prevailing 1.6–2.1 Å to 3.5 Å or above. Although most of the high-lying local maxima for the ring rotations still belong to dative bound adducts, these allude to the preference for dissociation during the ring rearrangements, as it can release the strain in these adducts. Overall, the PES scans suggest that the interconversion of the distinct conformational states of a **p**-adduct cannot take place in the dative bonding sp³ state, but instead the complete dissociation of the B–N bond is required for the transformation of isomers.

For comparison, we applied a similar PES screening for the ring rotation (E, F and G) barriers in the sp² **II** borane structure as well. The obtained PES profiles are depicted in Figure S37. The points with the highest energies lie between 14.3–19.6 kcal·mol⁻¹ above the starting point, which are much lower than the values obtained for the B–D rotations in the adducts. In order to evaluate the accuracy of these barrier heights, we started transition state searches from the highest lying points. These calculations resulted in structures with a single imaginary vibrational mode with frequencies between 46.0i cm⁻¹ and 48.5i cm⁻¹ that are all related to ring rotations. Relative energies of these structures are depicted as black dashed lines in Figure S37. The differences between the heights of the peaks in the PES scans and the energies of the true transition states corresponding to these peaks are on the scale of 0.7–7.7 kcal·mol⁻¹. These calculations not only reveal that the barrier heights (11.9–13.6 kcal·mol⁻¹) allow the more facile rotation of the rings in the sp² boranes on the NMR timescale, but also give an estimation about the inaccuracy of the PES scan evaluation of barrier heights. Considering these results, however, the estimated barrier heights for the A–D ring rotations in the **p**-adducts are still considered sufficiently high to exclude the interconversion of the distinct atropisomers through the dative bonding state.

We also carried out PES scans for borohydride [III-H] to monitor the rotational barriers of conformational changes. We investigated the rotation of the 3 rings around the axes defined in Figure S38 (B, C and D refer to the analogous axes in the piperidine complex defined in Figure S35). According to the scans, the barriers of these rotations are not higher than 27 kcal/mol and most of the estimated barriers range between 10 and 15 kcal/mol. These results clearly indicate that the rotation of the aryl rings in the borohydride complexes is kinetically feasible at room temperature.

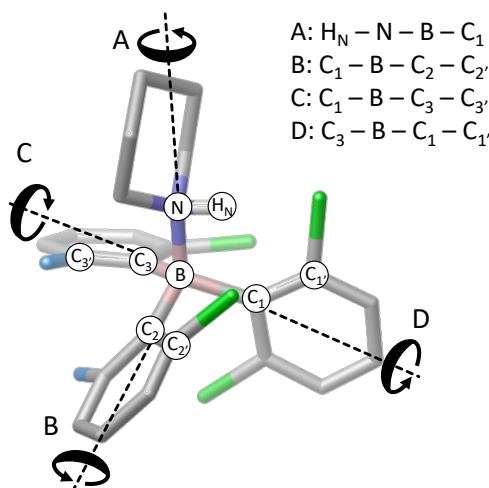


Figure S35. Potential energy surface scans carried out on the **p-II** adduct starting from the α conformation. A–D rotations are defined with the noted atoms. The axes of rotation were depicted as dashed lines, and positive rotation directions are signed with black curved arrows.

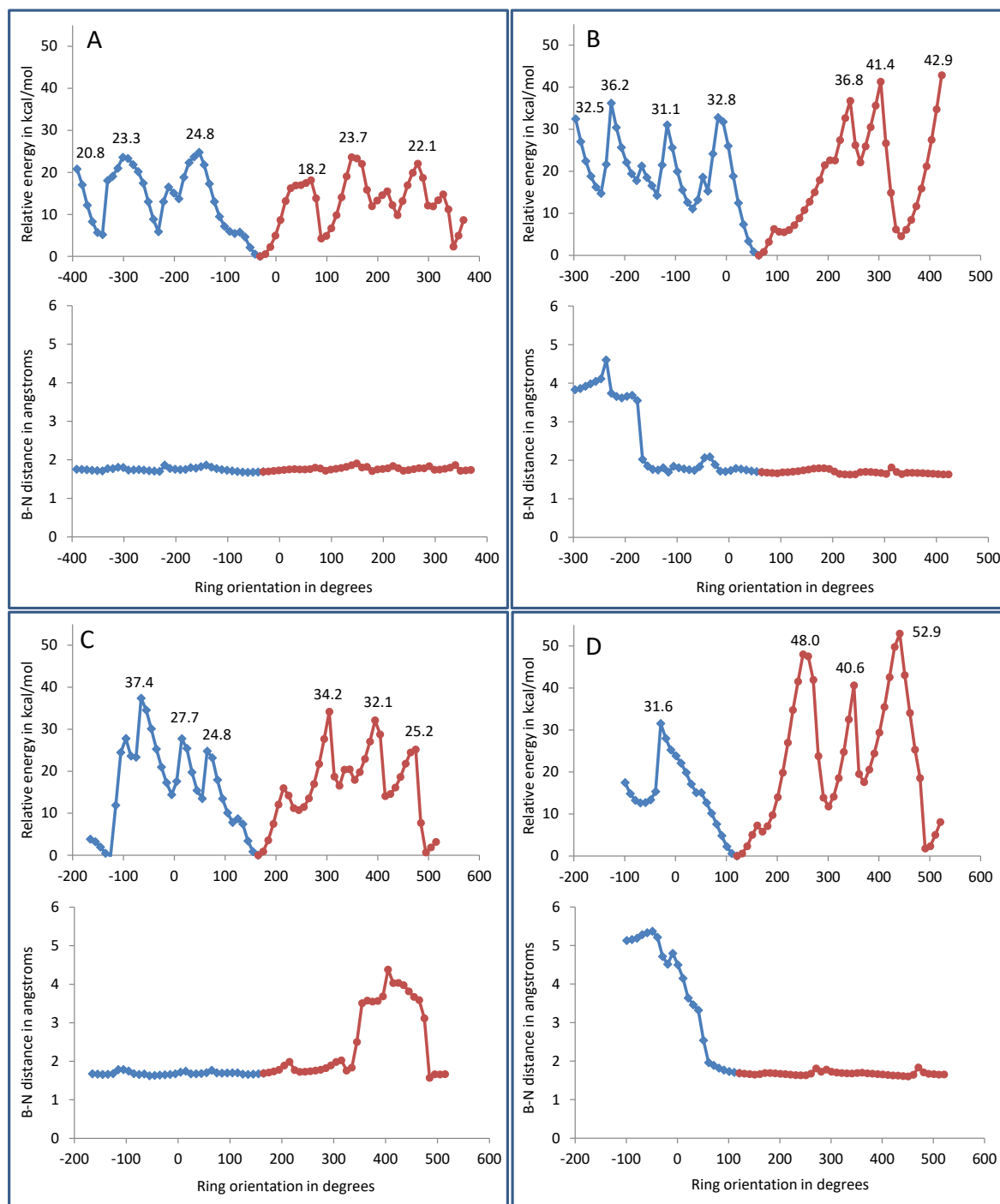


Figure S36. Results of the potential energy surface scans performed on $p-II(\alpha)$ towards negative direction (blue) and positive direction (red). In each of the four segments, the top plots depict the relative electronic energies, and the bottom plots depict the B–N interatomic distances in the system. Labels A–D refer to the rotations defined in Figure S35.

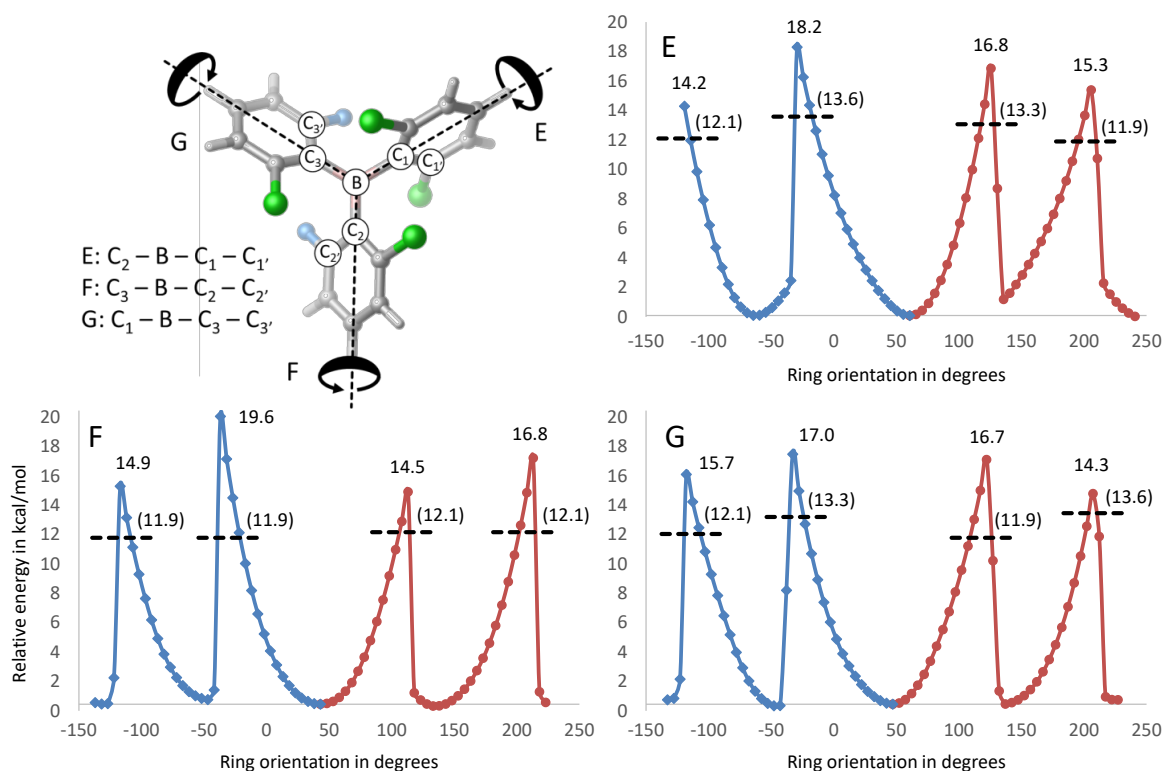


Figure S37. Potential energy surface scans carried out on **II**. (Top left) E, F, and G rotations are defined with the noted atoms. The axes of rotation were depicted as dashed lines, and positive rotation directions are signed with black curved arrows. (Top right, bottom left, and bottom right) Results of the potential energy surface scans towards (blue) negative direction and (red) positive direction. Relative energies of the transition states starting from the peaks are depicted with black dashed lines and given in brackets.

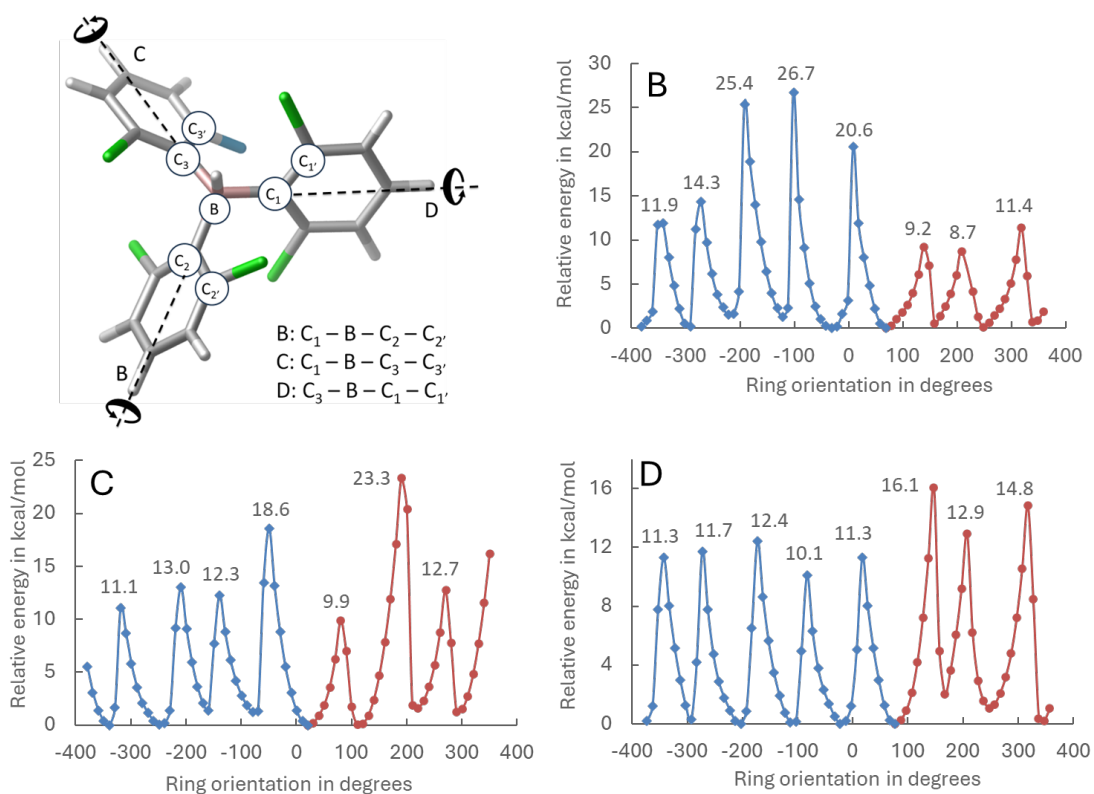


Figure S38. Potential energy surface scans (Top right, bottom left, and bottom right) carried out for **[III-H]** (Top left). B, C, and D rotations are defined with the noted atoms (see also Figure S35) and positive rotation directions are signed with black curved arrows. Results of the potential energy surface scans towards (blue) negative direction and (red) positive direction.

9. Aqueous Complexes and X-ray Crystallography

Despite the efforts to establish water-free conditions (dry solvents, glove box) aqueous forms of the dative **p**-borane adducts (**w**-borane) also emerged in the toluene solutions. Such clusters of interacting borane, **p** and water molecules feature broad ^{19}F NMR signals close to that of the sp^2 borane state. In the **p+I**, **p+II** and **p+III** mixtures respectively 1, 1 and 2 aqueous clusters were detected. In these species the spatial vicinity of **p** to boranes **I** and respectively **II** could be demonstrated through ^{19}F - ^1H HOESY correlations, see ^{19}F - ^1H HOESY spectra in Section 6. (Figures S28–S29) The aqueous clusters appear kinetically frozen as they do not undergo dynamic exchanges with the dative adduct or sp^2 forms at NMR timescale (Section 7) except for the **p+II** system at higher (>300 K) temperatures. The distinction of the aqueous clusters and the dative **p**-borane adducts could be made unequivocally using ^{19}F diffusional NMR spectroscopy. Given their larger size, the aqueous clusters were shown to diffuse about 20% and 30% slower than the corresponding dative **p**-adducts and the sp^2 state, respectively. (Figures S39–S41)

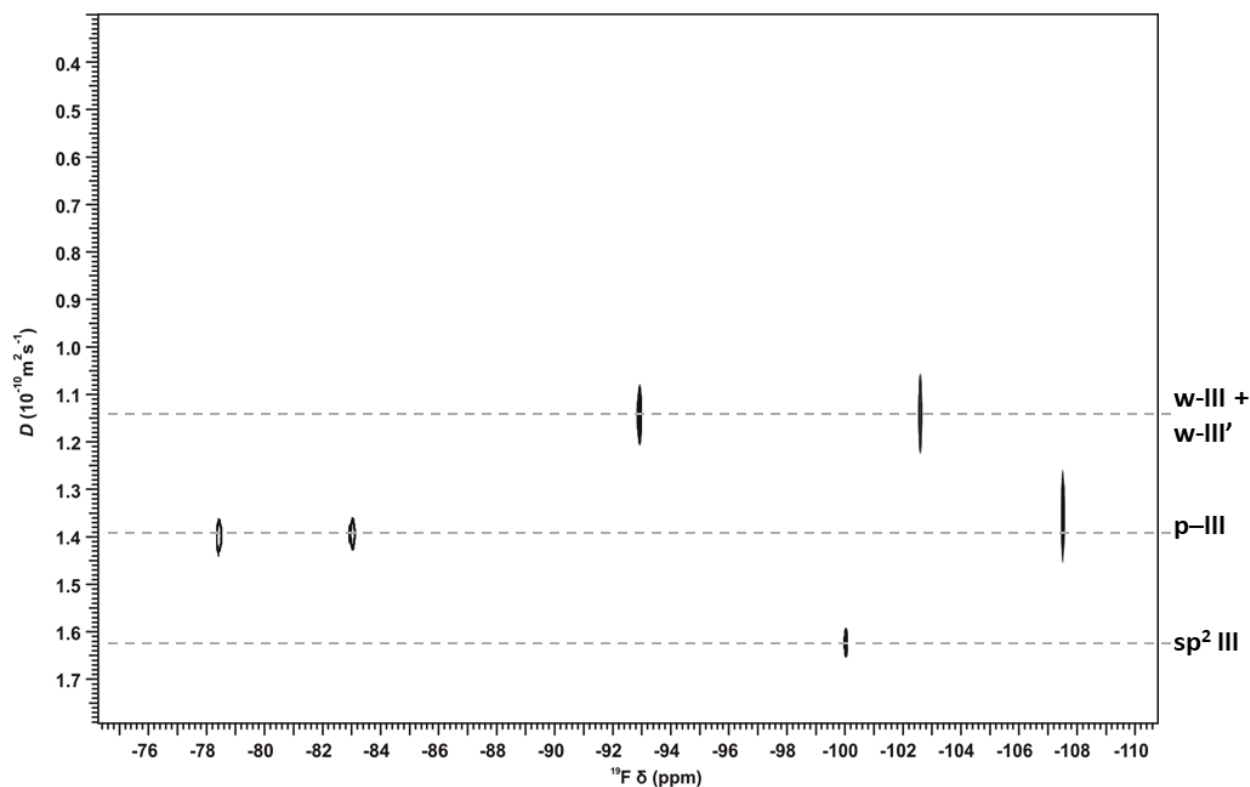


Figure S39. ^{19}F DOSY spectrum (376 MHz) of the mixture of **p** and **III** using a **p** to **III** ratio of 3:1 recorded at 243.2 K. There are clear differences in the diffusional coefficients of the distinct forms with the order of sp^2 **III** > **p-III** atropisomers > aqueous forms (**w-III**, **w-III'**).

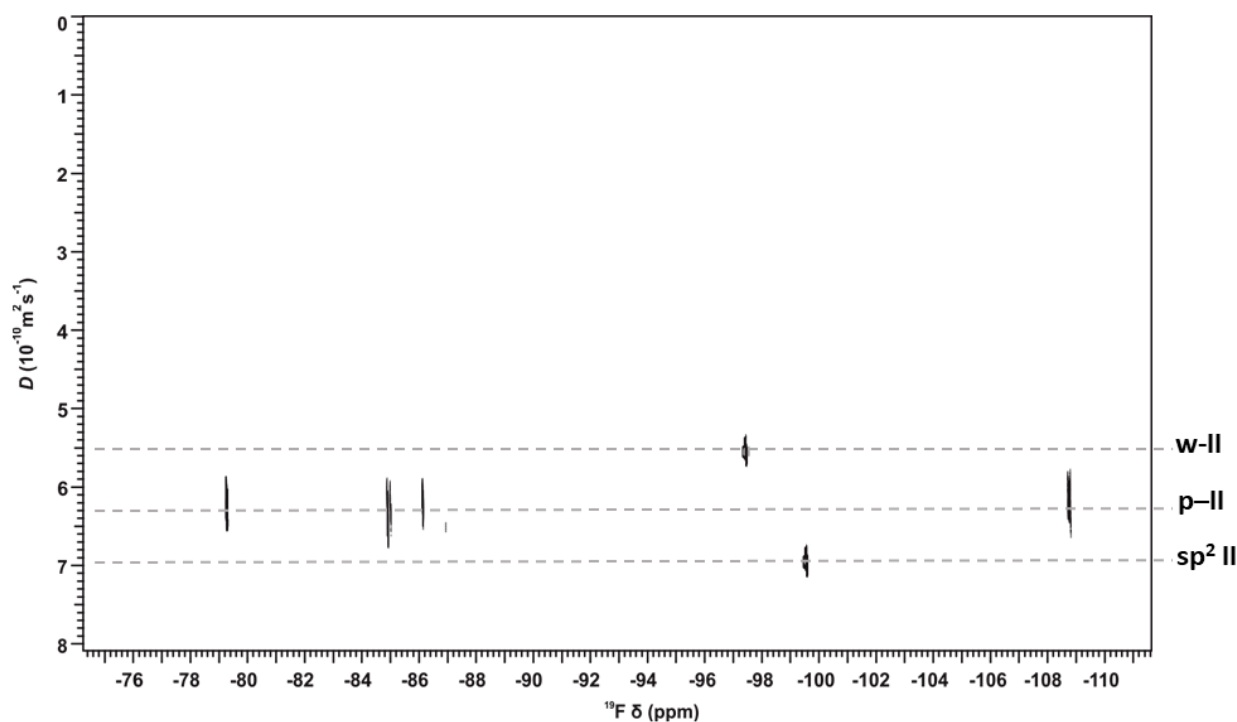


Figure S40. ^{19}F DOSY spectrum (376 MHz) of the mixture of **p** and **II** using a **p** to **II** ratio of 1:2 recorded at 298.2 K. There are clear differences in the diffusional coefficients of the distinct forms with the order of $\text{sp}^2 \text{II} > \text{p-II}$ atropisomers $>$ aqueous form (**w-II**).

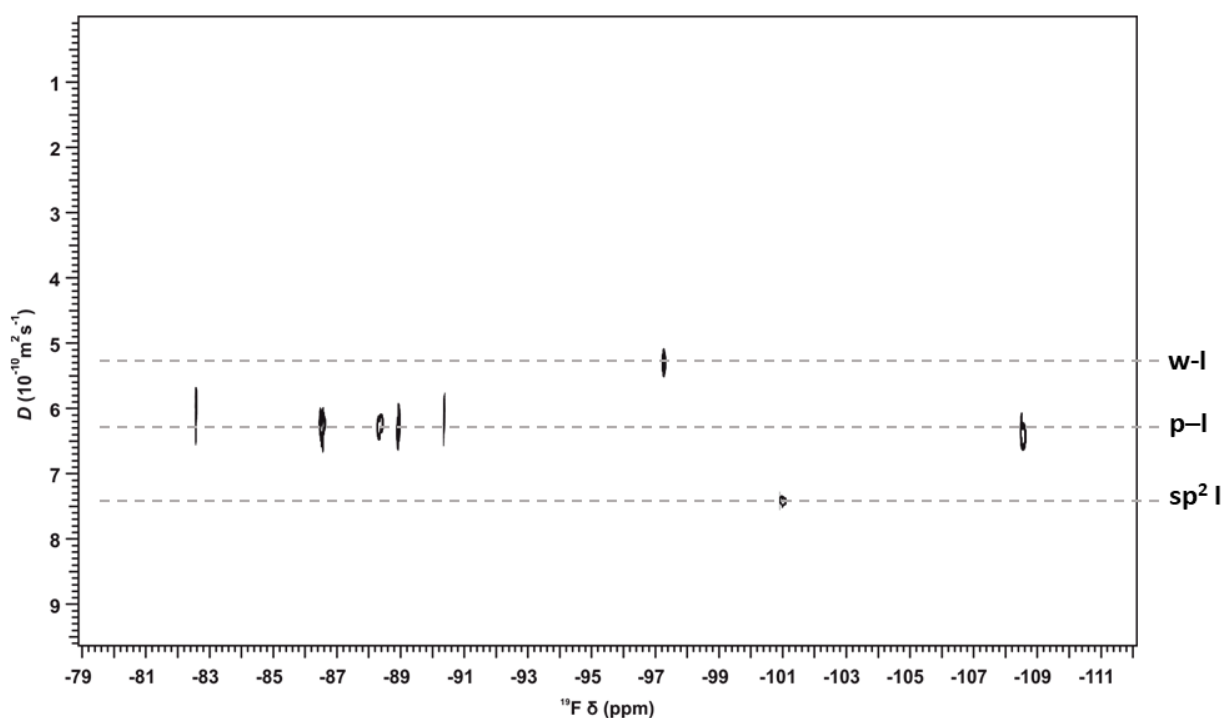


Figure S41. ^{19}F DOSY spectrum (376 MHz) of the mixture of **p** and **I** using a **p** to **I** ratio of 1:2 recorded at 298.2 K. There are clear differences in the diffusional coefficients of the distinct forms with the order of $\text{sp}^2 \text{I} > \text{p-I}$ atropisomers $>$ aqueous form (**w-I**).

Although the solution structure of the aqueous clusters was not investigated in detail, the crystal structures of the aqueous **p-III** adduct were determined using single crystal X-ray diffraction. Towards this, single crystals were grown from the mixture of **p** and **III** (3:1 ratio) using vapor diffusion directly in the NMR tube at 253.0 K. Based on the X-ray diffraction experiments, the interaction of **p** and **III** indeed shows water-mediated as the crystal structures features a OH^- bonded to the boron atom while a H^+ is taken up by a **p** molecule to form a $[\text{p-H}]^+ \cdots [\text{OH-III}]^-$ complex. However, multiple crystal disorders were observable causing variations in the number of **p** molecules per asymmetric unit and the conformation of the $[\text{OH-III}]^-$

unit as well. We distinguished crystal forms **1** and **2** based on the former aspect in which two and three **p** molecules complete the asymmetric unit, respectively. In **2** the appearance of the 3rd **p** molecule showed disorder as its presence could be confirmed in the ~60% of the asymmetric units. In **1** the orientation of the aryl rings appeared to be disordered. The two emerging conformers can be best characterized by the orientation of the fluorinated aryl ring which's Cl or F atom is points towards the O atom in 60% (form **1-A**) and 40% (form **1-B**) of the structures, respectively (Figure S42 and Figure S43). The arrangement of the [OH-III]⁻ unit is quasi-identical in **2** and **1-B**. (Table S17)

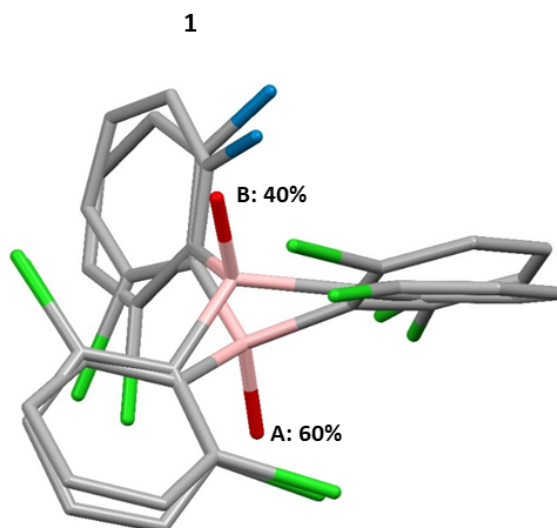


Figure S42. The overlay and relative ratio of the best fit structures in crystal form **1**. The following color coding was applied: blue – F, green – Cl, gray – C, red – O, pink – B.

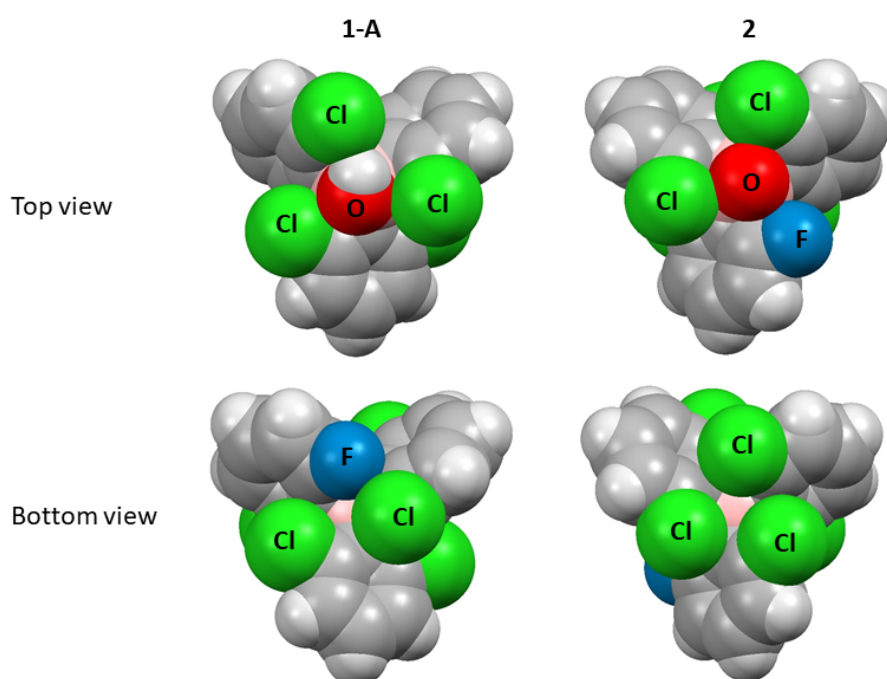
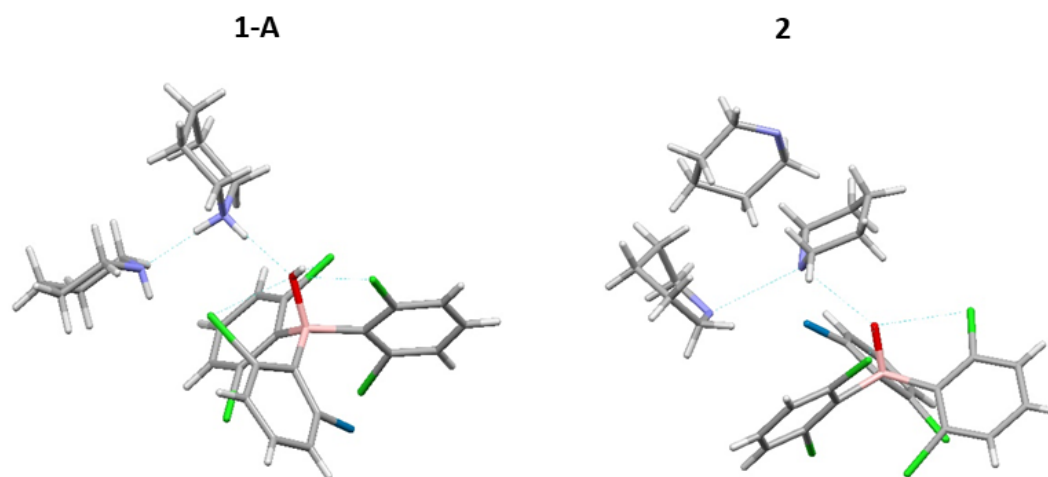


Figure S43. The top and bottom views of the [OH-III]⁻ unit of **1-A** and **2** are shown in vdW representation.

Table S17. List of the analyzed interatomic distances (r) in **1-B** and **2**.

Contact	r (Å) in 1-B	r (Å) in 2
O...N	2.714(3)	2.73(3)
O...B	1.495(3)	1.47(3)
O...Cl	3.0044(18)	2.909(15)
O...Cl	2.981(4)	2.899(15)
O...F	2.741(12)	2.764(17)
(O)H...Cl	2.32	

Close contacts detected for the OH⁻ oxygen to the halogen atoms unambiguously fixed its position in both forms (Table S17). The hydrogen atom positions could be determined based on the difference electron density map in case of **1**. Unfortunately, the crystal size and stability were sub-optimal for the localization of the water hydrogens and the p H^N-s in case of **2**. Nevertheless, based on the experimental data we can assume that the H-bonding pattern is similar in **1** and **2** (Figure S44). We conclude that the crystal structures demonstrate that for the water molecule (and subsequently for p) it is possible to attack both the fully chlorinated and the fluorinated sites of the [OH-III]⁻ unit. CCDC 2004799 (**1**) and 2004800 (**2**) contain the supplementary crystallographic data for this paper. The data is available in the Cambridge Crystallographic Data Centre via www.ccdc.cam.ac.uk/structures.

**Figure S44.** The plausible hydrogen-bonding system in the asymmetric unit of **1-A** and **2**. The water hydrogen and p H^N positions in **2** could not be found in the difference electron density map.

Crystal Clear^[34] (developed by Rigaku Company) software was used for data collection and the refinement of crystals **1** and **2**. Numerical absorption corrections or empirical correction^[35–36] were applied to the data. The structures were solved by direct methods. Anisotropic full-matrix least-squares refinements were performed on F^2 for all non-hydrogen atoms. Hydrogen atoms bonded to C atoms were placed in calculated positions and refined in a riding-model approximation. The computer programs used for the structure solution, refinement and analysis of the structures were Shelx^[37–38], Sir2014^[39], Wingx^[40] and Platon^[41]. Visualization software Mercury^[42] was used for the graphical representation of the described structures. For interatomic distance measurements the sum of vdW radius of the O+Cl and O+F atom pairs were specified around 3.27 Å and 2.99 Å, respectively^[43]. Further details on the crystallographic data, data collection and the refinement of **1** and **2** are collected in Table S18 and Figure S45.

Crystal data of **1**: C₁₈H₉BCl₅F, H₂O, 2C₅H₁₁N, *Fwt.*: 620.62, colourless, block, size: 0.50 x 0.25 x 0.20 mm, monoclinic, space group $P 2_1/n$, $a = 8.5595(2)$ Å, $b = 18.0868(4)$ Å, $c = 18.9345(4)$ Å, $\alpha = 90^\circ$, $\beta = 99.522(7)^\circ$, $\gamma = 90^\circ$, $V = 2890.94(13)$ Å³, $T = 103(2)$ K, $Z = 4$, $F(000) = 1288$, $D_x = 1.426$ Mg/m³, $\mu = 0.534$ mm⁻¹. A crystal of **1** was mounted on a fiber. Cell parameters were determined by least-squares using 131696 reflections in the range of $3.02^\circ \leq \vartheta \leq 29.095^\circ$. Intensity data were collected on a Rigaku RAXIS-RAPID II diffractometer (monochromator; Mo- $K\alpha$ radiation, $\lambda = 0.71075$ Å) at 103(2) K in the range of $3.025^\circ \leq \vartheta \leq 25.349^\circ$. A total of 116433 reflections were collected of which 5286 were unique ($R(\text{int}) = 0.0357$, $R(\sigma) = 0.0114$); intensities of 5089 reflections were greater than $2\sigma(I)$. Completeness to $\vartheta = 0.998$. A numerical absorption correction was applied to the data (the minimum and maximum transmission factors were 0.958676 and 0.986656, respectively). The structure was solved by direct methods (and subsequent difference syntheses). Anisotropic full-matrix least-squares refinement on F^2 for all non-hydrogen atoms yielded $R_1 = 0.0509$ and $wR^2 = 0.1165$ for 1332 [$I > 2\sigma(I)$] intensity data; and $R_1 = 0.0536$ and $wR^2 = 0.1180$ for all the 5286 unique intensity data (number of parameters = 410, goodness-of-fit = 1.195, the maximum and mean shift/esd is 0.000 and 0.000). The maximum and minimum residual electron density in the final

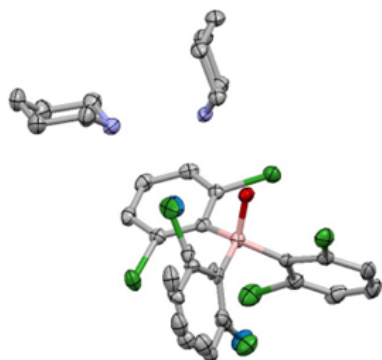
difference map was 0.67 and $-0.51 \text{ e} \cdot \text{\AA}^{-3}$. The weighting scheme applied was $w = 1/[\sigma^2(F_o^2) + (0.04443.6442P)^2 + 3.6442P]$ where $P = (F_o^2 + 2F_c^2)/3$. Hydrogen atomic positions were calculated from assumed geometries except H1O, H1NA, H1NB, H2N which were located via the difference maps. Hydrogen atoms were included in structure factor calculations, but they were not refined. The isotropic displacement parameters of the hydrogen atoms were approximated from the $U(\text{eq})$ value of the atom they were bonded to. In the refinement procedure of crystal **1** disorder conformations were considered. The occupancy of the C13A C14A C15A C16A C17A C18A C15A F1A and the C13B C14B C15B C16B C17B C18B C15B F1B rings were found to be 60% and 40%, respectively.

Crystal data of **2**: $\text{C}_{18}\text{H}_9\text{BCl}_5\text{F}$, H_2O , $3\text{C}_5\text{H}_{11}\text{N}$, *Fwt.*: 633.42, colourless, platelet, size: 0.25 x 0.25 x 0.01 mm, monoclinic, space group *Cc*, $a = 10.208(2) \text{\AA}$, $b = 17.008(3) \text{\AA}$, $c = 20.085(4) \text{\AA}$, $\alpha = 90^\circ$, $\beta = 91.581(6)^\circ$, $\gamma = 90^\circ$, $V = 3486(1) \text{\AA}^3$, $T = 123(2) \text{K}$, $Z = 4$, $Z' = 1$, $F(000) = 1310$, $D_x = 1.207 \text{ Mg/m}^3$, $\mu = 0.445 \text{ mm}^{-1}$. A crystal of **2** was mounted on a fiber. Cell parameters were determined by least-squares using 10248 reflections in the range of $3.045^\circ \leq \vartheta \leq 21.85^\circ$. Intensity data were collected on a Rigaku R-AXIS-RAPID II diffractometer (monochromator; Mo- $K\alpha$ radiation, $\lambda = 0.71075 \text{ \AA}$) at 123(2) K in the range of $3.052^\circ \leq \vartheta \leq 21.897^\circ$. A total of 14920 reflections were collected of which 4200 were unique [$R(\text{int}) = 0.1706$, $R(\sigma) = 0.1662$]; intensities of 2303 reflections were greater than $2\sigma(I)$. Completeness to $\vartheta = 0.992$. A numerical absorption correction was applied to the data (the minimum and maximum transmission factors were 0.971643 and 0.996687). The structure was solved by direct methods (and subsequent difference syntheses). Anisotropic full-matrix least-squares refinement on F^2 for all non-hydrogen atoms yielded $R_1 = 0.1116$ and $wR^2 = 0.2789$ for 1332 [$I > 2\sigma(I)$] intensity data; and $R_1 = 0.1705$ and $wR^2 = 0.3163$ for all the 4200 unique intensity data (number of parameters = 271, goodness-of-fit = 0.994, the maximum and mean shift/esd is 0.019 and 0.001). The absolute structure parameter is 0.5. (Friedel coverage: 0.997, Friedel fraction max.: 0.993, Friedel fraction full: 0.993). The maximum and minimum residual electron density in the final difference map was 0.71 and $-0.36 \text{ e} \cdot \text{\AA}^{-3}$. The weighting scheme applied was $w = 1/[\sigma^2(F_o^2) + (0.17860.0000P)^2 + 0.0000P]$ where $P = (F_o^2 + 2F_c^2)/3$. Hydrogen atomic positions were calculated from assumed geometries. Hydrogen atoms were included in structure factor calculations, but they were not refined. The isotropic displacement parameters of the hydrogen atoms were approximated from the $U(\text{eq})$ value of the atom they were bonded to. Two disordered **p** molecules were partially modelled in crystal **2**. The occupancy of the N2 C24 C25 C26 C27 C28 and N3 C29 C30 C31 C32 C33 rings showed 60%.

Table S18. Summary on the crystallographic data, data collections, structure determination and the refinement of crystals **1** and **2**.

crystal structure	1	2
CCDC	2004799	2004800
Empirical formula	C ₁₈ H ₁₀ BCl ₅ F, H ₂ O, 2C ₅ H ₁₁ N	C ₁₈ H ₁₀ BCl ₅ F, H ₂ O, 3C ₅ H ₁₁ N
Formula weight	620.62	633.42
Temperature (K)	103(2)	293(2)
Radiation and wavelength (Å)	Mo-K α , λ = 0.71075	Mo-K α , λ = 0.71075Å
Crystal system	monoclinic	monoclinic
Space group	<i>P</i> 21/ <i>n</i>	<i>C</i> c
Unit cell dimensions:		
<i>a</i> (Å)	8.5595(2)	10.208(2)
<i>b</i> (Å)	18.0868(4)	17.008(3)
<i>c</i> (Å)	18.9345(4)	20.085(4)
α (°)	90	90
β (°)	99.522(7)	91.581(6)
γ (°)	90	90
Volume	2890.94 (13)	3485.8(12)
<i>Z</i> ; <i>Z'</i>	4; 1	4; 1
Density (calculated) (Mg/m ³)	1.426	1.20
Absorption coefficient, μ (mm ⁻¹)	0.534	0.445
<i>F</i> (000)	1288	1310
Crystal colour, description	colourless, block	colourless, platelet
Crystal size (mm)	0.50 x 0.25 x 0.20	0.25 x 0.25 x 0.01
Absorption correction	numerical	numerical
Max. and min. transmission	0.958676 and 0.986656	0.971643 and 0.996687
ϑ -range for data collection	3.025° ≤ ϑ ≤ 25.349°	3.052° ≤ ϑ ≤ 21.897°
Index ranges	-10 ≤ <i>h</i> ≤ 10; -21 ≤ <i>k</i> ≤ 21; -22 ≤ <i>l</i> ≤ 22	-10 ≤ <i>h</i> ≤ 10; -17 ≤ <i>k</i> ≤ 17; -21 ≤ <i>l</i> ≤ 21
Reflections collected	116433	14920
Completeness to 2 ϑ	0.998	0.992
Independent reflections	5286 [<i>R</i> (int) = 0.0357]	4200 [<i>R</i> (int) = 0.1706]
Reflections <i>I</i> > 2 σ (<i>I</i>)	5089	2303
Data / restraints / parameters	5286 / 72 / 410	4200 / 121 / 271
Goodness-of-fit on <i>F</i> ²	1.195	0.994
Final <i>R</i> indices [<i>I</i> > 2 σ (<i>I</i>)]	<i>R</i> ₁ = 0.0509, <i>wR</i> ² = 0.1165	<i>R</i> ₁ = 0.1116, <i>wR</i> ² = 0.2789
<i>R</i> indices (all data)	<i>R</i> ₁ = 0.0536, <i>wR</i> ² = 0.1180	<i>R</i> ₁ = 0.1705, <i>wR</i> ² = 0.3163
Max. and mean shift/esd	0.000; 0.000	0.019; 0.001
Largest diff. peak and hole (e.Å ⁻³)	0.67 and -0.51	0.71 and -0.36

Direction 1 (50% ellipsoid)



Direction 2 (50% ellipsoid)

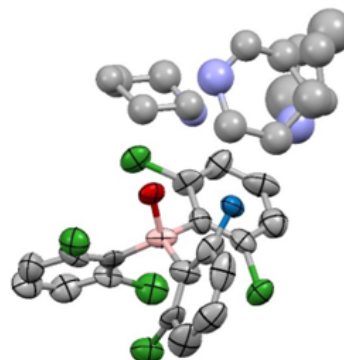


Figure S45. ORTEP style ellipsoid [40] representation of the asymmetric units of **1** and **2**. Hydrogen atoms are omitted for clarity.

10. Additional Borohydride and FIA Calculations

1) Test calculations using diffuse basis functions in the geometry optimization of the borohydride adducts

In order to check whether our computational protocol described in Section 1.2 can be reliably applied to the negatively charged borohydride species as well, we carried out test calculations for the four borohydride rotameric states derived from borane I. In these calculations, the geometries of the borohydride conformers (and that of borane I as well) were optimized using the 6-311++G(d,p) basis set, which includes diffuse functions for all atoms. LNO-CCSD(T)/CBS energies were computed using the reoptimized structures and the hydride affinities were estimated based on the electronic energies for both sets of optimized structures. The results are summarized in Figure S46.

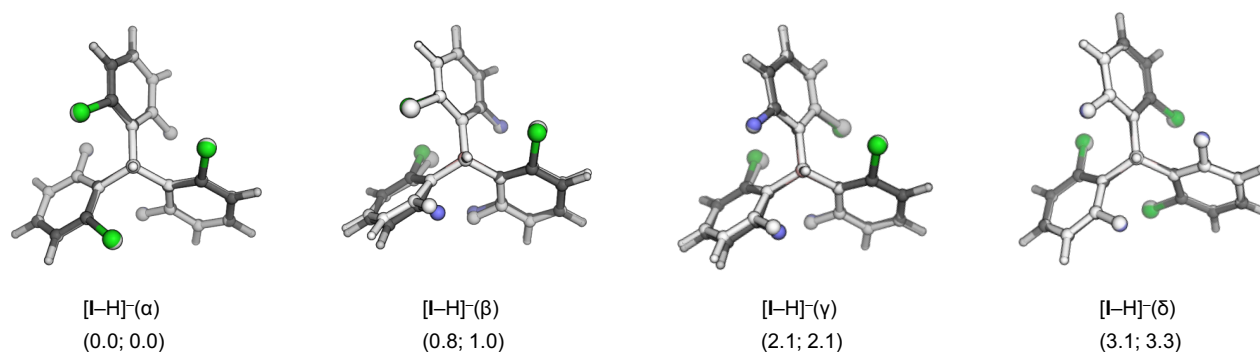


Figure S46. Overlay of optimized structures obtained with the 6-311G(d,p) and 6-311++G(d,p) basis sets. The original structures are in white, those obtained with the extended basis are colored. Relative stabilities are given in parentheses (in kcal/mol). First and second numbers correspond to results obtained with 6-311G(d,p) and 6-311++G(d,p) basis sets, respectively.

The overlay images display only slight variations in the orientation of the aryl groups, and the computed bond lengths differ by less than 0.005 Å. Our test calculations indicate that the hydride affinities obtained with our original protocol and those computed using the reoptimized structures differ by at most 0.2 kcal/mol, which confirms the relevance of the approximation used in our computational protocol.

2) Comparison of hydride and fluoride ion affinities

Calculations were carried out using our computational protocol to parallel the hydride ion and fluoride ion affinities (HIA and FIA) as two different measures of Lewis acidity. The FIA calculations were carried out for the four different rotameric states of fluoride adducts [I-F]⁻ with borane I, which are analogous to those of the hydride rotamers. The relative stabilities of hydride and fluoride species computed from the electronic energies are listed in Table S19. The results indicate that the relative stabilities of fluorides span a somewhat narrower energy range, the stability order of the rotamers follows that obtained for the analogous hydride forms.

Table S19. Relative stabilities (in kcal/mol) computed for various rotameric states of [I-H]⁻ hydride and [I-F]⁻ fluoride adducts.

	<i>hydrides</i>	<i>fluorides</i>
[I-X] ⁻ (α)	0.0	0.0
[I-X] ⁻ (β)	0.8	0.5
[I-X] ⁻ (γ)	2.1	1.6
[I-X] ⁻ (δ)	3.1	2.4

11. Additional Activation-Strain Analysis

To verify our assumption that the different stability of different hydride/piperidine complexes mainly originates from the difference in the back-strain, we carried out activation-strain analysis on some structures. In the activation-strain model^[44], the energy of adduct formation is separated into two terms, the strain energy and the interaction energy:

$$\Delta E = \Delta E_{\text{strain}} + \Delta E_{\text{int}}.$$

ΔE_{strain} is the energy required to distort the borane (and piperidine in the case of **p**-adducts) from their optimized geometry into their structure in the complex:

$$\Delta E_{\text{strain}} = \underbrace{E_{\text{borane}}^{\text{distorted}} - E_{\text{borane}}^{\text{opt}}}_{\Delta E_{\text{strain}}(\text{b})} \left(+ \underbrace{E_{\text{p}}^{\text{distorted}} - E_{\text{p}}^{\text{opt}}}_{\Delta E_{\text{strain}}(\text{p})} \right),$$

and ΔE_{int} is the energy gain from the interaction of the distorted molecules:

$$\Delta E_{\text{int}} = E_{\text{complex}} - E_{\text{borane}}^{\text{distorted}} - E_{\text{p/H}^+}^{\text{distorted}}.$$

This analysis was carried out at the B3LYP-D3/6-311G(d,p) level of theory.

We first compared the formation the borohydrides **[I-H]⁻(α)** and **[I-H]⁻(δ)**. These borohydrides can be derived from borane **I(β)** by the attack of a hydride-ion from the bottom and the top side respectively (see Table S3). Upon the bottom side attack, the chlorines of the aryl groups get closer to each other, while after a top side attack, the fluorine atoms will be close. The steric strain is expected to be smaller in the latter case, which is reflected in the 1.4 kcal/mol lower strain energy (Table S20). The interaction energy is 1.6 kcal/mol lower in this borohydride and thus the overall formation energy difference is 3.0 kcal/mol. These results suggest that the reduced steric strain and the larger interaction energy are equally important in the overall greater stability of the **[I-H]⁻(α)** adduct. However, we note that ΔE_{strain} is likely underestimated in the neutral borane as in the borohydride adduct, the negative charge is partially distributed among the aryl rings, and the repulsion is more enhanced between charged moieties.

Table S20. Strain, interaction and total formation energy of borohydrides **[I-H]⁻(α)** and **[I-H]⁻(δ)** [kcal/mol].

	ΔE_{strain}	ΔE_{int}	ΔE
[I-H]⁻(α)	23.1	-116.1	-93.0
[I-H]⁻(δ)	24.5	-114.5	-90.0

Next, we investigated the importance of steric strain in piperidine complexes. The activation-strain analysis was carried out for the most favored isomers of each adduct: **p-III(α)** (Table S4), **p-II(α)** (Table S5) and **p-I(α)** (Table S6). The results are collected in Table S21. The results reveal that the interaction energies and the strain energies originating from the distortion of the piperidine ($\Delta E_{\text{strain}}(\text{p})$) are similar in the three complexes and the changes in the stability can primarily be attributed to the changes in the back-strain ($\Delta E_{\text{strain}}(\text{b})$).

Table S21. Strain, interaction and total formation energy of piperidine adducts [kcal/mol].

	$\Delta E_{\text{strain}}(\text{b})$	$\Delta E_{\text{strain}}(\text{p})$	ΔE_{int}	ΔE
p-III(α)	48.5	3.4	-64.5	-12.6
p-II(α)	41.6	3.0	-63.9	-19.2
p-I(α)	36.0	3.2	-65.3	-26.0

12. ^{19}F NMR Spectra of the Quinuclidine+*Borane* Systems

In the presented piperidine–borane LA-LB adducts the *syn* positioned halogen atoms are able to form hydrogen bonds with the N–H group of the Lewis base which most likely increases the number of stable atropisomers per adduct. However, it is important to emphasize that this stabilizing effect is not prerequisite for atropisomer formation. To illustrate the atropisomeric dative adduct forming capacity of boranes **I** and **II** with a LB lacking N–H group, the ^{19}F spectra of the quinuclidine (1-azabicyclo[2.2.2]octane)+**I** and quinuclidine+**II** systems are shown in Figure S47. These were recorded during the LB screening described in Section 3 (see quinuclidine as entry C in Figure S2). Based on the observations with the **p**+borane systems, the downfield shifted (>-90 ppm) ^{19}F resonances indicate the presence of multiple atropisomers for both the quinuclidine–**I** and quinuclidine–**II** dative adducts. At ambient temperatures these adducts appear dynamic and kinetically more labile than the **p**–**I** and **p**–**II** adducts as only about 20% of the sp^2 borane forms adducts with the LB. Notably, in contrast to the **p**+borane systems, in the ^{19}F spectra of quinuclidine+**I** and quinuclidine+**II** systems no upfield shifted (<-107 ppm) ^{19}F NMR signals are present. This supports the assignment of the upfield shifted ^{19}F NMR signals of **p**–borane adducts to the N–H \cdots F hydrogen bonded *syn* fluorine atoms. (see SI section 5) Thus, the LB quinuclidine is also suitable to generate atropisomeric dative adducts with boranes **I** and **II** due to the directional anisotropy of the boranes, so the N–H \cdots Cl or N–H \cdots F hydrogen bond is not a prerequisite of multiple atropisomeric adduct formation. However, to demonstrate the MLA experimentally, we chose piperidine (**p**) as a model base which generated higher number of atropisomeric states for its respective dative adducts with **I**, and **II** (and also, with **III**). Also, for the **p**–borane adducts high quality ^{19}F NMR spectra could be obtained in a wide temperature range with sharp ^{19}F NMR signals that allowed their detailed structural and dynamic characterization of the **p**–borane systems.

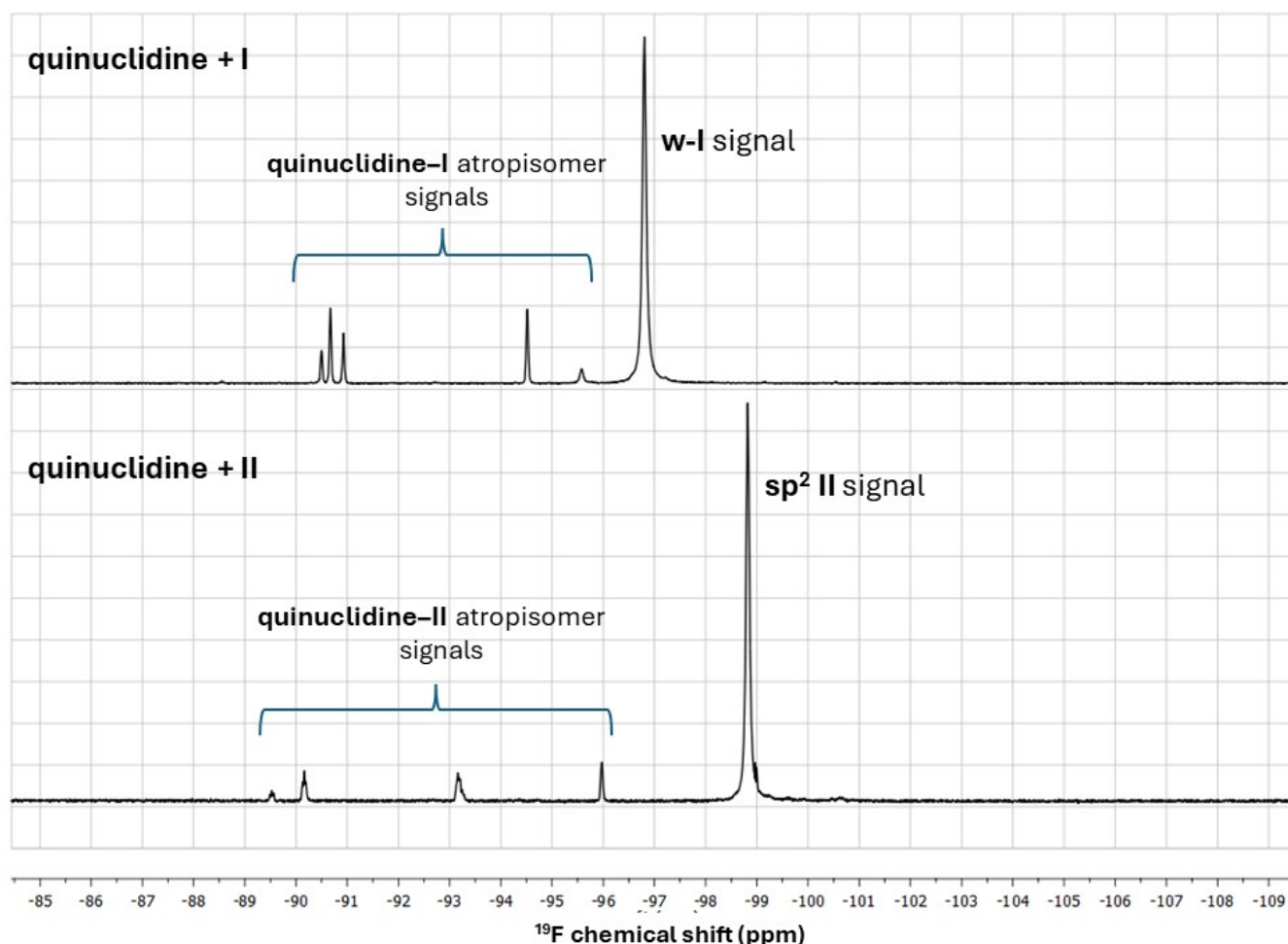


Figure S47. ^{19}F spectra (564 MHz) of the quinuclidine+**I** (top) and quinuclidine+**II** (bottom) systems using the quinuclidine to borane ratio of 3:1 recorded at 298.2 K in toluene-*d*₈.

References

- [24] C. L. Perrin, T. J. Dwyer, Application of two-dimensional NMR to kinetics of chemical exchange. *Chem. Rev.*, **1990**, *90*, 935–967. DOI: 10.1021/cr00104a002
- [25] Schrödinger Release 2017-1: Schrödinger, LLC, New York, NY, **2017**
- [26] a) A. D. Becke, Density-functional Thermochemistry. III. The Role of Exact Exchange. *J. Chem. Phys.*, **1993**, *98*, 5648–5652. DOI: 10.1063/1.464913 b) S. Grimme, J. Antony, S. Ehrlich, H. Krieg, A Consistent and Accurate Ab Initio Parameterization of Density Functional Dispersion Correction (DFT-D) for the 94 Elements H-Pu. *J. Chem. Phys.*, **2010**, *132*, 154104. DOI: 10.1063/1.3382344
- [27] M. J. Frisch, G. W. Trucks, H. B. Schlegel, G. E. Scuseria, M. A. Robb, J. R. Cheeseman, G. Scalmani, V. Barone, B. Mennucci, G. A. Petersson, H. Nakatsuji, M. Caricato, X. Li, H. P. Hratchian, A. F. Izmaylov, J. Bloino, G. Zheng, J. L. Sonnenberg, M. Hada, M. Ehara, K. Toyota, R. Fukuda, J. Hasegawa, M. Ishida, T. Nakajima, Y. Honda, O. Kitao, H. Nakai, T. Vreven, Jr J. A. Montgomery, J. E. Peralta, F. Ogliaro, M. Bearpark, J. J. Heyd, E. Brothers, K. N. Kudin, V. N. Staroverov, R. Kobayashi, J. Normand, K. Raghavachari, A. Rendell, J. C. Burant, S. S. Iyengar, J. Tomasi, M. Cossi, N. Rega, J. M. Millam, M. Klene, J. E. Knox, J. B. Cross, V. Bakken, C. Adamo, J. Jaramillo, R. Gomperts, R. E. Stratmann, O. Yazyev, A. J. Austin, R. Cammi, C. Pomelli, J. W. Ochterski, R. L. Martin, K. Morokuma, V. G. Zakrzewski, G. A. Voth, P. Salvador, J. J. Dannenberg, S. Dapprich, A. D. Daniels, Ö. Farkas, J. B. Foresman, J. V. Ortiz, J. Cioslowski, D. J. Fox, Gaussian 09, Revision D.01, Gaussian, Inc. Wallingford CT, **2009**
- [28] a) R. Krishnan, J. S. Binkley, R. Seeger, J. A. Pople, Self-consistent molecular orbital methods. XX. A basis set for correlated wave functions. *J. Chem. Phys.*, **1980**, *72*, 650–654. DOI: 10.1063/1.438955 b) A. D. McLean, G. S. Chandler, Contracted Gaussian basis sets for molecular calculations. I. Second row atoms, Z=11–18. *J. Chem. Phys.*, **1980**, *72*, 5639–5648. DOI: 10.1063/1.438980 c) T. Clark, J. Chandrasekhar, G. W. Spitznagel, P. v. R. Schleyer, Efficient diffuse function-augmented basis sets for anion calculations. III. The 3-21+G basis set for first-row elements, Li–F. *J. Comput. Chem.*, **1983**, *4*, 294–301. DOI: 10.1002/jcc.540040303 d) M. J. Frisch, J. A. Pople, J. S. Binkley, Self-consistent molecular orbital methods 25. Supplementary functions for Gaussian basis sets. *J. Chem. Phys.*, **1984**, *80*, 3265–3269. DOI: 10.1063/1.447079
- [29] A. V. Marenich, C. J. Cramer, D. G. Truhlar, Universal Solvation Model Based on Solute Electron Density and on a Continuum Model of the Solvent Defined by the Bulk Dielectric Constant and Atomic Surface Tensions. *J. Phys. Chem. B*, **2009**, *113*, 6378–6396. DOI: 10.1021/jp810292n
- [30] a) M. Kállay, P. R. Nagy, D. Mester, Z. Rolik, G. Samu, J. Csontos, J. Csóka, P. B. Szabó, L. Gyevi-Nagy, B. Hégyel, I. Ladjánszki, L. Szegedy, B. Ladóczki, K. Petrov, M. Farkas, P. D. Mezei, A. Ganyecz, The MRCC Program System: Accurate Quantum Chemistry from Water to Proteins. *J. Chem. Phys.*, **2020**, *152*, 074107. DOI: 10.1063/1.5142048 b) M. Kállay, P. R. Nagy, D. Mester, Z. Rolik, G. Samu, J. Csontos, J. Csóka, P. B. Szabó, L. Gyevi-Nagy, B. Hégyel, I. Ladjánszki, L. Szegedy, B. Ladóczki, K. Petrov, M. Farkas, P. D. Mezei, A. Ganyecz, R. A. Horváth, MRCC, a Quantum Chemical Program Suite. (<https://www.mrcc.hu/>)
- [31] T. H. Dunning, Gaussian basis sets for use in correlated molecular calculations. I. The atoms boron through neon and hydrogen. *J. Chem. Phys.*, **1989**, *90*, 1007–1023. DOI: 10.1063/1.456153
- [32] a) A. Karton, J. M. L. Martin, Comment on: “Estimating the Hartree–Fock limit from finite basis set calculations” [Jensen F (2005) *Theor Chem Acc* 113:267]. *Theor. Chem. Acc.*, **2006**, *115*, 330–333. DOI: 10.1007/s00214-005-0028-6 b) T. Helgaker, W. Klopper, H. Koch, J. Noga, Basis-set convergence of correlated calculations on water. *J. Chem. Phys.*, **1997**, *106*, 9639–9646. DOI: 10.1063/1.473863
- [33] a) F. London, The quantum theory of inter-atomic currents in aromatic combinations, *J. Phys. Radium*, **1937**, *8*, 397–409. DOI: 10.1051/jphysrad:01937008010039700 b) R. McWeeny, Perturbation Theory for Fock-Dirac Density Matrix. *Phys. Rev.*, **1962**, *126*, 1028. DOI: 10.1103/PhysRev.126.1028 c) R. Ditchfield, Self-consistent perturbation theory of diamagnetism. 1. Gauge-invariant LCAO method for N.M.R. chemical shifts. *Mol. Phys.*, **1974**, *27*, 789–807. DOI: 10.1080/00268977400100711 d) J. R. Cheeseman, G. W. Trucks, T. A. Keith, and M. J. Frisch, A Comparison of Models for Calculating Nuclear Magnetic Resonance Shielding Tensors. *J. Chem. Phys.*, **1996**, *104*, 5497–509. DOI: 10.1063/1.471789
- [34] CrystalClear SM 1.4.0, Rigaku/MSI Inc. **2008**
- [35] NUMABS: T. Higashi, Rigaku/MSI Inc. **1998**, rev. **2002**
- [36] R. H. Blessing, An empirical correction for absorption anisotropy. *Acta Cryst.*, **1995**, *A51*, 33–38. DOI: 10.1107/S0108767394005726
- [37] G. M. Sheldrick, A short history of SHELX. *Acta Cryst.*, **2008**, *A64*, 112–122. DOI: 10.1107/S0108767307043930
- [38] G. M. Sheldrick, Crystal structure refinement with SHELXL. *Acta Cryst.*, **2015**, *C71*, 3–8. DOI: 10.1107/S2053229614024218
- [39] M. C. Burla, R. Caliandro, B. Carrozzini, G. L. Cascarano, C. Cuocci, C. Giacovazzo, M. Mallamo, A. Mazzzone, G. Polidori, Crystal structure determination and refinement via SIR2014. *J. Appl. Crystallogr.*, **2015**, *48*, 306–309. DOI: 10.1107/S1600576715001132
- [40] L. J. Farrugia, WinGX and ORTEP for Windows: an update. *J. Appl. Crystallogr.*, **2012**, *45*, 849–854. DOI: 10.1107/S0021889812029111
- [41] A. L. Spek, Structure validation in chemical crystallography. *Acta Cryst.*, **2009**, *D65*, 148–155. DOI: 10.1107/S090744490804362X
- [42] C. F. Macrae, P. R. Edgington, P. McCabe, E. Pidcock, G. P. Shields, R. Taylor, M. Towler, J. van de Streek, Mercury: Visualization and analysis of crystal structures. *J. Appl. Crystallogr.*, **2006**, *39*, 453–457. DOI: 10.1107/S002188980600731X
- [43] A. Bondi, van der Waals Volumes and Radii. *J. Phys. Chem.*, **1964**, *68*, 441–451. DOI: 10.1021/j100785a001
- [44] W. J. van Zeist, F. M. Bickelhaupt: The activation strain model of chemical reactivity. *Org. Biomol. Chem.*, **2010**, *8*, 3118–3127. DOI: 10.1039/B926828F

List of Atomic Coordinates

Boranes:

III(α):				II(α):			
B	-0.03735100	-0.05510100	-0.06874000	B	-0.06775800	0.02352000	-0.13018700
C	-1.61019800	0.01204900	-0.12890800	C	-1.39155000	0.85234000	-0.25232300
C	0.80990700	1.26476500	0.07559300	C	1.30310400	0.79633500	-0.06227300
C	0.67285000	-1.44540700	-0.18244700	C	-0.10154000	-1.54081500	-0.13519500
C	1.72700000	-1.88194100	0.63656900	C	0.66155800	-2.37712800	0.69784300
C	2.33212700	-3.12385900	0.48658100	C	0.60158900	-3.76448500	0.63241300
C	1.89468100	-3.97501700	-0.52455300	C	-0.23117800	-4.36622600	-0.30624300
C	0.85484400	-3.59395100	-1.36602900	C	-1.00433800	-3.58878500	-1.16181700
C	0.27169900	-2.35559400	-1.16663700	C	-0.92589800	-2.21290600	-1.04709100
Cl	2.28131700	-0.87212200	1.96822300	Cl	1.69842800	-1.68289800	1.93960000
H	3.12940200	-3.41799900	1.15560300	H	1.19772100	-4.36020400	1.31023900
H	2.36714200	-4.94139500	-0.65364900	H	-0.27664100	-5.44688800	-0.36864900
H	0.49297800	-4.22834100	-2.16433300	H	-1.65841000	-4.02177500	-1.90702200
F	-0.72132000	-1.99146200	-2.00904900	F	-1.67143700	-1.47783200	-1.90280400
C	1.82887800	1.60461000	-0.82957400	C	2.28881200	0.66203000	-1.04713600
C	2.58223700	2.76663800	-0.72451900	C	3.49694300	1.34677100	-1.00902100
C	2.33812700	3.63707900	0.33164600	C	3.75251100	2.20094300	0.05847900
C	1.34848600	3.34716700	1.26354600	C	2.80788700	2.37114500	1.06552000
C	0.60516600	2.18278400	1.11761500	C	1.60749100	1.67784700	0.98243100
Cl	2.15902300	0.56432700	-2.21552400	Cl	1.98045400	-0.38264800	-2.43562000
H	3.34432000	2.98210400	-1.46136000	H	4.21857300	1.21252700	-1.80370600
H	2.92235600	4.54434400	0.42911600	H	4.69257000	2.73765100	0.10553200
H	1.15383300	4.00871800	2.09699200	H	2.99633600	3.02669000	1.90522500
Cl	-0.59227100	1.83585700	2.36350100	Cl	0.44864800	1.87232200	2.29863400
C	-2.42061500	-0.70936700	0.76197000	C	-2.54261800	0.64156100	0.52371800
C	-3.80839400	-0.66191700	0.73543700	C	-3.69507500	1.40545700	0.38594800
C	-4.43821300	0.11893000	-0.22755300	C	-3.72966800	2.41467500	-0.57285900
C	-3.68577300	0.84331200	-1.14468500	C	-2.62022400	2.66441300	-1.37306600
C	-2.29920300	0.78271600	-1.07687800	C	-1.48916400	1.88902700	-1.18562900
Cl	-1.67229700	-1.67963600	2.03159000	Cl	-2.53386600	-0.58711400	1.78706600
H	-4.38055800	-1.22585700	1.45988900	H	-4.54757000	1.21362100	1.02334200
H	-5.52026200	0.16173100	-0.26390100	H	-4.62710400	3.00959600	-0.69304900
H	-4.16135000	1.44606400	-1.90673100	H	-2.61384700	3.43718600	-2.13038200
Cl	-1.39288200	1.68047600	-2.29423300	F	-0.42489400	2.13411700	-1.98356800

II(B):				II(y):			
B	0.00000000	0.00000000	0.06568300	B	0.00000000	0.00000000	-0.17947300
C	1.32676300	0.33940800	-0.69139000	C	0.00000000	0.00000000	1.39572600
C	0.00000000	0.00000000	1.64168700	C	0.40754300	-1.29575500	-0.96011700
C	-1.32676300	-0.33940800	-0.69139000	C	-0.40754300	1.29575500	-0.96011700
C	-2.53627200	0.23307600	-0.28066500	C	-1.27961500	1.20115500	-2.05232700
C	-3.75483200	0.00769900	-0.89652700	C	-1.74566400	2.28255500	-2.77751000
C	-3.79348400	-0.86069600	-1.98161100	C	-1.30745400	3.55309600	-2.41988800
C	-2.63014600	-1.48006700	-2.43057900	C	-0.42629200	3.71953500	-1.35603700
C	-1.42659100	-1.20798000	-1.79214300	C	0.00000000	2.60352600	-0.64443300
F	-2.51787900	1.09578400	0.75963400	F	-1.73680800	-0.02223400	-2.40456400
H	-4.63806400	0.50847400	-0.52263200	H	-2.43401300	2.11511200	-3.59532900
H	-4.73421000	-1.06049300	-2.48052000	H	-1.65144000	4.41915100	-2.97254900
H	-2.65296100	-2.16874200	-3.26417900	H	-0.06844400	4.70172200	-1.07868000
Cl	0.00000000	-2.05599100	-2.38157500	Cl	1.14952900	2.88627500	0.65999800
C	-0.20052500	-1.16745400	2.38432000	C	1.27961500	-1.20115500	-2.05232700
C	-0.19781800	-1.19153800	3.77328600	C	1.74566400	-2.28255500	-2.77751000
C	0.00000000	0.00000000	4.46412200	C	1.30745400	-3.55309600	-2.41988800
C	0.19781800	1.19153800	3.77328600	C	0.42629200	-3.71953500	-1.35603700
C	0.20052500	1.16745400	2.38432000	C	0.00000000	-2.60352600	-0.64443300
Cl	-0.41764200	-2.69142400	1.52091700	F	1.73680800	0.02223400	-2.40456400
H	-0.34504300	-2.12600200	4.29821300	H	2.43401300	-2.11511200	-3.59532900
H	0.00000000	0.00000000	5.54762600	H	1.65144000	-4.41915100	-2.97254900
H	0.34504300	2.12600200	4.29821300	H	0.06844400	-4.70172200	-1.07868000
Cl	0.41764200	2.69142400	1.52091700	Cl	-1.14952900	-2.88627500	0.65999800
C	1.42659100	1.20798000	-1.79214300	C	-1.15191500	0.27642500	2.14362400
C	2.63014600	1.48006700	-2.43057900	C	-1.17474900	0.27536300	3.53205900
C	3.79348400	0.86069600	-1.98161100	C	0.00000000	0.00000000	4.22382100
C	3.75483200	-0.00769900	-0.89652700	C	1.17474900	-0.27536300	3.53205900
C	2.53627200	-0.23307600	-0.28066500	C	1.15191500	-0.27642500	2.14362400
Cl	0.00000000	2.05599100	-2.38157500	Cl	-2.67474000	0.57460500	1.30323500
H	2.65296100	2.16874200	-3.26417900	H	-2.09773400	0.48261500	4.05686300
H	4.73421000	1.06049300	-2.48052000	H	0.00000000	0.00000000	5.30729500
H	4.63806400	-0.50847400	-0.52263200	H	2.09773400	-0.48261500	4.05686300
F	2.51787900	-1.09578400	0.75963400	Cl	2.67474000	-0.57460500	1.30323500

I(α):				I(β):			
B	-0.09109900	-0.10607600	0.08122300	B	0.00000000	0.00000000	0.22995100
C	1.00805600	-1.21229900	-0.05594700	C	0.00000000	-1.56574500	0.25364600
C	0.29315300	1.40988500	0.16243900	C	1.35597500	0.78287300	0.25364600
C	-1.59961300	-0.52448700	0.15972700	C	-1.35597500	0.78287300	0.25364600
C	-2.62560100	0.02338000	-0.62420100	C	-1.69050600	1.82657100	-0.62144800
C	-3.95406500	-0.36989900	-0.50999100	C	-2.90485500	2.49986700	-0.56196500
C	-4.29601600	-1.33644000	0.43184400	C	-3.82937800	2.14345300	0.41638700
C	-3.31922500	-1.91189600	1.23807500	C	-3.54743100	1.11862700	1.31396000
C	-2.00866300	-1.49954100	1.07336800	C	-2.33188300	0.46701200	1.20243500
Cl	-2.23452500	1.21445600	-1.86462700	Cl	-0.57450100	2.26828200	-1.91191900
H	-4.70379300	0.07226800	-1.15208000	H	-3.12130400	3.28486900	-1.27387700
H	-5.33007200	-1.64300100	0.53444900	H	-4.77569600	2.66755300	0.47597600
H	-3.55060000	-2.66229000	1.98252700	H	-4.24181100	0.81935900	2.08793200
F	-1.06936700	-2.05594200	1.87428600	F	-2.06312600	-0.51912400	2.09013900
C	-0.26005600	2.21678500	1.16145400	C	1.57038600	1.78596300	1.20243500
C	0.03362200	3.55777800	1.33183400	C	2.74247500	2.51285100	1.31396000
C	0.92178300	4.15466500	0.44322200	C	3.77097400	2.24461200	0.41638700
C	1.49733100	3.41208300	-0.58434800	C	3.61737600	1.26574500	-0.56196500
C	1.18409100	2.06359700	-0.70268100	C	2.42711000	0.55073600	-0.62144800
F	-1.10917000	1.64564600	2.04745500	F	0.58198800	2.04628200	2.09013900
H	-0.42859000	4.10365400	2.14368400	H	2.83049100	3.26383700	2.08793200
H	1.16699200	5.20469900	0.54834100	H	4.69801700	2.80209800	0.47597600
H	2.17830200	3.87058400	-1.28849700	H	4.40543200	1.06069400	-1.27387700
Cl	1.90409100	1.18335500	-2.04891800	Cl	2.25164000	-0.63660800	-1.91191900
C	2.20014200	-1.27008900	0.68503100	C	-0.73660400	-2.37730700	-0.62144800
C	3.15137000	-2.26759200	0.50683800	C	-0.71252000	-3.76561200	-0.56196500
C	2.93407500	-3.25008100	-0.45510300	C	0.05840400	-4.38806600	0.41638700
C	1.77156200	-3.24327100	-1.21834400	C	0.80495600	-3.63147900	1.31396000
C	0.84575100	-2.24048600	-0.99152000	C	0.76149700	-2.25297600	1.20243500
Cl	2.51756400	-0.07862700	1.94455800	Cl	-1.67713900	-1.63167400	-1.91191900
H	4.04568000	-2.27279000	1.11502600	H	-1.28412800	-4.34556300	-1.27387700
H	3.67555500	-4.02530300	-0.60688800	H	0.07767900	-5.46965100	0.47597600
H	1.57182500	-3.98802800	-1.97740400	H	1.41132000	-4.08319600	2.08793200
F	-0.26781900	-2.23727000	-1.75981700	F	1.48113800	-1.52715700	2.09013900

Hydride Complexes:

[III-H] ⁻ (α):				[III-H] ⁻ (β):			
C	0.4819280	1.4448770	0.1930300	C	-1.2035620	-1.1088490	0.3300020
B	-0.0270040	-0.0968840	0.4433760	B	0.0045900	-0.0329660	0.5826750
H	-0.0669230	-0.1646490	1.6465150	H	0.0095910	0.0944070	1.7824920
C	1.0158520	-1.2811340	0.0250130	C	-0.3056360	1.4812030	0.0345520
C	-1.5687500	-0.3901830	-0.0395750	C	1.5198650	-0.5906550	0.2847710
C	-2.3732310	-1.3037640	0.6668450	C	2.6161220	-0.0297960	0.9697630
C	-3.7173470	-1.5522920	0.4069730	C	3.9274870	-0.4864810	0.8935190
C	-4.3412560	-0.8746130	-0.6326870	C	4.2166410	-1.5786370	0.0853430
C	-3.6000620	0.0090660	-1.4051670	C	3.1948630	-2.1655030	-0.6481430
C	-2.2554810	0.2134450	-1.1057600	C	1.9010660	-1.6594990	-0.5451500
Cl	-1.6763750	-2.2762230	1.9864160	Cl	2.3851460	1.4030890	2.0017660
H	-4.2591010	-2.2677810	1.0124470	H	4.7040890	0.0108470	1.4605220
H	-5.3904410	-1.0455430	-0.8481260	H	5.2302650	-1.9583560	0.0166010
H	-4.0481260	0.5301920	-2.2416450	H	3.3920800	-2.9991040	-1.3101950
Cl	-1.4008740	1.2844270	-2.2396480	Cl	0.7288280	-2.4222060	-1.6443170
C	2.2091810	-1.5140190	0.7235720	C	-1.2458820	2.2893750	0.7022760
C	3.0926350	-2.5587770	0.4610440	C	-1.5200820	3.6178030	0.3951140
C	2.7956850	-3.4525240	-0.5614840	C	-0.8348260	4.2250350	-0.6494410
C	1.6329510	-3.2759730	-1.3038100	C	0.0850690	3.4825940	-1.3769150
C	0.7993620	-2.2114310	-0.9953250	C	0.3128940	2.1523260	-1.0338110
Cl	2.6992850	-0.3990300	2.0195950	Cl	-2.2208600	1.6154630	2.0310800
H	3.9957390	-2.6616220	1.0489190	H	-2.2605890	4.1607580	0.9684840
H	3.4679600	-4.2749260	-0.7803790	H	-1.0259160	5.2623340	-0.9021150
H	1.3612560	-3.9346190	-2.1198200	H	0.6162870	3.9183530	-2.2135200
F	-0.2962350	-2.0765060	-1.7913660	Cl	1.4243650	1.2933290	-2.1240470
C	1.5119200	1.8973270	-0.6498900	C	-2.2238910	-1.1126240	-0.6284980
C	1.9734160	3.2101200	-0.7091160	C	-3.2664280	-2.0395660	-0.6699110
C	1.3792850	4.1785690	0.0879100	C	-3.3148220	-3.0526500	0.2787130
C	0.3265900	3.8173190	0.9187980	C	-2.3180590	-3.1260580	1.2469500
C	-0.0857500	2.4894470	0.9493240	C	-1.3151140	-2.1707320	1.2373440
Cl	2.2930510	0.7998630	-1.8128650	Cl	-2.2211190	0.0706300	-1.9553410
H	2.7805050	3.4632200	-1.3847670	H	-4.0175080	-1.9667060	-1.4460420
H	1.7249240	5.2060240	0.0535370	H	-4.1167770	-3.7824970	0.2580210
H	-0.1726010	4.5499060	1.5401390	H	-2.2984740	-3.9024100	2.0021970
Cl	-1.4594190	2.1615530	2.0347630	F	-0.3609300	-2.3068560	2.1973230

[II-H]-(α):			[II-H]-(β):				
C	1.1929590	0.9740780	0.0328570	C	0.8313130	1.3058370	0.3821430
B	-0.0972160	0.0288250	0.4082190	B	-0.0763920	-0.0509530	0.5381840
H	-0.1582900	0.0626980	1.6125850	H	-0.1031330	-0.2179500	1.7330840
C	0.0969090	-1.5625060	0.0861600	C	0.5876870	-1.4205010	-0.0509880
C	-1.5172220	0.6513510	-0.1102230	C	-1.6535250	0.1424960	0.1191750
C	-2.7415620	0.3642930	0.5090220	C	-2.6623710	-0.5769590	0.7870630
C	-3.9666810	0.9202570	0.1454030	C	-4.0294470	-0.4180030	0.5805680
C	-4.0108570	1.8238430	-0.9102010	C	-4.4678990	0.5032180	-0.3619680
C	-2.8366260	2.1393560	-1.5848550	C	-3.5306820	1.2162690	-1.0971930
C	-1.6513550	1.5461780	-1.1749520	C	-2.1745210	1.0104270	-0.8554230
Cl	-2.7978580	-0.8138400	1.8420080	Cl	-2.2294810	-1.8358560	1.9717560
H	-4.8650160	0.6432430	0.6822220	H	-4.7324250	-1.0118820	1.1508320
H	-4.9530670	2.2713350	-1.2073130	H	-5.5286400	0.6505200	-0.5340620
H	-2.8167810	2.8250370	-2.4233550	H	-3.8381660	1.9164820	-1.8635610
F	-0.5494310	1.8764550	-1.9033670	Cl	-1.0874160	1.8945390	-1.9515100
C	1.0196980	-2.3575010	0.7801860	C	1.6913710	-2.0420960	0.5502440
C	1.1741520	-3.7319350	0.6087170	C	2.2544770	-3.2441620	0.1273210
C	0.3651700	-4.3920330	-0.3086790	C	1.7032260	-3.8988150	-0.9682490
C	-0.5673380	-3.6642630	-1.0404880	C	0.6123210	-3.3343980	-1.6204270
C	-0.6633760	-2.2974270	-0.8282490	C	0.1031940	-2.1324320	-1.1516090
Cl	2.1178710	-1.6018460	1.9595440	Cl	2.4958320	-1.2597030	1.9302260
H	1.9166210	-4.2671500	1.1867720	H	3.1111610	-3.6511970	0.6490570
H	0.4648530	-5.4620650	-0.4546700	H	2.1244980	-4.8369890	-1.3126580
H	-1.2131090	-4.1263000	-1.7774380	H	0.1531530	-3.7956480	-2.4864330
F	-1.5630310	-1.6457660	-1.6151730	F	-0.9386810	-1.6214820	-1.8631890
C	2.1514810	0.7540960	-0.9702320	C	0.5402340	2.3608880	1.2578290
C	3.2897100	1.5311480	-1.1694570	C	1.2383740	3.5533220	1.3532830
C	3.5103870	2.6342700	-0.3559640	C	2.3314900	3.7515410	0.5151700
C	2.5770520	2.9505880	0.6227690	C	2.6770450	2.7604400	-0.3938640
C	1.4619820	2.1337960	0.7835510	C	1.9255570	1.5850790	-0.4454840
Cl	1.9408910	-0.5575680	-2.1550910	F	-0.5237150	2.2306020	2.0961630
H	3.9816330	1.2752120	-1.9617840	H	0.9161130	4.2958740	2.0732450
H	4.3922730	3.2504810	-0.4937780	H	2.9035100	4.6716540	0.5642520
H	2.7040290	3.8189310	1.2567410	H	3.5122970	2.8916130	-1.0698680
Cl	0.3119300	2.6781200	2.0308100	Cl	2.4186000	0.4438030	-1.7185370

[II-H]-(γ):			[II-H]-(δ):				
C	1.4446310	0.8656700	0.1851930	C	0.9737620	-1.2124510	0.2073580
B	0.0216720	0.1448470	0.5680450	B	-0.0312120	-0.0048440	0.6837570
H	0.0158340	0.0823280	1.7731070	H	0.0839510	-0.0095220	1.8858990
C	-0.0506730	-1.4307630	0.1040880	C	-1.6304920	-0.2951750	0.4732050
C	-1.2917860	1.0581370	0.2337050	C	0.4543300	1.4964730	0.2475070
C	-2.5261350	0.8562140	0.8695590	C	0.0768590	2.5607090	1.0768740
C	-3.6565840	1.6491240	0.6848790	C	0.4521060	3.8845820	0.9163430
C	-3.5872980	2.7306230	-0.1858920	C	1.2719460	4.2177360	-0.1575670
C	-2.3969560	2.9869580	-0.8575570	C	1.6758500	3.2223190	-1.0377070
C	-1.3097420	2.1546690	-0.6337420	C	1.2565990	1.9086000	-0.8228730
Cl	-2.7311940	-0.5282450	1.9677930	F	-0.7383360	2.3029830	2.1350480
H	-4.5713530	1.4150370	1.2142400	H	0.0966990	4.6222270	1.6256850
H	-4.4546360	3.3625630	-0.3427880	H	1.5863120	5.2441730	-0.3122010
H	-2.2922150	3.8071140	-1.5576030	H	2.2994100	3.4529850	-1.8919910
F	-0.1954060	2.4457290	-1.3586470	Cl	1.7624720	0.7468860	-2.0703400
C	0.7583240	-2.3812140	0.7579330	C	-2.2219970	-1.2502190	1.3116510
C	0.7306060	-3.7527680	0.5281920	C	-3.5683950	-1.5738170	1.3499230
C	-0.1530020	-4.2619240	-0.4145630	C	-4.4361930	-0.9101600	0.4879470
C	-0.9668830	-3.3859250	-1.1188530	C	-3.9268820	0.0387200	-0.3887920
C	-0.8893120	-2.0197600	-0.8584990	C	-2.5578140	0.3120950	-0.3827150
Cl	1.9491600	-1.8577700	1.9756560	F	-1.4239050	-1.9475640	2.1647350
H	1.3922210	-4.4046670	1.0843120	H	-3.9076700	-2.3329890	2.0442830
H	-0.1988310	-5.3285800	-0.6055960	H	-5.4968280	-1.1367080	0.4923200
H	-1.6513060	-3.7479470	-1.8754710	H	-4.5733280	0.5576740	-1.0850170
Cl	-1.9186560	-1.0220990	-1.9137660	Cl	-2.0216100	1.4642130	-1.6269890
C	1.9894320	1.7830240	1.0920420	C	0.7272990	-2.2177780	-0.7438790
C	3.2105620	2.4256170	0.9563080	C	1.5828720	-3.2823920	-1.0182260
C	3.9784320	2.1658450	-0.1742320	C	2.7915410	-3.3766480	-0.3425020
C	3.4954570	1.2871710	-1.1354560	C	3.1278060	-2.3952050	0.5811920
C	2.2557030	0.6775380	-0.9399340	C	2.2311940	-1.3604310	0.8255030
F	1.2840100	2.0969770	2.2123310	Cl	-0.7190000	-2.1581120	-1.7781060
H	3.5327170	3.1112460	1.7308330	H	1.3035830	-4.0143870	-1.7654190
H	4.9397190	2.6495700	-0.3096600	H	3.4711350	-4.1975830	-0.5440560
H	4.0601450	1.0787410	-2.0352010	H	4.0726620	-2.4241050	1.1088050
Cl	1.7073520	-0.3614980	-2.2743050	Cl	2.8015490	-0.1434620	1.9945760

[I-H] ⁻ (α):			[I-H] ⁻ (β):				
C	0.0000000	1.5796600	-0.0636700	C	1.3530610	0.8663960	0.2463930
B	0.0000000	0.0000000	0.3635700	B	-0.0583120	0.0918480	0.5703270
H	0.0000000	0.0000000	1.5708290	H	-0.0889940	-0.0732120	1.7650360
C	1.3680250	-0.7898300	-0.0636700	C	-0.0466230	-1.4264980	-0.0546960
C	-1.3680250	-0.7898300	-0.0636700	C	-1.4165260	0.9495230	0.2490250
C	-1.8075350	-1.9477360	0.5917960	C	-2.6727670	0.5648800	0.7462290
C	-2.9953700	-2.6206440	0.3093020	C	-3.8573680	1.2749300	0.5652950
C	-3.8223390	-2.1352200	-0.6969340	C	-3.8286740	2.4649560	-0.1530820
C	-3.4376430	-1.0020290	-1.4057580	C	-2.6195610	2.9119650	-0.6715560
C	-2.2397700	-0.3845040	-1.0779240	C	-1.4752190	2.1546330	-0.4582970
Cl	-0.7991760	-2.6718670	1.8684160	Cl	-2.8268080	-0.9451750	1.6771760
H	-3.2588420	-3.5082830	0.8702520	H	-4.7812540	0.8961380	0.9834790
H	-4.7534310	-2.6401270	-0.9303070	H	-4.7387230	3.0348450	-0.3056990
H	-4.0363490	-0.5912290	-2.2098120	H	-2.5374730	3.8300780	-1.2408760
F	-1.9103890	0.6951170	-1.8404050	F	-0.3383600	2.6667310	-1.0047510
C	2.5905570	-0.5915030	0.5917960	C	0.7929830	-2.4325280	0.4437610
C	3.7672300	-1.2837450	0.3093020	C	0.8140820	-3.7508120	-0.0105320
C	3.7603250	-2.2426330	-0.6969340	C	-0.0514720	-4.1269740	-1.0305120
C	2.5866040	-2.4760720	-1.4057580	C	-0.9076970	-3.1783400	-1.5793150
C	1.4528760	-1.7474460	-1.0779240	C	-0.8720440	-1.8826520	-1.0872850
Cl	2.7134930	0.6438270	1.8684160	Cl	1.9431540	-2.0578540	1.7511600
H	4.6676830	-1.0680990	0.8702520	H	1.4976850	-4.4627200	0.4342240
H	4.6631320	-2.7965280	-0.9303070	H	-0.0547470	-5.1481230	-1.3959710
H	2.5301940	-3.1999660	-2.2098120	H	-1.5948890	-3.4141190	-2.3828940
F	0.3532060	-2.0020040	-1.8404050	F	-1.7135890	-1.0040850	-1.6968360
C	0.7868950	2.1319500	-1.0779240	C	2.0371460	1.5222400	1.2759260
C	0.8510390	3.4781010	-1.4057580	C	3.2721530	2.1440830	1.1547640
C	0.0620150	4.3778530	-0.6969340	C	3.9037770	2.1407390	-0.0837320
C	-0.7718590	3.9043890	0.3093020	C	3.2786370	1.5292340	-1.1638960
C	-0.7830220	2.5392400	0.5917960	C	2.0361990	0.9257620	-0.9751850
F	1.5571830	1.3068870	-1.8404050	F	1.4790020	1.5771490	2.5151240
H	1.5061550	3.7911960	-2.2098120	H	3.7109650	2.6135760	2.0270040
H	0.0902990	5.4366550	-0.9303070	H	4.8709250	2.6154700	-0.2093420
H	-1.4088410	4.5763810	0.8702520	H	3.7359660	1.5244540	-2.1450650
Cl	-1.9143170	2.0280400	1.8684160	Cl	1.2947190	0.2416760	-2.4391130

[l-H]-(γ):			[l-H]-(δ):				
C	0.9974600	-1.2434910	0.2031030	C	-1.3576880	0.8340250	0.4031920
B	-0.0902260	-0.1172150	0.6713680	B	0.0000000	0.0000000	0.7877840
H	-0.0243480	-0.1333300	1.8767340	H	0.0000000	0.0000000	1.9963030
C	-1.6519550	-0.4823230	0.3174440	C	1.4011300	0.7587800	0.4031920
C	0.2724710	1.4373720	0.2822310	C	-0.0434430	-1.5928040	0.4031920
C	-0.3731860	2.4339560	1.0278610	C	0.7336900	-2.4615110	1.1817670
C	-0.1687970	3.7988680	0.9092330	C	0.7767000	-3.8409770	1.0599310
C	0.7548150	4.2531960	-0.0273930	C	-0.0081480	-4.4471680	0.0836880
C	1.4292770	3.3307100	-0.8156740	C	-0.7947140	-3.6550100	-0.7422770
C	1.1704710	1.9683060	-0.6519470	C	-0.7864570	-2.2693260	-0.5721130
F	-1.2902400	2.0543860	1.9592950	F	1.5374530	-1.9304660	2.1425450
H	-0.7298920	4.4722720	1.5459340	H	1.4194620	-4.4080540	1.7224650
H	0.9424380	5.3147850	-0.1461710	H	0.0000000	-5.5248220	-0.0386110
H	2.1442770	3.6531680	-1.5617560	H	-1.4014930	-4.0951140	-1.5233550
Cl	2.0514380	0.9077890	-1.7776280	Cl	-1.7549810	-1.3657600	-1.7592320
C	-2.4094840	-1.2071790	1.2450620	C	1.7648860	1.8661500	1.1817670
C	-3.7536970	-1.5271650	1.1161460	C	2.9380330	2.5931300	1.0599310
C	-4.4318580	-1.1149710	-0.0257980	C	3.8554340	2.2165280	0.0836880
C	-3.7443990	-0.4103280	-1.0064000	C	3.5626880	1.1392620	-0.7422770
C	-2.3922120	-0.1249100	-0.8169230	C	2.3585230	0.4535720	-0.5721130
F	-1.8099660	-1.6609790	2.3791520	F	0.9031060	2.2967070	2.1425450
H	-4.2376290	-2.0892260	1.9059340	H	3.1077550	3.4333170	1.7224650
H	-5.4834170	-1.3473050	-0.1553830	H	4.7846360	2.7624110	-0.0386110
H	-4.2385250	-0.0918720	-1.9154610	H	4.2472190	0.8338290	-1.5233550
Cl	-1.5972040	0.7087930	-2.1700000	Cl	2.0602740	-0.8369780	-1.7592320
C	2.2836400	-1.3151320	0.7612690	C	-1.5720660	1.8157550	-0.5721130
C	3.2340970	-2.2855790	0.4533760	C	-2.7679740	2.5157470	-0.7422770
C	2.9140470	-3.2750780	-0.4693800	C	-3.8472860	2.2306400	0.0836880
C	1.6575990	-3.2669770	-1.0642540	C	-3.7147330	1.2478460	1.0599310
C	0.7578710	-2.2689950	-0.7166410	C	-2.4985760	0.5953610	1.1817670
Cl	2.8075800	-0.0733010	1.9225180	Cl	-0.3052920	2.2027380	-1.7592320
H	4.2062030	-2.2575060	0.9288060	H	-2.8457270	3.2612850	-1.5233550
H	3.6386590	-4.0409760	-0.7235810	H	-4.7846360	2.7624110	-0.0386110
H	1.3586020	-4.0077110	-1.7961360	H	-4.5272180	0.9747370	1.7224650
F	-0.4390180	-2.3182620	-1.3625350	F	-2.4405600	-0.3662400	2.1425450

p-adducts:

p-III(α):			p-III(β):				
N	-0.2794430	-1.6900370	0.1296650	N	-1.0403940	-1.0318390	-0.9836420
B	0.0804090	-0.0371120	0.0441250	B	0.0387720	-0.0609960	-0.0706920
C	-0.1043400	0.6280610	1.5692660	C	1.1540280	-1.1682350	0.4432000
C	1.6012490	0.0125530	-0.6406430	C	0.5625540	1.1821450	-1.0866490
C	-1.1113660	0.7976410	-0.8292280	C	-0.7764030	0.7350700	1.1790640
C	0.2384760	-2.4883850	-1.0415600	C	-0.8702260	-1.1266190	-2.4812630
C	-0.3678840	-3.8917840	-1.1013000	C	-2.1045720	-1.7530480	-3.1252730
C	-0.1948980	-4.6582440	0.2139980	C	-2.3410470	-3.1674540	-2.5850800
C	-0.6920640	-3.8059130	1.3867710	C	-2.4322130	-3.1351780	-1.0558240
C	0.0153620	-2.4539410	1.3966340	C	-1.2327640	-2.4228910	-0.4289940
C	2.8030160	-0.2708880	0.0508130	C	1.8870330	1.5864330	-1.4072560
C	4.0820360	-0.1454840	-0.4813180	C	2.2024500	2.6573540	-2.2448190
C	4.2379110	0.2397490	-1.8029220	C	1.2041180	3.4240110	-2.8171540
C	3.1078710	0.4314650	-2.5786180	C	-0.1138800	3.1117170	-2.5345630
C	1.8456090	0.2886480	-2.0072130	C	-0.3910090	2.0342980	-1.7001080
C	-2.3341580	0.3507200	-1.3717460	C	-2.1307350	0.7124170	1.5721510
C	-3.3484480	1.1618180	-1.8735760	C	-2.7103500	1.5254110	2.5423760
C	-3.1793730	2.5343260	-1.8944790	C	-1.9304920	2.4431720	3.2229520
C	-1.9755640	3.0564640	-1.4518110	C	-0.5769590	2.4972900	2.9378330
C	-0.9930760	2.2066850	-0.9573910	C	-0.0432630	1.6600120	1.9651320
C	0.8045870	1.5096860	2.1831750	C	2.0064670	-1.7694720	-0.4925790
C	0.6248590	2.1366690	3.4069850	C	2.9680050	-2.7286080	-0.2409140
C	-0.5422060	1.9164540	4.1194860	C	3.1127790	-3.1842110	1.0628860
C	-1.5090480	1.0817010	3.5780530	C	2.2645860	-2.6958940	2.0448830
C	-1.2777120	0.4827580	2.3428000	C	1.3006050	-1.7377640	1.7231350
Cl	0.5440150	0.4102950	-3.2137670	Cl	-2.1512860	1.8081160	-1.4817240
Cl	2.8294310	-0.8794380	1.7260760	Cl	3.3608860	0.8406800	-0.7566510
Cl	0.5129800	3.0399130	-0.5683070	Cl	1.7106630	1.7619560	1.8430740
Cl	-2.7427620	-1.3837870	-1.5878130	Cl	-3.3396250	-0.4274980	0.8975170
Cl	-2.6487680	-0.5141440	1.7853350	Cl	0.2039300	-1.3695750	3.0658630
F	1.9712810	1.8235280	1.5755330	F	1.8894930	-1.4008180	-1.8025940
H	-1.2952760	-1.7138810	0.0464280	H	-1.9365100	-0.5636240	-0.8548050
H	1.3218880	-2.5364280	-0.9325660	H	0.0106110	-1.7309350	-2.6727250
H	0.0169530	-1.9323740	-1.9485040	H	-0.6783500	-0.1324770	-2.8702830
H	-1.4321840	-3.8169870	-1.3428960	H	-1.9587020	-1.7675600	-4.2091680
H	0.1034430	-4.4266910	-1.9308610	H	-2.9800370	-1.1209730	-2.9330290
H	-0.7275490	-5.6120530	0.1710950	H	-3.2495620	-3.6004160	-3.0122530
H	0.8658000	-4.8910940	0.3672690	H	-1.5066100	-3.8109400	-2.8894640
H	-1.7763840	-3.6561530	1.3206800	H	-3.3569880	-2.6346740	-0.7546860
H	-0.5002700	-4.3038930	2.3413940	H	-2.4758900	-4.1478370	-0.6445950
H	-0.2767750	-1.8462380	2.2462450	H	-1.3378410	-2.3415590	0.6507320
H	1.0897690	-2.5960430	1.4457390	H	-0.3170180	-2.9760490	-0.6321010
H	4.9407380	-0.3538540	0.1422080	H	3.2430470	2.8858880	-2.4300700
H	5.2266370	0.3570560	-2.2298960	H	1.4493620	4.2576870	-3.4639160
H	3.1896990	0.6783410	-3.6283470	H	-0.9278640	3.6908800	-2.9488600
H	-4.2556190	0.7080340	-2.2485260	H	-3.7665760	1.4300050	2.7537730
H	-3.9603990	3.1820260	-2.2734430	H	-2.3668170	3.0895520	3.9746430
H	-1.7799680	4.1193480	-1.4955720	H	0.0796790	3.1703010	3.4724090
H	1.4101860	2.7887740	3.7661800	H	3.5804650	-3.0858900	-1.0582480
H	-0.7052600	2.3950170	5.0774380	H	3.8627630	-3.9263680	1.3081950
H	-2.4411700	0.8983240	4.0949220	H	2.3263690	-3.0620620	3.0606180

p-III(y):			p-III(4):				
N	-0.9127570	-1.4377490	0.5772180	N	-0.5929430	1.6059690	0.3297510
B	-0.0591460	-0.0747970	0.0087980	B	0.0112000	0.0360910	-0.0768270
C	-1.0909290	0.7201270	-1.0698220	C	1.2811200	0.3341380	-1.1032600
C	0.1352220	1.0336130	1.2590180	C	0.3087360	-0.7514230	1.3752810
C	1.3189430	-0.7441110	-0.6451590	C	-1.2183900	-0.8804660	-0.8196940
C	-0.8743680	-2.6014430	-0.3802330	C	-0.3288930	2.2205590	1.6857600
C	-1.9881880	-3.6062180	-0.0811090	C	-1.2572110	3.4068620	1.9320510
C	-1.9591820	-4.0832270	1.3760470	C	-1.0245510	4.4977960	0.8818980
C	-1.9218920	-2.8830760	2.3309400	C	-1.1959940	3.9115090	-0.5228500
C	-0.7561570	-1.9606920	1.9805630	C	-0.3505390	2.6527760	-0.7315060
C	1.2995940	1.7744490	1.6056070	C	1.5034100	-1.3701770	1.8290040
C	1.3595810	2.7038000	2.6438130	C	1.6476260	-1.9791750	3.0760800
C	0.2414820	2.9783240	3.4103320	C	0.5800800	-2.0488880	3.9527740
C	-0.9442250	2.3330950	3.1069420	C	-0.6388320	-1.5236240	3.5587190
C	-0.9691650	1.4165170	2.0609860	C	-0.7425600	-0.9124640	2.3140730
C	1.5540640	-0.9428550	-2.0261890	C	-2.5214810	-0.5323150	-1.2277740
C	2.7285240	-1.4660100	-2.5658670	C	-3.4973910	-1.4107730	-1.6918390
C	3.7408190	-1.8965180	-1.7271460	C	-3.2068250	-2.7577570	-1.8049320
C	3.5455670	-1.8284330	-0.3572440	C	-1.9266440	-3.1810340	-1.4910490
C	2.3684740	-1.2816390	0.1410390	C	-0.9859090	-2.2620280	-1.0407990
C	-2.4083110	0.3743230	-1.3988100	C	1.2302940	0.0047650	-2.4686140
C	-3.2883180	1.0844770	-2.1955790	C	2.2477060	0.1983250	-3.3927950
C	-2.8618440	2.2764750	-2.7577720	C	3.4202830	0.8103440	-2.9847860
C	-1.5631960	2.6958970	-2.5110650	C	3.5305090	1.2357800	-1.6676000
C	-0.7265100	1.9297750	-1.7042940	C	2.4809580	1.0074910	-0.7841750
CI	-2.6192270	0.7684860	1.8015610	CI	-2.4006950	-0.3156390	2.0019360
CI	2.8566900	1.6653510	0.7601760	CI	2.9694940	-1.5521230	0.8499720
CI	2.3229560	-1.3050830	1.9222210	CI	0.6231490	-2.9565180	-0.8489160
CI	0.3302040	-0.6354200	-3.2783120	CI	-3.1414440	1.1523750	-1.2201670
CI	0.9190860	2.5339970	-1.5958900	CI	2.7807910	1.6722070	0.8373730
F	-2.9582940	-0.8010440	-0.9192180	F	0.1036560	-0.5296700	-3.0006290
H	-1.8741730	-1.1106790	0.5493020	H	-1.6003640	1.4521770	0.3211460
H	0.1108300	-3.0592500	-0.2865230	H	0.7046330	2.5447500	1.7017300
H	-0.9683970	-2.2088590	-1.3892150	H	-0.4465930	1.4591570	2.4465770
H	-2.9522570	-3.1377460	-0.3011090	H	-2.3013380	3.0715430	1.9109200
H	-1.8828020	-4.4503850	-0.7686770	H	-1.0689690	3.7870790	2.9401970
H	-2.8242680	-4.7181570	1.5854940	H	-0.0075070	4.8919600	0.9952710
H	-1.0656050	-4.6973880	1.5415080	H	-1.7105630	5.3360800	1.0303330
H	-2.8637030	-2.3241090	2.2810190	H	-2.2508990	3.6797820	-0.6935560
H	-1.8057810	-3.2130740	3.3671970	H	-0.9076120	4.6382350	-1.2880290
H	-0.6785640	-1.1153370	2.6584520	H	0.7085930	2.9001800	-0.6992500
H	0.1766840	-2.5120730	2.0272950	H	-0.5585160	2.1992420	-1.6980650
H	2.2948350	3.2112040	2.8364670	H	2.6027450	-2.4135850	3.3378540
H	0.2887440	3.6975200	4.2189950	H	0.6898060	-2.5253680	4.9194480
H	-1.8503670	2.5388980	3.6602650	H	-1.5078280	-1.5839060	4.1997440
H	2.8260720	-1.5472860	-3.6398430	H	-4.4737290	-1.0288280	-1.9569740
H	4.6593000	-2.3022410	-2.1338870	H	-3.9557220	-3.4586870	-2.1527610
H	4.2999040	-2.1849080	0.3307890	H	-1.6376420	-4.2169010	-1.6068700
H	-4.2826020	0.6867740	-2.3507100	H	2.0845850	-0.1277160	-4.4116780
H	-3.5229350	2.8634390	-3.3833380	H	4.2328910	0.9719100	-3.6826000
H	-1.1801950	3.6067560	-2.9508790	H	4.4206960	1.7412370	-1.3190240

p-II(α):			p-II(β):				
N	-0.1042560	1.6800010	-0.2973210	N	0.1723390	-1.5977570	-0.6633040
B	0.0911460	0.0104660	-0.1241450	B	-0.0134820	-0.0628100	-0.0065620
C	1.7310310	-0.1499600	0.0395810	C	0.9893300	0.9850500	-0.8536620
C	-0.8040660	-0.5914600	1.1689660	C	-1.6518310	0.2284720	-0.1257100
C	-0.6075690	-0.7251690	-1.4550010	C	0.6529130	-0.0189110	1.5234740
C	0.7937680	2.4936020	0.6013150	C	-0.0652900	-2.8075260	0.1964400
C	0.3896530	3.9669290	0.6335690	C	0.5000950	-4.0579510	-0.4741430
C	0.3455310	4.5726620	-0.7734030	C	-0.1545340	-4.2865670	-1.8419970
C	-0.5290840	3.7093790	-1.6891580	C	-0.0321020	-3.0271230	-2.7077000
C	-0.0550500	2.2581290	-1.6894220	C	-0.5398350	-1.7850510	-1.9770230
C	-1.7176440	0.0419170	2.0356300	C	-2.2585230	0.9721000	-1.1664690
C	-2.5215410	-0.5980060	2.9759500	C	-3.6193250	1.2594640	-1.2533440
C	-2.4416610	-1.9708620	3.1238080	C	-4.4891410	0.7618330	-0.2993430
C	-1.5334880	-2.6686840	2.3447660	C	-3.9849630	-0.0461330	0.7063900
C	-0.7513410	-1.9874690	1.4201980	C	-2.6187570	-0.3028700	0.7634020
C	0.0063360	-1.7009880	-2.2614880	C	0.0779510	0.6670220	2.6094420
C	-0.5895540	-2.3630720	-3.3248130	C	0.6454220	0.8166000	3.8650080
C	-1.9042720	-2.0770910	-3.6547750	C	1.8907740	0.2639050	4.1173970
C	-2.5941420	-1.1371450	-2.9028580	C	2.5432370	-0.4123090	3.0968620
C	-1.9460460	-0.5057570	-1.8447910	C	1.9289860	-0.5220980	1.8520540
C	2.5720870	0.0067420	1.0706100	C	1.9487660	0.6354350	-1.8111430
C	3.9507170	-0.0980450	-1.0789910	C	2.8680070	1.4757200	-2.4146990
C	4.6000060	-0.3491670	0.1222960	C	2.8696550	2.8166650	-2.0663640
C	3.8515300	-0.4469920	1.2858790	C	1.9394880	3.2650250	-1.1388670
C	2.4625820	-0.3256620	1.2304160	C	1.0398930	2.3693040	-0.5693490
CI	0.4208210	-3.0214810	0.5996880	CI	-2.2051330	-1.4052000	2.1039790
CI	-1.9489430	1.8205730	2.1056460	CI	-1.3570240	1.6024850	-2.5661160
CI	-2.9825080	0.6614700	-0.9820800	CI	2.9489720	-1.3593810	0.6461840
F	1.2800510	-2.0896770	-2.0224010	F	-1.1360440	1.2487620	2.4792350
CI	1.6869840	-0.3340460	2.8267810	CI	-0.1343560	3.1091380	0.5155750
F	2.0137550	0.3151230	-2.2785600	F	2.0277370	-0.6677720	-2.2675450
H	-1.0547140	1.8533840	0.0291220	H	1.1639630	-1.6340870	-0.8880780
H	1.8070010	2.3830050	0.2165390	H	-1.1385990	-2.9056950	0.3349780
H	0.7655800	2.0499760	1.5934530	H	0.3826640	-2.6280410	1.1700820
H	-0.5906400	4.0678320	1.1095380	H	1.5857660	-3.9522470	-0.5848040
H	1.1027530	4.5009690	1.2680340	H	0.3327790	-4.9129900	0.1868700
H	-0.0274890	5.5996700	-0.7362090	H	0.2973910	-5.1440250	-2.3478410
H	1.3613860	4.6162720	-1.1847330	H	-1.2150680	-4.5251440	-1.6957450
H	-1.5755070	3.7509210	-1.3631440	H	1.0135790	-2.8648470	-2.9899820
H	-0.5051500	4.0810540	-2.7174990	H	-0.5971700	-3.1363360	-3.6377390
H	-0.6656650	1.6383790	-2.3383200	H	-0.3838430	-0.8917310	-2.5728760
H	0.9718530	2.1857690	-2.0365500	H	-1.6047400	-1.8602580	-1.7532460
H	-3.1985600	-0.0127990	3.5831220	H	-3.9821120	1.8622160	-2.0746940
H	-3.0639230	-2.4853460	3.8458640	H	-5.5485780	0.9825560	-0.3501230
H	-1.4136330	-3.7382760	2.4520670	H	-4.6389490	-0.4794240	1.4507790
H	-0.0026170	-3.0954310	-3.8636530	H	0.0906750	1.3649190	4.6150630
H	-2.3905890	-2.5830890	-4.4798920	H	2.3543520	0.3649400	5.0911280
H	-3.6246170	-0.8928450	-3.1222390	H	3.5237590	-0.8421170	3.2501730
H	4.4792920	0.0167940	-2.0162440	H	3.5559850	1.0587840	-3.1384350
H	5.6783220	-0.4469830	0.1564550	H	3.5762990	3.5043670	-2.5143510
H	4.3320070	-0.6043510	2.2419450	H	1.8945260	4.3085400	-0.8579070

p-II(y):			p-II(4):				
N	0.9767750	-1.2697210	-0.7876820	-0.2105430	0.9031160	-1.3421410	
B	0.0295570	-0.0597120	-0.0621960	0.0804530	-0.0414340	0.0101090	
C	0.6207300	0.1969390	1.4829930	C	-0.1389260	-1.6596120	-0.3430280
C	0.2998820	1.3829220	-0.8830020	C	1.6129770	0.4042030	0.4978340
C	-1.4848480	-0.7162450	-0.1465160	C	-1.1271470	0.1942450	1.1503700
C	0.6155010	-2.6626380	-0.3397340	C	0.2120270	2.3418200	-1.1810420
C	1.7310270	-3.6520290	-0.6723050	C	-0.3322430	3.2280720	-2.3015880
C	2.0666540	-3.6373020	-2.1687690	C	0.0407910	2.6986060	-3.6903760
C	2.3468150	-2.2049910	-2.6413600	C	-0.3527310	1.2222560	-3.8128060
C	1.1927220	-1.2718470	-2.2778910	C	0.2681240	0.4085700	-2.6810920
C	-0.6568430	2.3084440	-1.3793910	C	2.8064000	-0.0626470	-0.1048740
C	-0.3351870	3.5026300	-2.0248390	C	4.0934290	0.2712650	0.3045310
C	0.9856270	3.8693730	-2.2102030	C	4.2700560	1.1443660	1.3653810
C	1.9794360	3.0357350	-1.7279160	C	3.1533260	1.6969850	1.9672740
C	1.6200700	1.8537020	-1.0893830	C	1.8813080	1.3444230	1.5203590
C	-2.1075750	-0.8291010	-1.3978010	C	-0.9584860	-0.5237850	2.3492200
C	-3.3383570	-1.3993610	-1.6594270	C	-1.8638720	-0.6227360	3.3867970
C	-4.0497650	-1.9408960	-0.5967650	C	-3.0740810	0.0492590	3.2784070
C	-3.4874300	-1.9218400	0.6703620	C	-3.3183460	0.8065540	2.1445490
C	-2.2307240	-1.3452980	0.8686510	C	-2.3599870	0.8673710	1.1317600
C	1.7146740	-0.4292090	2.0908040	C	0.6685030	-2.6835220	0.1881850
C	2.2340120	-0.1643810	3.3454190	C	0.4637660	-4.0432860	0.0141900
C	1.6373930	0.8214820	4.1156280	C	-0.6245220	-4.4784860	-0.7262200
C	0.5386260	1.4951210	3.6015590	C	-1.4947530	-3.5372880	-1.2560960
C	0.0620170	1.1756120	2.3336700	C	-1.2456430	-2.1840560	-1.0398390
CI	3.0586350	0.9501750	-0.5203390	CI	0.6037170	2.2764080	2.3400260
CI	-2.4140870	2.1201970	-1.2191520	CI	2.8167500	-1.1680120	-1.5051910
CI	-1.6175830	-1.5535090	2.5195110	CI	-2.8491450	1.9797950	-0.1849040
F	-1.4593920	-0.3313560	-2.4918060	F	0.2174440	-1.1663430	2.5410450
CI	-1.3937180	2.0403590	1.8587360	CI	-2.5196700	-1.1216580	-1.6990150
F	2.3925920	-1.4323160	1.4246370	F	1.7519260	-2.3770420	0.9345930
H	1.9002310	-1.0959910	-0.3985560	H	-1.2282170	0.9191250	-1.4118240
H	-0.3116580	-2.9320460	-0.8457160	H	1.3021290	2.3483710	-1.1718260
H	0.4165620	-2.6316430	0.7284330	H	-0.1326120	2.6837450	-0.2096180
H	2.6183520	-3.3968150	-0.0838290	H	-1.4209970	3.2933560	-2.2138300
H	1.4161010	-4.6498570	-0.3537910	H	0.0549060	4.2398530	-2.1511590
H	2.9228480	-4.2851620	-2.3751910	H	-0.4423830	3.2958450	-4.4682320
H	1.2179320	-4.0409500	-2.7344010	H	1.1230480	2.7935250	-3.8408320
H	3.2726120	-1.8312500	-2.1877630	H	-1.4434840	1.1132100	-3.7879790
H	2.4925960	-2.1737110	-3.7248870	H	-0.0156330	0.8046750	-4.7656450
H	1.3820730	-0.2505240	-2.5969250	H	0.0368460	-0.6491790	-2.7607820
H	0.2704390	-1.5990950	-2.7488630	H	1.3493360	0.5132930	-2.6939410
H	-1.1358070	4.1418850	-2.3710390	H	4.9431240	-0.1589350	-0.2078450
H	1.2364430	4.7967120	-2.7108050	H	5.2653280	1.4046920	1.7050400
H	3.0248800	3.2916420	-1.8339000	H	3.2532270	2.4099480	2.7743650
H	-3.7150760	-1.3933250	-2.6738010	H	-1.5974440	-1.2117900	4.2545660
H	-5.0243100	-2.3865810	-0.7552510	H	-3.8120620	-0.0059650	4.0691920
H	-4.0041330	-2.3645490	1.5110170	H	-4.2422660	1.3578590	2.0351820
H	3.0915160	-0.7312750	3.6834200	H	1.1686410	-4.7283180	0.4670140
H	2.0175730	1.0593490	5.1015010	H	-0.8028240	-5.5360430	-0.8783550
H	0.0348750	2.2591480	4.1780780	H	-2.3693670	-3.8379840	-1.8167670

p-II(6):			p-II(5):				
N	-0.1139210	-1.6622660	0.2043390	N	1.2248020	-1.2471190	-0.5717830
B	0.0744930	-0.0018280	-0.0335420	B	0.1291650	-0.0594030	-0.0671320
C	1.5245360	0.1088610	-0.8347030	C	-0.4973040	0.7115750	-1.4113240
C	-1.2377120	0.6216600	-0.9137250	C	-0.9187420	-0.8808940	0.9226710
C	-0.0540420	0.7750440	1.4362430	C	1.0485500	1.1731580	0.6319540
C	0.3493020	-2.4954750	-0.9654510	C	1.7462890	-2.0936620	0.5572090
C	-0.0981310	-3.9534090	-0.8513550	C	3.0161300	-2.8419770	0.1504200
C	0.3313210	-4.5823510	0.4785490	C	2.8086510	-3.6774890	-1.1183740
C	-0.1174300	-3.6979910	1.6472240	C	2.2040600	-2.8146370	-2.2331750
C	0.4091090	-2.2757110	1.4767430	C	0.9263380	-2.1311980	-1.7495130
C	-2.4425030	0.0168770	-1.3296290	C	-1.9495740	-1.7218430	0.4375550
C	-3.5362180	0.6758820	-1.8885940	C	-2.8774890	-2.3875820	1.2324160
C	-3.4781040	2.0398180	-2.1033180	C	-2.8024690	-2.2754020	2.6108960
C	-2.3072490	2.7064860	-1.7833270	C	-1.7674320	-1.5428150	3.1664840
C	-1.2433700	2.0070370	-1.2259150	C	-0.8517530	-0.9002400	2.3363790
C	0.8207370	1.7779930	1.8921210	C	2.4426690	1.3074710	0.5906690
C	0.6907490	2.4869770	-2.3712490	C	3.1924950	2.3803150	1.0422230
C	-0.3848940	2.2275580	3.9105270	C	2.5347080	3.4619420	1.6042660
C	-1.3144840	1.2711300	3.5274150	C	1.1511070	3.4195940	1.6997110
C	-1.1360650	0.5936560	2.3246410	C	0.4561460	2.3105920	1.2268750
C	1.5531700	0.2501720	-2.1031240	C	0.4181740	1.0938140	-2.4061110
C	2.6853960	0.3674280	-3.0202900	C	0.1603680	1.8180520	-3.5534890
C	3.9291000	0.3014070	-2.4115020	C	-1.1391960	2.2531220	-3.7691840
C	3.9971470	0.0828350	-1.0425800	C	-2.1114480	1.9472550	-2.8302800
C	2.8229890	-0.0267390	-0.3001230	C	-1.7956140	1.2034740	-1.6901340
CI	0.1864830	3.0130300	-0.9751170	CI	0.4777800	-0.1548380	3.2534690
CI	-2.7548020	-1.7524080	-1.2535900	CI	-2.1914430	-2.0486620	-1.2967460
CI	-2.4447870	-0.5636970	1.9681450	CI	-1.2818060	2.3827990	1.4803070
F	1.8930060	2.1381020	1.1527270	F	3.2276700	0.2910730	0.0752710
CI	3.1176960	-0.4080290	1.4139890	CI	-3.2007560	0.9495710	-0.6432520
F	0.3824810	0.2394450	-2.9254660	F	1.7373960	0.7266000	-2.2594960
H	-1.1245620	-1.7898090	0.2486920	H	2.0181690	-0.6915260	-0.8773420
H	1.4366660	-2.4285860	-0.9851840	H	0.9475150	-2.7823270	0.8363280
H	-0.0308200	-2.0322280	-1.8735690	H	1.9364130	-1.4409840	1.4041660
H	-1.1857940	-4.0119970	-0.9504270	H	3.8160560	-2.1119490	-0.0094500
H	0.3232720	-4.5031450	-1.6979310	H	3.3273360	-3.4745230	0.9866890
H	-0.0804130	-5.5906990	0.5732160	H	3.7541770	-4.1211160	-1.4417600
H	1.4234810	-4.6793440	0.5030380	H	2.1251080	-4.5072790	-0.9008930
H	-1.2119460	-3.6796950	1.7143260	H	2.9236540	-2.0545830	-2.5610930
H	0.2501660	-4.0915520	2.5990700	H	1.9648840	-3.4225450	-3.1103560
H	0.1284890	-1.6368100	2.3081230	H	0.4670630	-1.5250300	-2.5257360
H	1.4927040	-2.2791200	1.4131240	H	0.2008790	-2.8751750	-1.4326290
H	-4.4189020	0.1097340	-2.1526150	H	-3.6494680	-2.9826370	0.7638700
H	-4.3210640	2.5693810	-2.5301160	H	-3.5261570	-2.7741870	3.2443070
H	-2.2022190	3.7670300	-1.9681430	H	-1.6503520	-1.4728980	4.2393350
H	1.4402430	3.2315190	3.3116580	H	4.2690140	2.3388900	0.9401990
H	-0.5073320	2.7685120	4.8409740	H	3.0871390	4.3201680	1.9665130
H	-2.1768670	1.0524070	4.1423520	H	0.5994750	4.2362070	2.1454560
H	2.5638210	0.4981670	-4.0876010	H	0.9735230	2.0318430	-4.2346700
H	4.8364020	0.3963000	-2.9956640	H	-1.3913390	2.8283110	-4.6516260
H	4.9521140	-0.0090740	-0.5433700	H	-3.1302780	2.2825850	-2.9682420

p-II(7):			
N	-0.8613490	-1.5152370	0.2868290
B	-0.0594610	-0.0594410	-0.0789280
C	-1.1381240	0.8575580	-1.0050130
C	0.1696280	0.8201740	1.3286320
C	1.2858590	-0.5726210	-0.8976640
C	-0.8458620	-2.5000300	-0.8539800
C	-1.9177680	-3.5754280	-0.6737060
C	-1.7869430	-4.2905060	0.6768290
C	-1.7274880	-3.2696390	1.8204010
C	-0.6136510	-2.2536260	1.5744780
C	1.3457370	1.4916510	1.7610450
C	1.4437440	2.2151010	2.9499810
C	0.3528510	2.3397770	3.7911330
C	-0.8451380	1.7569070	3.4157130
C	-0.9064690	1.0450840	2.2227830
C	1.3756420	-0.4821280	-2.2952460
C	2.4442280	-0.9012320	-3.0734240
C	3.5228680	-1.5117370	-2.4544230
C	3.4884260	-1.7055590	-1.0799350
C	2.3929950	-1.2554920	-0.3483300
C	-2.4547190	0.5319100	-1.3543500
C	-3.3619010	1.3230650	-2.0382300
C	-2.9646220	2.5832360	-2.4520440
C	-1.6683450	2.9917850	-2.1744400
C	-0.8055480	2.1443170	-1.4852240
CI	-2.5606430	0.4391810	1.9003810
CI	2.8617970	1.5583980	0.8435920
CI	2.5198290	-1.6125770	1.3899920
F	0.3312410	0.0165720	-3.0067340
CI	0.8231900	2.7769720	-1.2886460
F	-2.9829420	-0.6994180	-1.0061860
H	-1.8295490	-1.2151290	0.3606290
H	0.1523110	-2.9375310	-0.8840930
H	-0.9969180	-1.9441570	-1.7767180
H	-2.9039220	-3.1085560	-0.7561930
H	-1.8342060	-4.2875110	-1.4998550
H	-2.6188670	-4.9850140	0.8215360
H	-0.8674440	-4.8883970	0.6850390
H	-2.6869640	-2.7477310	1.9168200
H	-1.5414650	-3.7666020	2.7767360
H	-0.5339410	-1.5271820	2.3786770
H	0.3413560	-2.7607190	1.4882380
H	2.3856700	2.6839820	3.1996050
H	0.4294230	2.8993860	4.7155060
H	-1.7314440	1.8554620	4.0276330
H	2.3954910	-0.7495570	-4.1438160
H	4.3746900	-1.8481570	-3.0329500
H	4.3045570	-2.1972940	-0.5683980
H	-4.3535230	0.9316000	-2.2236320
H	-3.6466510	3.2333140	-2.9860720
H	-1.3099010	3.9603290	-2.4958980

p-l(α):			p-l(β):				
B	-0.0180730	0.0702040	0.0751240	B	-0.0848270	0.1235850	-0.0516030
C	1.1224120	-0.2556560	1.2483320	C	-1.7078480	0.3487660	0.1861020
C	0.4772380	-0.8370690	-1.2316100	C	0.7626090	1.4567320	-0.5919400
N	0.0768490	1.6972070	-0.3236810	N	-0.0298720	-1.0781270	-1.2145000
C	-1.6031260	-0.1134060	0.5137390	C	0.7618650	-0.3148710	1.3139980
C	-1.0358490	2.1628170	-1.2250430	C	-0.9931880	-2.2091900	-0.9596520
C	-0.7067800	3.5201470	-1.8417990	C	-0.7161700	-3.4036770	-1.8703700
C	-0.4228840	4.5703510	-0.7608060	C	-0.7406620	-3.0024120	-3.3495300
C	0.6454660	4.0599450	0.2144900	C	0.1959010	-1.8126970	-3.5890630
C	0.2666420	2.6947080	0.7860670	C	-0.1410240	-0.6528380	-2.6555240
C	2.4816140	0.1042380	1.1455840	C	-2.5115660	-0.1844010	1.2113920
C	3.4728610	-0.2125050	2.0705710	C	-3.8843210	0.0404200	1.3279990
C	3.1375780	-0.9577930	3.1918240	C	-4.5419180	0.8033140	0.3746270
C	1.8245940	-1.3703380	3.3550120	C	-3.8215740	1.3143620	-0.6969170
C	0.8789360	-1.0201520	2.4033880	C	-2.4630830	1.0638660	-0.7535190
C	-2.6666950	-0.6066140	-0.2667950	C	1.5858200	-1.4023460	1.6422560
C	-3.9850330	-0.7071060	-0.1805680	C	2.3086140	-1.5224920	2.8297540
C	-4.3179230	-0.2680720	1.4532880	C	2.2322730	-0.5209330	3.7844380
C	-3.3315850	0.2907600	2.2549400	C	1.4250410	0.5823910	3.5395940
C	-2.0425750	0.3573620	1.7591920	C	0.7350420	0.6419340	2.3450850
C	0.4717730	-2.2487170	-1.1912940	C	2.0711020	1.4052880	-1.1101950
C	0.9517740	-3.0702590	-2.2072480	C	2.8309430	2.5072320	-1.4947740
C	1.4786150	-2.5050390	-3.3608230	C	2.2985000	3.7794430	-1.3439140
C	1.5085190	-1.1238740	-3.4765140	C	1.0286530	3.9162800	-0.8041880
C	1.0181180	-0.3622510	-2.4303030	C	0.3157870	2.7823420	-0.4451440
CI	3.0975280	1.0330710	-0.2519700	CI	-1.8665210	-1.2837380	2.4490230
F	-0.3622560	-1.4952330	2.6574400	F	-1.8301160	1.5712930	-1.8523410
CI	-2.4563850	-1.1026570	-1.9584740	CI	1.7797180	-2.8323550	0.5818100
F	-1.1390070	0.9571530	2.5889970	F	-0.0634260	1.7244650	2.1829230
CI	-0.2345910	-3.1027340	0.1784010	CI	2.9280870	-0.1489030	-1.3011170
F	1.0835240	0.9982740	-2.6628150	F	-0.8969930	3.0367980	0.0945000
H	0.9256390	1.7589380	-0.8824290	H	0.9047470	-1.4762620	-1.1195910
H	-1.9383480	2.2142020	-0.6152430	H	-1.9939160	-1.8141800	-1.1335200
H	-1.1902070	1.4049190	-1.9874240	H	-0.9210300	-2.4799580	0.0903620
H	0.1623890	3.4086380	-2.4993210	H	0.2584550	-3.8343520	-1.6189600
H	-1.5443380	3.8279960	-2.4740880	H	-1.4634660	-4.1742320	-1.6609670
H	-0.1086870	5.5136910	-1.2154760	H	-0.4588590	-3.8494630	-3.9806590
H	-1.3463370	4.7759310	-0.2057040	H	-1.7613890	-2.7183040	-3.6332010
H	1.6135270	3.9809340	-0.2947120	H	1.2384860	-2.1139390	-3.4309400
H	0.7828770	4.7595720	1.0437990	H	0.1237460	-1.4594040	-4.6215580
H	1.0304100	2.3125660	1.4583370	H	0.5190050	0.1951510	-2.8120150
H	-0.6654090	2.7504350	1.3433050	H	-1.1601390	-0.3092210	-2.8151190
H	4.4892010	0.1167200	1.9021480	H	-4.4242970	-0.3939610	2.1583840
H	3.8941740	-1.2191480	3.9216220	H	-5.6065710	0.9844880	0.4596120
H	1.5043840	-1.9644460	4.2009980	H	-4.2794180	1.9040330	-1.4803430
H	-4.7379640	-1.1189940	-0.4775630	H	2.9203440	-2.3990930	2.9939090
H	-5.3383630	-0.3464490	1.8084270	H	2.7901730	-0.6040680	4.7090780
H	-3.5313140	0.6693670	3.2488280	H	1.3081680	1.3902570	4.2499990
H	0.8994030	-4.1440980	-2.0886460	H	3.8262660	2.3606680	-1.8917880
H	1.8557860	-3.1340750	-4.1578080	H	2.8733170	4.6511320	-1.6323010
H	1.9017410	-0.6193450	-4.3493310	H	0.5678190	4.8825140	-0.6448700

p-l(v):			p-l(δ):		
B	0.0208580	-0.0579480	B	-0.0969160	-0.0525920
C	-1.2385780	-0.4538610	C	1.0400840	-0.5318000
C	-0.4447480	-0.5127470	C	0.1001620	-1.1570670
N	0.0693650	1.7018850	N	-1.6224440	-0.3023670
C	1.5359900	-0.3989650	C	-0.1425750	1.5375060
C	0.6941680	2.4233970	C	-2.7461580	0.2224220
C	0.3440110	3.9097560	C	-4.0874740	-0.3575720
C	0.8193510	4.5455820	C	-4.3561320	-0.0777060
C	0.2869460	3.7566100	C	-3.1672930	-0.5325870
C	0.6137110	2.2696810	C	-1.8630620	0.0852400
C	-1.4838490	-1.8133430	C	2.2524400	0.0590550
C	-2.5731400	-2.2848110	C	3.1381080	-0.5498450
C	-3.5123100	-1.3917410	C	2.8616320	-1.8013330
C	-3.3303320	-0.0386780	C	1.6917370	-2.4454980
C	-2.2251170	0.3663730	C	0.8564360	-1.7985180
C	2.7301460	-0.4037750	C	-0.3941490	2.0952630
C	3.9787410	-0.7559770	C	-0.4387660	3.4665220
C	4.1041610	-1.1049190	C	-0.2765560	4.3679860
C	2.9828770	-1.0647280	C	-0.0995860	3.8868180
C	1.7687120	-0.7032310	C	-0.0543580	2.5175310
C	-1.5351210	-0.0047100	C	1.2613520	-1.1676250
C	-1.9881340	-0.5033680	C	1.5373290	-2.1087920
C	-1.3564760	-1.6063050	C	0.6352250	-3.1349680
C	-0.2949500	-2.1844150	C	-0.5282230	-3.1946020
C	0.1188130	-1.6390340	C	-0.7430070	-2.2279110
Cl	-0.3583830	-3.0677670	Cl	2.8259410	1.6400970
F	-2.1455840	1.7408530	F	-0.2794020	-2.5058890
Cl	2.7836800	0.0690340	Cl	-0.7616160	1.0970140
F	0.7409140	-0.6160020	F	0.0824180	2.1160880
Cl	-2.5078450	1.3690580	Cl	2.4713310	0.0980210
F	1.1569410	-2.2866340	F	-1.9387420	-2.3890980
H	-0.9118990	1.9705670	H	-1.7162170	-1.3147050
H	1.7699130	2.2806450	H	-2.7350680	1.3091760
H	0.3509190	1.9535560	H	-2.5285620	-0.0277410
H	-0.7406850	4.0289390	H	-4.0839340	-1.4368600
H	0.8018640	4.4048450	H	-4.8768280	0.0688990
H	0.5032660	5.5906200	H	-5.2754660	-0.5737010
H	1.9159550	4.5426460	H	-4.5076080	0.9991160
H	-0.7987680	3.8747210	H	-3.0820430	-1.6260440
H	0.7162170	4.1331470	H	-3.3099730	-0.2490010
H	0.1967460	1.6969530	H	-1.0073370	-0.2360560
H	1.6914430	2.1031980	H	-1.9069490	1.1704150
H	-2.6713740	-3.3477810	H	4.0466560	-0.0297030
H	-4.3660050	-1.7471300	H	3.5517690	-2.2685400
H	-4.0157420	0.7148730	H	1.4156370	-3.4260280
H	4.8396670	-0.7538480	H	-0.6136280	3.8132370
H	5.0691650	-1.3885400	H	-0.3063930	5.4338590
H	3.0200700	-1.2973920	H	0.0121710	4.5381070
H	-2.8308970	-0.0359640	H	2.4531280	-2.0250960
H	-1.6967260	-2.0126070	H	0.8378840	-3.8745770
H	0.2306540	-3.0521180	H	-1.2731490	-3.9674750

p-l(5):			p-l(6):				
B	0.0731220	-0.0310860	0.0784750	B	0.1402900	0.0432700	-0.0083880
C	1.5499320	0.1709470	0.8079960	C	-0.3714920	-0.7203210	1.3811900
C	-0.0303290	-1.2800670	-1.0179180	C	1.0907590	-1.1330040	-0.7635000
N	-0.2016480	1.4431650	-0.6500730	N	1.1861840	1.3012210	0.3882260
C	-1.1830510	-0.3779460	1.1378180	C	-0.9918860	0.7951940	-0.9442700
C	0.0796650	2.6190610	0.2520220	C	1.6580880	2.0801850	-0.8099430
C	-0.4434430	3.9268170	-0.3407430	C	2.8863160	2.9217970	-0.4667420
C	0.1132430	4.1746390	-1.7475140	C	2.6137080	3.8572900	0.7181330
C	-0.1290400	2.9490410	-2.6362710	C	2.0442150	3.0701900	1.9056680
C	0.4396700	1.6902050	-1.9873040	C	0.8206420	2.2575050	1.4844360
C	1.6336590	0.5384970	2.1590760	C	-1.6226660	-1.2979920	1.7050480
C	2.7974110	0.7493140	2.8801660	C	-1.8608960	-2.0160280	2.8801910
C	4.0144920	0.6238130	2.2273330	C	-0.8519050	-2.2059420	3.8109790
C	4.0251950	0.3144040	0.8744150	C	0.4059330	-1.6806960	3.5523040
C	2.8218110	0.1080860	0.2021260	C	0.5873880	-0.9873430	2.3715050
C	-2.4566660	0.1778260	1.3467990	C	-0.8901090	0.7897810	-2.3437230
C	-3.4358100	-0.3603550	-1.853480	C	-1.7658530	1.3966650	-3.2281390
C	-3.1722820	-1.5182400	2.8969970	C	-2.8313870	2.1214920	-2.7147040
C	-1.9240310	-2.1129310	2.7680610	C	-2.9669010	2.2410460	-1.3386020
C	-1.0008710	-1.5336460	1.9201370	C	-2.0564760	1.6050160	-0.4961110
C	-1.0438260	-1.4306680	-1.9840200	C	0.5423660	-2.2580570	-1.4205000
C	-1.1870530	-2.5201360	-2.8396080	C	1.2788120	-3.3162160	-1.9460610
C	-0.2969840	-3.5795230	-2.7395830	C	2.6625710	-3.3156550	-1.8449820
C	0.7049480	-3.5261480	-1.7830050	C	3.2791150	-2.2421730	-1.2248970
C	0.8063450	-2.4113740	-0.9649110	C	2.4900510	-1.2191450	-0.7246140
F	0.4861240	0.7594480	2.8596680	CI	-3.0571180	-1.1916840	0.6757560
CI	3.0389620	-0.2421300	-1.5307380	F	1.8706960	-0.5252280	2.1835230
CI	-3.0026700	1.7120820	0.5939440	F	0.1717650	0.1721220	-2.9287530
F	0.2017580	-2.1535930	1.8621360	CI	-2.3519380	1.9253310	1.2289820
CI	-2.3260600	-0.2056180	-2.1815770	CI	-1.1956200	-2.4074430	-1.6535610
F	1.8128930	-2.4718120	-0.0669170	F	3.2403480	-0.2047530	-0.1560960
H	-1.2070750	1.4572240	-0.8225650	H	2.0073120	0.8147250	0.7364520
H	1.1612700	2.6611790	0.3797820	H	0.8257510	2.7091420	-1.1284940
H	-0.3625690	2.4076520	1.2227520	H	1.8657160	1.3735050	-1.6098450
H	-1.5366330	3.9003980	-0.3749690	H	3.7196870	2.2510960	-0.2338750
H	-0.1705070	4.7411620	0.3364670	H	3.1767020	3.4925810	-1.3534170
H	-0.3417970	5.0667930	-2.1859060	H	3.5272740	4.3836060	1.0075200
H	1.1918010	4.3639680	-1.6857090	H	1.8875050	4.6219660	0.4164730
H	-1.2024810	2.8139920	-2.8148330	H	2.8054090	2.3933730	2.3125210
H	0.3398950	3.0774480	-3.6157740	H	1.7551620	3.7444080	2.7167880
H	0.2927410	0.8088490	-2.6050880	H	0.4061220	1.6860620	2.3111970
H	1.5073940	1.8009630	-1.8156630	H	0.0398170	2.9132030	1.1066040
H	2.7212930	1.0139700	3.9267830	H	-2.8483790	-2.4219950	3.0522670
H	4.9451960	0.7776090	2.7599080	H	-1.0434470	-2.7611860	4.7210260
H	4.9578900	0.2269680	0.3339560	H	1.2441000	-1.8013770	4.2260040
H	-4.3912170	0.1385110	2.2737040	H	-1.5877570	1.2945740	-4.2906380
H	-3.9255420	-1.9443360	3.5482260	H	-3.5396070	2.6046890	-3.3768900
H	-1.6439570	-3.0081290	3.3078020	H	-3.7714370	2.8225420	-0.9094360
H	-1.9959070	-2.5353640	-3.5574310	H	0.7581030	-4.1300280	-2.4323260
H	-0.3933670	-4.4388550	-3.3920140	H	3.2459780	-4.1349190	-2.2465920
H	1.4206850	-4.3264750	-1.6474540	H	4.3530950	-2.1676730	-1.1150650

p-(7):			p-(8):				
B	-0.0410830	-0.0923420	0.1311740	B	0.0684810	-0.0006500	0.2739700
C	-1.1039060	1.1809480	0.3356100	C	1.2419020	-1.1931860	0.1666690
C	-1.0022240	-1.3014700	-0.5090350	C	0.9685640	1.4099860	0.2692840
N	0.5100860	-0.5859510	1.6487440	N	-0.6700520	-0.1492150	1.7983250
C	1.3440550	0.2596770	-0.6902910	C	-1.1941060	-0.1068170	-0.7684040
C	0.9264310	-2.0287470	1.8849100	C	-1.2700870	1.0547120	2.5048820
C	2.4289330	-2.3122380	1.8726780	C	-2.7914830	1.1961730	2.4316720
C	3.2205720	-1.3167870	2.7202650	C	-3.5194650	-0.1108840	2.7453500
C	2.9130280	0.0981030	2.2311440	C	-3.0093320	-1.1979810	1.7994910
C	1.4243410	0.3999990	2.3533600	C	-1.5091200	-1.3998680	1.9739960
C	-1.6769040	1.8456680	-0.7721100	C	1.9726670	-1.4060220	-1.0231570
C	-2.6331240	2.8524040	-0.6847540	C	3.0184410	-2.3129420	-1.1641040
C	-3.0872650	3.2674370	0.5597550	C	3.4161300	-3.0815730	-0.0789330
C	-2.5686300	2.6648420	1.6946550	C	2.7553350	-2.9214550	1.1283980
C	-1.6208130	1.6674010	1.5414730	C	1.7225990	-2.0017880	1.2042950
C	1.9607660	1.5126680	-0.8647590	C	-1.6658770	-1.2295300	-1.4734670
C	3.1739840	1.7001680	-1.8525000	C	-2.8000220	-1.2168950	-2.2868430
C	3.8585470	0.6072180	-2.0397210	C	-3.5529510	-0.0573380	-2.4049760
C	3.3304980	-0.6653950	-1.8625120	C	-3.1757720	1.0727650	-1.6907280
C	2.1236630	-0.7862640	-1.2005410	C	-2.0388250	1.0003820	-0.9085840
C	-2.0561550	-1.9313380	0.1852500	C	1.1371930	2.4119170	-0.7162910
C	-2.9179660	-2.8869210	-0.3468980	C	2.0293560	3.4802480	-0.5894220
C	-2.7753880	-3.2631510	-1.6743040	C	2.8173770	3.6145140	0.5426320
C	-1.7791480	-2.6711580	-2.4339030	C	2.7116700	2.6647610	1.5481550
C	-0.9445380	-1.7317740	-1.8481040	C	1.8191530	1.6264950	1.3657600
Cl	-1.1580110	1.4686090	-2.4139010	Cl	1.5686480	-0.5188660	-2.4880980
F	-1.1723760	1.1525330	2.7404400	F	1.1479460	-1.9376620	2.4575180
Cl	1.2870310	3.0099460	-0.1898080	Cl	-0.9021540	-2.8249230	-1.3402830
F	1.6941350	-2.0693530	-1.0145640	F	-1.7534450	2.1254170	-0.1906990
Cl	-2.4248060	-1.5358530	1.8882590	Cl	0.2554660	2.4535840	-2.2522890
F	-0.0220070	-1.2160050	-2.6933300	F	1.7892200	0.7242120	2.4049840
H	-0.3550340	-0.5206310	2.1771520	H	0.1517850	-0.3401330	2.3602880
H	0.4137320	-2.6362960	1.1436240	H	-0.7829940	1.9399360	2.1039780
H	0.5271040	-2.2903730	2.8693100	H	-0.9786460	0.9530690	3.5550270
H	2.5576360	-3.3339060	2.2436690	H	-3.0690380	1.9807440	3.1426000
H	2.8099030	-2.3030050	0.8541430	H	-3.0930280	1.5491310	1.4482650
H	2.9438540	-1.4122700	3.7782460	H	-3.3366470	-0.4091740	3.7858540
H	4.2908630	-1.5275850	2.6491820	H	-4.5988560	0.0233230	2.6361190
H	3.4431270	0.8476350	2.8262210	H	-3.4911410	-2.1587900	2.0032370
H	3.2475360	0.2171510	1.1990600	H	-3.2469090	-0.9360650	0.7667580
H	1.1425440	0.3806180	3.4094870	H	-1.3148750	-1.7631100	2.9867530
H	1.1871390	1.3883270	1.9719710	H	-1.1251810	-2.1446880	1.2827600
H	-3.0071460	3.3066260	-1.5923290	H	3.5087350	-2.4090660	-2.1234030
H	-3.8319600	4.0497610	0.6403980	H	4.2291490	-3.7907260	-0.1749020
H	-2.8769660	2.9394180	2.6949120	H	3.0164070	-3.4821380	2.0163900
H	3.5730580	2.7000950	-1.6325680	H	-3.0880770	-2.1189640	-2.8093550
H	4.7993170	0.7461700	-2.5585010	H	-4.4328960	-0.0411110	-3.0365910
H	3.8240140	-1.5580500	-2.2240380	H	-3.7306680	2.0009380	-1.7294620
H	-3.6920220	-3.3159480	0.2747410	H	2.0971970	4.2019390	-1.3920230
H	-3.4390310	-4.0005540	-2.1091720	H	3.5061440	4.4452640	0.6354270
H	-1.6247900	-2.9120600	-3.4776010	H	3.3006010	2.6991230	2.4552720

p-I(9):

B	0.0681200	-0.0473320	0.1491820
C	1.3332380	-1.1631970	0.0965130
C	0.8213670	1.3785630	-0.2759990
N	-0.4732980	0.0113900	1.7413240
C	-1.2862880	-0.4548060	-0.7033010
C	-1.1901870	1.2408040	2.2687770
C	-2.7128210	1.1460210	2.3509560
C	-3.1788930	-0.1362720	3.0374490
C	-2.6066350	-1.3240530	2.2658890
C	-1.0829410	-1.2818530	2.2592910
C	1.8977710	-1.6225410	-1.1169400
C	3.0213390	-2.4387400	-1.2148550
C	3.6717330	-2.8663180	-0.0660780
C	3.1701300	-2.4735850	1.1628030
C	2.0476510	-1.6621700	1.1951810
C	-2.3205350	0.4091690	-1.1188300
C	-3.4767170	-0.0083800	-1.7751100
C	-3.6676510	-1.3571980	-2.0439800
C	-2.7069660	-2.2694830	-1.6342020
C	-1.5803570	-1.7971690	-0.9814260
C	1.7320830	2.1025840	0.5208170
C	2.4364050	3.2340550	0.1161430
C	2.2802150	3.7044570	-1.1790730
C	1.4240850	3.0313460	-2.0356560
C	0.7381460	1.9191080	-1.5741410
Cl	1.1837980	-1.2023620	-2.6735640
F	1.6392580	-1.3728860	2.4827690
Cl	-2.2773500	2.1648860	-0.8231560
F	-0.7242120	-2.7683450	-0.5574490
Cl	2.1265910	1.6073840	2.1911540
F	-0.0778970	1.3559800	-2.4928970
H	0.4172670	0.0557580	2.2273550
H	-0.8797770	2.0818950	1.6535250
H	-0.7947240	1.4025630	3.2759190
H	-3.0575330	2.0351230	2.8877220
H	-3.1542120	1.1929530	1.3578160
H	-2.8335180	-0.1637200	4.0790450
H	-4.2709680	-0.1778950	3.0598650
H	-2.8995640	-2.2749870	2.7210710
H	-2.9986330	-1.3237700	1.2468570
H	-0.7205100	-1.4014930	3.2831520
H	-0.6682640	-2.0922240	1.6672750
H	3.3735820	-2.7347120	-2.1937360
H	4.5489720	-3.4981020	-0.1315690
H	3.6173860	-2.7745700	2.1010610
H	-4.2143930	0.7248430	-2.0718070
H	-4.5603720	-1.6899570	-2.5595200
H	-2.8056600	-3.3344300	-1.7989820
H	3.1060280	3.7238160	0.8099690
H	2.8249530	4.5787330	-1.5139640
H	1.2613830	3.3438870	-3.0587910